PETROPHYSICAL ANALYSIS OF MARI DEEP 6 AND MARI DEEP 9, CENTRAL INDUS BASIN, PAKISTAN

BY

YASIR AJMAL
UMAR FAROOQ
MODASSAR HUSSAIN

B.S - Geology
Session 2005-2009

Faculty of Earth and Environmental Sciences
Bahria University Islamabad


بسم الله الرحمن الرحيم

DEDICATION

We dedicate this thesis to our parents. Without their patience, understanding, support and most of all their love, the completion of this work would not have been possible.

ACKNOWLEDGEMENTS

First of all we are thankful to Almighty ALLAH for giving us strength and skills to face the hardships during the completion of this project. Secondly, we gratefully acknowledge the guidance and resources provided by our H.O.D Dr. Shahina Tariq, our internal supervisor Mr. Mohsin Munir and all faculty members. We are heartily thankful to our supervisor Mr. M. Zahid whose encouragement, guidance and support from the initial to the final level enabled us to develop an understanding of the subject.

Lastly, we offer our regards and blessings to all those who supported us in any respect during the completion of this project.

TABLE OF CONTENTS

CHAPTER #1

Introduction to our Thesis Project

1.1 Introduction

Petroleum is vital to many industries, and is of importance to the maintenance of industrialized civilization itself, and thus is a critical concern for many nations. Oil accounts for a large percentage of the world's energy consumption, ranging from a low of 32% for Europe and Asia, up to a high of 53% for the Middle East. In other words, the economy of the world is being controlled by the energy sector. The energy resources and reserves are being used as indicator of economy and political stability of a country. Petroleum and related energy reserves of a country constitute its most important assets. The role of hydrocarbon availability, exploration and development is directly related to the overall development and prosperity of the human being.

The petroleum exploration and its exploitation have gained special importance over the past few decades to meet the increasing demand of the world energy. Due to its importance this field has developed special interests of the scientists and various hydrocarbon agencies and a number of new geophysical techniques and methods have been developed to explore and exploit the hydrocarbon buried in subsurface geological formations. Geophysical well logging is one of the strong tools which are used to evaluate the formation characteristic features having potential for hydrocarbon development. Well logging, also known as borehole logging is the practice of making a detailed record (log) of the geologic formations penetrated by a borehole. The log may be based either on visual inspection of samples brought to the surface (geological logs) or on physical measurements made by instruments lowered into the borehole (geophysical logs). Well logging is done when drilling boreholes for oil and gas, groundwater, minerals, and for environmental and geotechnical studies.

The oil and gas industry records rock and fluid properties to find hydrocarbon zones in the geological formations within the Earth's crust. A logging procedure consists of lowering a 'logging tool' on the end of a wire-line into an oil well (or hole) to measure the rock and fluid properties of the formation. An interpretation of these measurements is then made to locate and quantify potential depth zones containing oil and gas (hydrocarbons). Logging tools developed over the years measure the electrical, acoustic, radioactive, electromagnetic, and other properties of the rocks and their contained fluids. Logging is usually performed as the logging tools are pulled out of the hole. This data is recorded to a printed record called a "Well Log" and is normally transmitted digitally to office locations. Well logging usually refers to downhole

measurements made via instrumentation that is lowered into the well at the end of a wire-line cable. The wire-line consists of an outer wire rope and an inner group of wires. The outer rope provides strength for lowering and lifting the heavy instruments and the inner wiring provides for transmission of power to the downhole equipment and for data telemetry uphole to the recording equipment on the surface.

Although most logs are run to evaluate oil and gas wells, increasing numbers are being run yearly for other purposes, including evaluation of the geothermal energy and ground water. Well log analysis in petroleum industry for oil and gas emphasis the evaluation of basic petrophysical properties of formations containing hydrocarbons.

1.2 Objectives set for the thesis project

The aim of the study was to interpret the hydrocarbon potential in the deep reservoirs of Mari Gas Field by evaluating their well logs which includes porosity calculation, shale volume calculation, water saturation calculation, hydrocarbon saturation calculation, permeability calculation and to resolve lithology.

1.3 General Introduction to the study area

Mari Gas field is located in Central Indus Basin, in a regional structural area commonly referred as the Mari-Kandkhot High. This High was created in Late Cretaceous by extensional tectonics, which resulted in response to the spreading axis between Madagascar and Indian continent. The Mari-Kandkhot High (figure 1.1) is trending NW-SE, uplift and is separated from Jacobabad–Khairpur High by Panno-Aquil Low. Mari structure is more or less similar to Khairpur High. During Late Tertiary Mari Anticline was formed due to inversion. Multiple reservoirs have been successfully tapped in the Mari D& PL including Pirkoh Limestone, Habib Rahi Limestone, Sui Main Limestone at shallow level and Lower Goru Sandstones at deeper level (After Naseer et.al; 2007).

Mari Gas Field was introduced by Esso Eastern Inc (EEI) discovered this field in 1957 with the drilling of first well – Mari X-1. It was drilled to the depth of 11110 feet. The gas was encountered at the depth of 2300 feet in Lower Kirthar Range commonly known as Habib Rahi Limestone. This field was brought on production in 1967 when the required infrastructure was

established to supply 30 MMSCF/Day gas to fertilizer plant of Esso Pakistan Fertilizer Company Limited, now Engro Chemical Pakistan Limited.

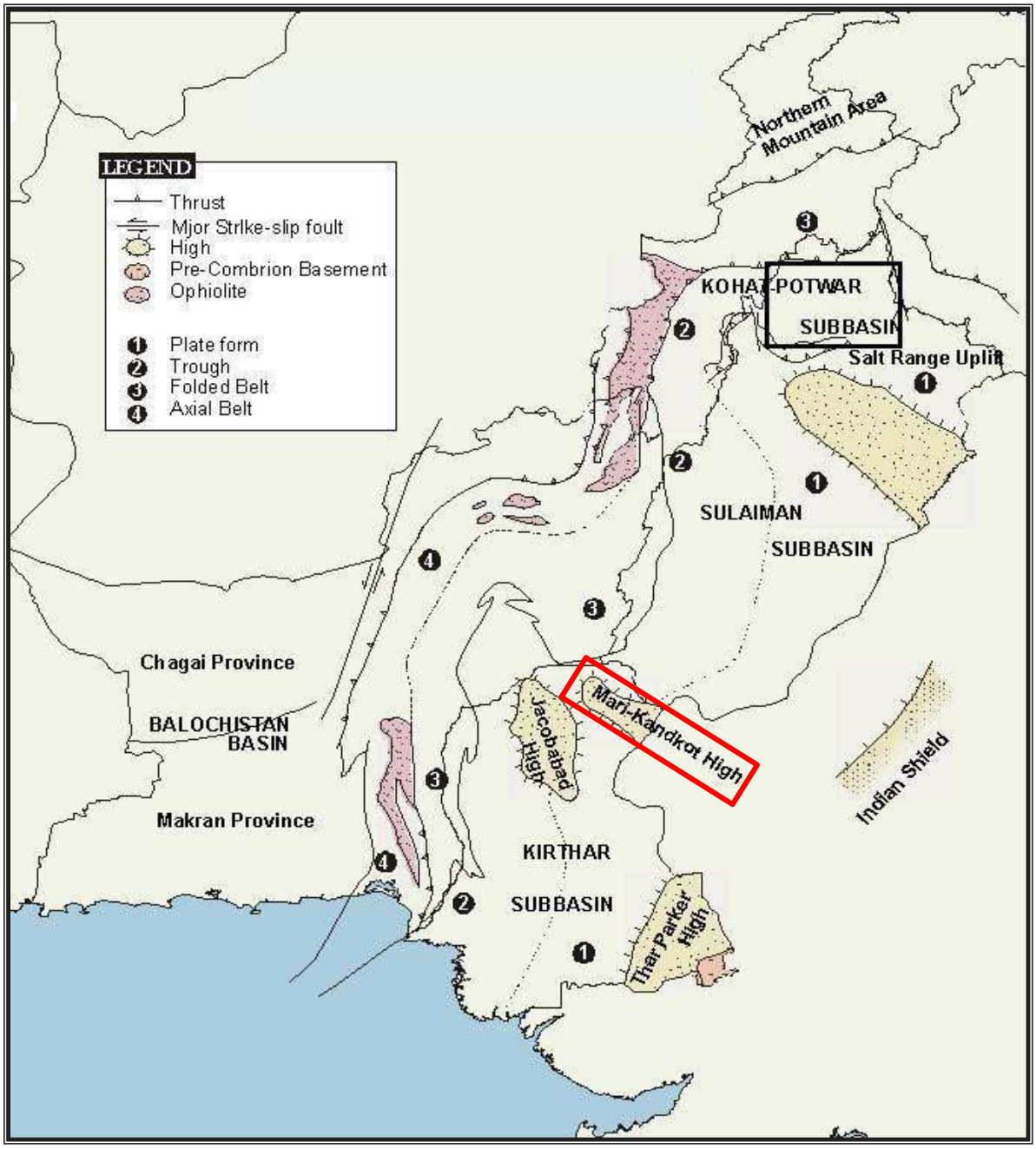

Figure 1.1: Map showing Tectonic Zone of Pakistan. Mari-Kandkhot High is highlighted by red box (After Kazmi; 1982).

Mari Gas Field was owned by Pak Stanvac Petroleum Project (PSPP), a joint venture between Government of Pakistan as 49% interest owner and EEI as 51% interest owner and operator with

marketing rights over entire production from the field. The field was operated under this arrangement till 1983 when Fauji Foundation acquired the entire 51% interest of EEI in PSPP along with its branch office and operated the field till December 22, 1985. Fauji Foundation, Government of Pakistan and Oil and Gas Development Corporation (now Oil and Gas Development Company Limited) incorporated Mari Gas Company Ltd as an unlisted public limited company on December 04, 1984 to take over the assets, liabilities and operation of Fauji Foundation (Mari Gas) and Pak Stanvac Petroleum Project. The Company commenced business in its own name on December 23, 1985.

1.4 Location of the study area

The Mari structure is located in the Central Indus Basin, of the Thar slope platform which gently slopes westwards. Mari Gas Field, located at Daharki, District Ghotki, Sindh, approximately 96 kilometers North of Sukkur.

1.5 Exploration history

According to Abbasi (1998), the hydrocarbon exploration history of the Mari area started in 1957 when Esso eastern Inc. drilled the first well, Mari X-1 and tested gas in Habib Rahi Limestone at depth of 625.7 (mss). As a result of this success, two deeper wells were drilled by Esso. Mari X-2 and Mari X-3 were drilled in 1957 and 1959 in the lower Goru Formation. Mari X-2 didn't flow commercial quality of gas from Habib Rahi Formation as it was located on the western flank of Mari structure. Mari X-3 tested gas at a rate of 29 MMSCF/ day from Habib Rahi Reservoir. These three wells established Gas-in-place reserves, which were estimated to be 4 TCF at that time.

1.6 Development of Mari Gas field

Mari Gas field was developed in phases according to the demand for gas consumption.

1.6.1 Phase I

The first development phase was initiated in December 1965 and completed in March 1966 with the completion of drilling of five development wells yielding a total production of 30 MMSCF/day for Exxon fertilizer. The project was completed at a total cost of about Rs.8.5 million.

1.6.2 Phase II

Another fertilizer plant (Pak Saudi) was built in Mirpur Mathello ten years after completion of Phase-I. To meet the demand for this plant Phase-II of development was initiated in November 1977 and completed in February 1978. Further 9 production wells were drilled to meet the additional demand of 80 MMSCF/D for Pak Saudi Fertilizer. The total cost of the project was Rs.28.7 million.

1.6.3 Phase III

Phase III started in May 1981 and completed in July 1981. In this phase III new wells were drilled and completed at a cost of Rs.42 million. This was done to meet the demand of natural gas for another fertilizer plant at Goth Machi. This plant required 90 MMSCF/D of natural gas for operations. With the completion of Phase-III the production capacity of the field was increased from 110 MMSCF/D to 200 MMSCF/D.

1.6.4 Phase IV

In October 1985, 27 developments and 3 steps out wells were drilled. The project was completed in March 1986 at a cost of Rs.257 million. This was done to fulfill the need of gas for power generation. 100 MMSCF/D of gas to be used at WAPDA's Guddu Power Station.

1.6.5 Phase V

The demand for natural gas kept increasing over the period of time. Fertilizer manufacturers in the area i.e. FFC & Engro installed additional urea manufacturing plants at Goth Machi and Daharki in that way asking MGCL to provide additional gas. Phase V Part I & II development projects were undertaken to meet the demand for 100 MMSCF/D of additional gas in April 1993 and completed in August 1994. Phase-V development programme increased the field production from 300 MMSCF/D to 400 MMSCF/D.

1.7 Petroleum prospects of study area

Reservoir sands in the Middle Indus Platform area were charged from the underlying regionally proven organic-rich shales (Sembar Formation) and from the organic-rich shales within the Lower Goru Member. These shales contain terrestrial organic matter, a TOC in the range of 0.5 – 1.7%, with Type III Kerogen and have been in gas generation phase since late Cretaceous-early Tertiary times. This timing of H-C generation, expulsion and migration coincide with the Early Paleocene and then the Late Eocene structuration. A part of the most significant phase of hydrocarbon generation that took place in the Eocene and younger times is preserved in the form of present-day gas and condensate accumulations in the Middle and Lower Indus platform fields (After Ahmad et.al, 2004).

The lower part of the Habib Rahi Limestone Member (horizon 'HA') and the Pirkoh Limestone & Marl Member (horizon 'PA') is interpreted as shallow shelf (platform edge/shoals) deposits which have excellent reservoir characteristics in Mari field. The average porosity at Mari field is estimated as good to very good (15-20%). Two types of secondary porosities i.e., solution enlarged intra skeletal and matrix micro-porosities enabled the Habib Rahi Limestone with main reservoir characteristics in Mari gas field, which has estimated gas in place of 6 TCF (Trillion Cubic Feet); the recoverable gas reserves are estimated at 4 TCF. The porosity development is facies controlled so reservoir potentials are high in those areas where shallow shelf (platform edge/shoals) facies are thickly deposited (After Sheikh et.al; 2004).

1.8 Hydrocarbon potential of reservoir rocks of study area

In Mari Field, gas has encountered in two main reservoirs. First is shallow reservoir of Habib Rahi Limestone of the Middle to Upper Eocene Kirthar Formation and the second is Lower Goru Sand which is a deep reservoir.

1.8.1 Habib Rahi Limestone

In the Eastern part of fold belt at Mari Field, gas has been encountered in the Habib Rahi Limestone of the Middle to Upper Eocene Kirthar Formation. It is widespread over the western part of the Indus basin but absent in most of wells drilled in the southern part of the Thar slope platform (After Abbasi et.al; 1998). The Habib Rahi Limestone is divided into three lobes the

eastern lobe, the western lobe and the southern lobe based on porosity and permeability distribution, as shown in table 1.1.

Parameters	Eastern Lobe	Western Lobe	Southern Lobe
Porosity (%)	25	20	18
Permeability (mD)	40-70	10-15	5-9

Table 1.1: Properties of different lobes of Habib Rahi Limestone (After Abbasi et.al; 1998).

The Habib Rahi Limestone has been divided into two intervals.

a. Habib Rahi reservoir zone-A

The upper interval, Zone- A, is approximately 10.7 m thick and is composed of shaly limestone and thin limestone beds. Zone-A exhibits poor reservoir quality.

b. Habib Rahi reservoir zone-B

Zone-B, which is approximately 91.4 m thick, contains virtually the entire gas reserves, is a good quality reservoir with porosity varying from 19 to 25 percent and permeability varying from 5 to 70 millidarcies.

Properties	Layer-1	Layer-2
Log Porosity (%)	22.6	19.3
Core Porosity (%)	22.0	20.8
Core Permeability (mD)	12.1	08.2
Sw (Log) (%)	24.2	35.8

Table 1.2: Difference between two layers of the Habib Rahi zone-B (After Abbasi et.al; 1998)

The Habib Rahi Zone-B has been divided into two layers on the basis of resistivity log response for use in reservoir simulation. No lithological differences can be seen from the core descriptions. However, Petrophysical properties in Layer-2 appear to be poor and more variable

than in Layer-1 (After Abbasi et.al, 1998). The average properties for the two layers are listed in table 1.2.

1.8.2 Lower Goru sands

The discoveries at Mari Deep in recent years have proven the importance of Early Cretaceous (Lower Goru) Sandstone Play in the basin. Presently the discoveries from lower Goru sands are restricted mainly to the south-eastern part of the basin while from Tertiary reservoirs these have been mainly made in the central and north-western parts of the study area (After Khan et.al; 1999).

1.8.3 Lower Goru sand division

Lower Goru Sands have been divided into three main intervals A, B & C (from bottom to top) by OMV and PPL. These sands continue to be the major exploration target in the south-eastern part of the study area. Lower Goru Sands (A, B & C) were probably deposited on a ramp type margin as indicated by regional seismic geometry of these deposits. Generally Lower Goru Sands run almost parallel in NE-SW direction in a back stepping pattern in relatively narrow fair way. Productive sand units are relatively thin with thickness ranging from 5 to 10 m and are beyond seismic resolution (After Khan et.al; 1999).

1.9 Gas reserves of the Mari Gas Field

Following tables shows the gas reserves of the Mari Gas field

Gas In Place	**10,530 BCF**
Recoverable Reserves	6,800 BCF
Produced till April 2008	3,434 BCF
Balance Recoverable Reserves	3,366 BCF

Table 1.3: Habib Rahi reservoir (Courtesy Mari Gas Ltd.)

Gas In Place	**1,861 BCF**
Recoverable Reserves	1,210 BCF
Produced till April 2008	-
Balance Recoverable Reserves	1,210 BCF

Table 1.4: Goru B reservoir (Courtesy Mari Gas Ltd.)

Gas In Place	**65 BCF**
Recoverable Reserves	42 BCF
Produced till April 2008	9 BCF
Balance Recoverable Reserves	33 BCF

Table 1.5: SML/Pirkoh reservoir (Courtesy Mari Gas Ltd.)

CHAPTER # 2

Introduction to Petrophysics

2.1 Introduction

Petrophysics (petro is Latin for "rock" and physics is the study of nature) is the study of the physical and chemical properties that describe the occurrence and behavior of rocks, soils and fluids. Petrophysics mainly studies reservoirs of resources, including ore deposits and oil or natural gas reservoirs. Petrophysicists in the oil and gas industry typically are employed in helping the engineers and other geoscientists understand the rock properties of the reservoir. Petrophysicists evaluate the reservoir rock properties by employing well log measurements, in which a string of measurement tools are inserted in the borehole, core measurements, in which rock samples are retrieved from subsurface, and sometimes seismic measurements, and combining them with geology and geophysics.

Petrophysical studies are utilized by petroleum engineering, geology, mineralogy, exploration geophysics and other related studies. Some of the key properties studied in petrophysics are lithology, porosity, water saturation, permeability, density, solid mechanics, magnetization, electrical conductivity, thermal conductivity and radioactivity.

2.2 Conventional Petrophysical properties

Most petrophysicists are employed to compute what are commonly called conventional (or reservoir) petrophysical properties. These are:

2.2.1 Lithology

Lithology gives us the answer of the question that what type of rock is it? When combined with local geology and core study, geoscientists can use log measurements such as natural gamma, neutron, density, Photoelectric, resistivity or their combination to determine the lithology downhole.

2.2.2 Porosity

The porosity of the rock is the number of the pore (void) space in a rock, as shown in figure 2.1. It is measured as a fraction, between 0 – 1, or as a percentage between 0 – 100 % and is represented by the symbol φ. The porosity depends on the shape, surface, texture, angularity, orientation, and degree of cementation and size distribution of the grains, which make up the

rock. Porosity can be divided into three categories primary porosity, secondary porosity and effective porosity.

a. Primary porosity

The pore spaces left between the fragments of the rock forming material during the time of deposition is known as the primary porosity.

b. Secondary porosity

Secondary porosity is the porosity which develops after the process of deposition. It develops due to dissolution, fractures, pits and other discontinuities in the bulk volumes of matrix. The contribution of the secondary to the overall bulk porosity is generally small yet it can lead to dramatic increases in bulk permeability.

c. Effective porosity

The degree to which pores within the material are interconnected is known as effective porosity. Effective porosity is the only capacity, which can make contribution to the flow. Pores initially present but subsequently seals off by cementation or recrystallization effects are of no interest.

Porosity is typically measured using an instrument that measures the reaction of the rock to bombardment by neutrons or by gamma rays. Sonic wave speed and NMR logs are also measured to derive rock porosity.

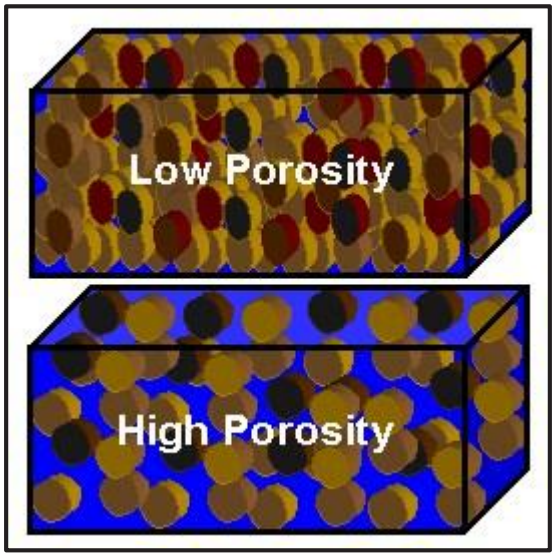

Figure 2.1: Diagram showing porosity in a rock unit.

2.2.3 Saturation

The saturation of a formation is the fraction of its pore volume occupied by the fluid considered. Water saturation, then, is the fraction (or percentage) of the pore volume that contains formation water. If nothing but water exists in the pores, a formation has a water saturation of 100%. The symbol for saturation is S, various subscripts are used to denote saturation of a particular fluid (S, for water saturation, S, for oil saturation, S, for hydrocarbon saturation, etc.).

Oil, or gas, saturation is the fraction of the pore volume that contains oil, or gas. The pores must be saturated with some fluid. Thus, the summation of all saturations in a given formation rock must total to 100%. Although there are some rare instances ‘of saturating fluids other than water, oil, and gas (such as carbon dioxide or simply air), the existence of a water saturation less than 100% generally implies a hydrocarbon saturation equal to 100% less the water saturation (or 1 - S_w).

The water saturation of a formation can vary from 100% to a quite small value, but it is seldom, if ever, zero. No matter how “rich” the oil or gas reservoir rock may be, there is always a small amount of capillary water that cannot be displaced by the oil. Similarly, for an oil- or gas-bearing reservoir rock, it is impossible to remove all the hydrocarbons by ordinary fluid drives or recovery techniques. Some hydrocarbons remain trapped in parts of the pore volume.

2.2.4 Permeability

Permeability is the property of a rock which allows the liquid to pass through or in other words it is simply the measure to the ease with which a fluid can pass through a rock (figure 2.2). Just as with porosity, the packing, shape, and sorting of granular materials control their permeability. Although a rock may be highly porous, if the voids are not interconnected, then fluids within the closed, isolated pores cannot move hence making the rock impermeable. The symbol most commonly used for permeability is K. Permeability is measured in Darcy, but the permeability in petroleum-producing rocks is usually expressed in units called milliDarcys (one milliDarcy is 1/1000 of a Darcy).

Permeability is also divided into three sub categories namely absolute permeability, effective permeability, and relative permeability.

a. Absolute permeability

The measurement of the permeability, or ability to flow or transmit fluids through a rock, conducted when a single fluid, or phase, is present in the rock. This is the property of the rock and not of the fluid flowing through it. Absolute permeability is measured with the fluid which saturates 100% of the pore space.

b. Effective permeability

The ability to preferentially flow or transmit a particular fluid when other immiscible fluids are present in the reservoir (e.g. effective permeability of gas in a gas-water reservoir). The relative saturations of the fluids as well as the nature of the reservoir affect the effective permeability. The effective permeability is always less than the absolute permeability for the rock.

c. Relative permeability

It is the ratio of the effective permeability to the absolute permeability. If a single fluid is present in a rock, its relative permeability is 1.0. Calculation of relative permeability allows comparison of the different abilities of fluids to flow in the presence of each other, since the presence of more than one fluid generally inhibits flow.

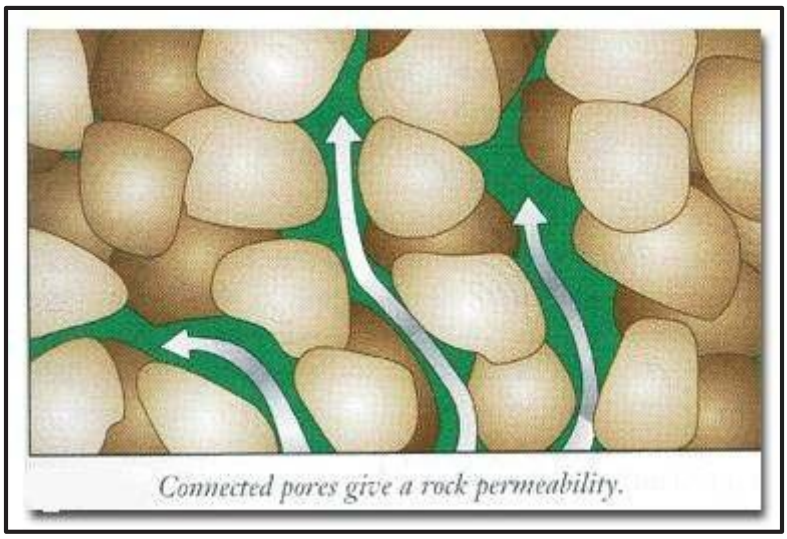

Figure 2.2: Diagram showing permeability in a rock

2.2.5 Thickness of the reservoir

Thickness of rock with enough permeability to deliver fluids to a well bore. This property is often called “Net reservoir rock.” In the oil and gas industry, another quantity “Net Pay” is

computed which is the thickness of rock that can deliver hydrocarbons to the well bore at a profitable rate.

Reservoir models are built upon their measured and derived properties to estimate the amount of hydrocarbon present in the reservoir, the rate at which that hydrocarbon can be produced to the Earth's surface through wellbores and the fluid flow in rocks. In the water resource industry, similar models are used to compute how much water can be produced to the surface over long periods of time, without depleting the aquifer.

2.3 Methods of formation evaluation

In petroleum exploration and development, formation evaluation is used to determine whether a potential oil or gas field is commercially viable. Essentially, it is the process of "recognizing a commercial well when we drill one". Only in rare cases do oil and gas wells come in with a fountain of gushing oil. In real life, that is a blowout and usually also a financial and environmental disaster. Modern rotary drilling uses a heavy mud as a lubricant and as a means of producing a confining pressure against the formation face in the borehole, preventing blowouts. This is a double edged sword mud filtrate soaks into the formation around the borehole and a mud cake plasters the sides of the hole. These factors obscure the possible presence of oil or gas in even very porous formations. Further complicating the problem is the widespread occurrence of small amounts of petroleum in the rocks of many sedimentary provinces. In fact, if a sedimentary province is absolutely barren of traces of petroleum, one is probably foolish to continue drilling there.

The formation evaluation problem is a matter of answering two questions:

1. What are the lower limits for porosity, permeability and upper limits for water saturation that permit profitable production from a particular formation or pay zone; in a particular geographic area; in a particular economic climate?
2. Do any of the formations in the well under consideration exceed these lower limits?

It is complicated by the impossibility of directly examining the formation. It is, in short, the problem of looking at the formation indirectly.

Formation Evaluation Techniques are:

1. Coring
2. Mud logging
3. Wire-line logging

2.3.1 Coring

One way to get more accurate samples of the formation at a certain depth in the well is coring. There are two techniques commonly used at present. The first is the "whole core", a cylinder of rock, usually about 3" to 4" in diameter and, with good luck, up to 50 feet to 60 feet long. It is cut with a "core barrel", a hollow pipe tipped with a ring shaped, diamond chip studded bit that can cut a plug and retain it in a trip to the surface. If no shale or fractures are encountered, the full 60 foot length of the core barrel can be filled. More often the plug breaks while drilling, usually at the aforementioned shale or fractures and the core barrel jams, very slowly grinding the rocks in front of it to powder. This signals the driller to give up on getting a full length core and to pull up the pipe.

Taking a full core is an expensive operation that usually stops or slows drilling for at least the better part of a day. A full core can be invaluable for later reservoir evaluation. One of the tragedies of the oil business is the huge amount of money that has been spent for cores that have been lost because of the high cost of storage. Once a section of well has been drilled, there is, of course, no way to core it without drilling another well.

The other, cheaper, technique for obtaining samples of the formation is "Sidewall Coring". In this method, a steel cylinder a coring gun has hollow-point steel bullets mounted along its sides. These bullets are moored to the gun by short steel cables. The coring gun is lowered to the bottom of the well and the bullets are fired individually as the gun is pulled up the hole. The mooring cables ideally pull the hollow bullets and the enclosed plug of formation loose and the gun carries them to the surface. Advantages of this technique are low cost and the ability to sample the formation after it has been drilled. Disadvantages are possible non recovery because of lost or misfired bullets and a slight uncertainty about the sample depth. Sidewall cores are often shot "on the run" without stopping at each core point because of the danger of differential sticking. Most service company personnel are skilled enough to minimize this problem, but it can be significant if depth accuracy is important.

2.3.2 Mud logging

The simplest and most direct tool is well cuttings examination. Some older oilmen ground the cuttings between their teeth and tasted to see if crude oil was present. Today, a well-site geologist or mud-logger uses a low powered stereoscopic microscope to determine the lithology of the formation being drilled and to estimate porosity and possible oil staining. A portable ultraviolet light chamber or "Spook Box" is used to examine the cuttings for fluorescence. Fluorescence can be an indication of crude oil staining, or of the presence of fluorescent minerals. They can be differentiated by placing the cuttings in a solvent filled watch glass or dimple dish. The solvent is usually carbon tetrachlorethane. Crude oil dissolves and then redeposit as a fluorescent ring when the solvent evaporates. The written strip chart recording of these examinations is called a sample log or mud-log.

Mud logging (or Well-site Geology) is a well logging process in which drilling mud and drill bit cuttings from the formation are evaluated during drilling and their properties recorded on a strip chart as a visual analytical tool and stratigraphic cross sectional representation of the well. The drilling mud which is analyzed for hydrocarbon gases, by use of a gas chromatograph, contains drill bit cuttings which are visually evaluated by a mud-logger and then described in the mud log. The total gas, chromatograph record, lithological sample, pore pressure, shale density, etc (all lagged parameters because they are circulated up to the surface from the bit) are plotted along with surface parameters such as Rate Of Penetration (ROP), Weight On Bit (WOB), etc. on the mud-log which serve as a tool for the mud-logger, drilling engineers, mud engineers, and other service personnel charged with drilling and producing the well.

2.3.3 Wire-line logging

In 1928, the Schlumberger brothers in France developed the workhorse of all formation evaluation tools: the electric log. Electric logs have been improved to a high degree of precision and sophistication since that time, but the basic principle has not changed. The detail description is big topic so concentrated in another chapter.

CHAPTER # 3

History and development in well logging

3.1 Developments in well logging

Well logging is a relatively young science, but initial work in the field dates back over 140 years. As early as 1869, Lord Kelvin in Britain was making interpretations of heat flow in shallow well bores by measuring temperature versus depth. 100 years later, the Apollo astronauts set up heat flow experiments in the lunar regolith. The holes were only 1.5 to 3.2 meters deep and the logging tool was stationary, but the results were recorded versus depth, so these surveys are the first logs recorded off planet Earth. The first surface measurements of electrical resistance of rocks were made by Conrad Schlumberger in 1912. This was repeated on the Moon by Apollo astronauts also.

Figure 3.1: Dave Scott of Apollo 15 running the first logs on the Moon in 1971 (NASA Photo)

The initial success with surface resistivity led Conrad and his brother Marcel Schlumberger to consider similar measurements in boreholes. In 1927, they convinced the Pechlebronn Oil Company, drilling in Alsace, France, to try such electrical measurements as an aid to understanding the rock layers. The first such log in the USA was run on 17 August l929 for Shell Oil Company in Kern County, California. Logs were run that same year in Venezuela, Russia, and India.

Year	DEVELOPMENT
1869	First temperature log Lord Kelvin
1883	Single electrode resistivity log patented by Fred Brown
1912	First surface resistivity survey (Conrad Schlumberger)
1927	First multi-electrode electrical survey in a wellbore (in France)
1929	First electrical survey in California (also Venezuela, Russia, India)
1931	First SP log, first sidewall core gun
1932	First deviation survey, first bullet perforator
1933	First commercial temperature log
1936	First SP dipmeter
1937	First electrical log in Canada (for gold in Ontario)
1938	First gamma ray log, first neutron log
1939	First electrical log in Alberta
1941	Archie's Laws published, first caliper log
1945	First commercial neutron log
1947	First resistivity dipmeter, first induction log described
1948	First microlog, first shaped charge perforator
1948	Rw from SP published
1949	First laterolog
1952	First microlaterolog

1954	Added caliper to microlog
1956	First commercial induction log, nuclear magnetic log described
1957	First sonic log, first density log
1960	First sidewall neutron log (scaled in porosity units)
1960	First thermal decay time log
1961	First digitized dipmeter log
1962	First compensated density log (scaled in density/porosity units)
1962	First computer aided log analysis, first logarithmic resistivity scale
1963	First transmission of log images by telecopier (predecessor to FAX)
1964	First measurement while drilling logs described
1965	First commercial digital recording of log data
1966	First compensated neutron log
1969	First experimental PE curve on density log
1971	First extraterrestrial temperature log Apollo 15
1976	First desktop computer aided log analysis system LOG/MATE
1977	First computerized logging truck
1982	First use of email to transmit data via ARPaNet (predecessor to Internet)
1983	First transmission of log data by satellite from wellsite to computer center
1985	First resistivity microscanner

Table 3.1: Table showing development in well logging through time

3.1.1 The early years (1929 - 1949)

The first recognizable technical paper on log interpretation, by the Schlumberger brothers and E.G. Leonardon, describing the electrical resistivity log, was published in 1934. Log analysis using these new tools involved curve-shape recognition - still a valid and commonly used qualitative approach to interpretation. Log curve shapes are determined visually from the appearance of the recorded data when plotted versus depth. These curve shapes were related to rock sample and core description data to determine general rules-of-thumb for separating permeable, porous, oil bearing beds from non-productive zones.

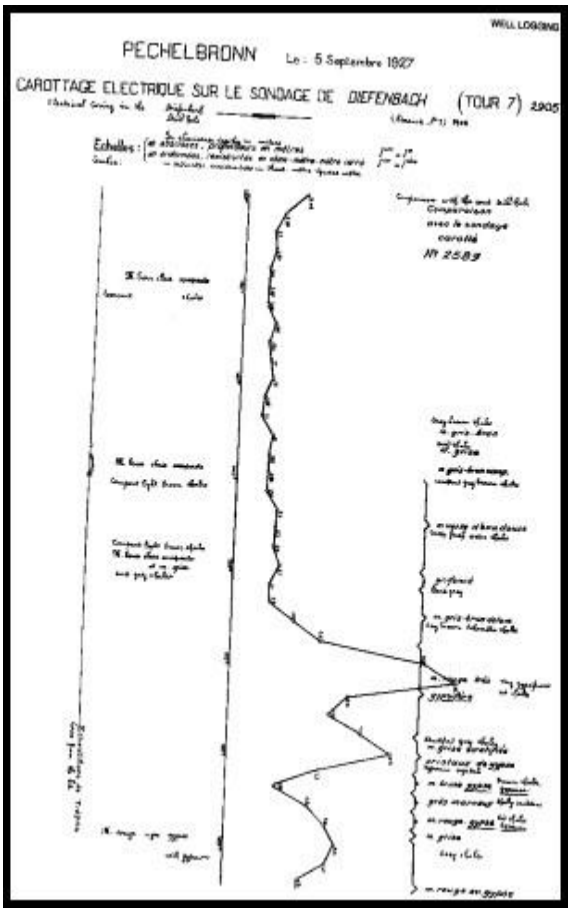

Figure 3.2: First Schlumberger log 1927

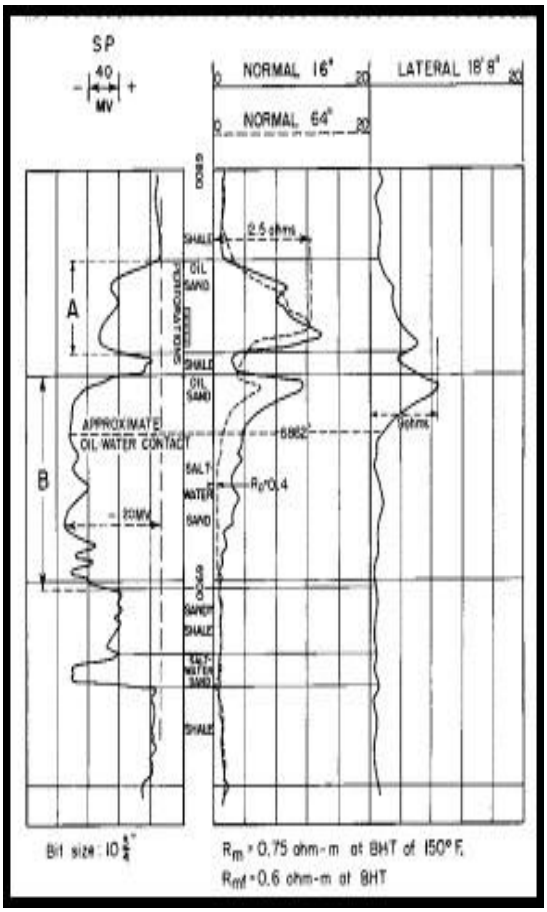

Figure 3.3: Curve shape analysis 1950

The early success of curve shape interpretation was quite accidental. It depended on the fact that the formation water in the first wells logged was quite conductive due to dissolved salt. Had these logs been run in west Texas at the beginning of the twenties, the fresh water sands may have given such confused interpretations that well logging might never have become popular.

Seven years after the original Schlumberger paper, in 1941, G. E. Archie developed the empirical data behind the concept of "formation factor" - a term used to relate the porosity, the resistivity log reading, and the water saturation in the zone. This revolutionized log analysis, as the subject was now quantitative rather than only qualitative. In practice, however, the errors due to borehole effects on the measurements and uncertainty about other items relating formation factor to porosity, prevented really accurate results.

W. O. Winsauer, with others, modified the Archie equation slightly in 1952. This formula is used today but is commonly known as the Archie equation. M. P. Tixier of Schlumberger published the details of the so-called Rocky Mountain or resistivity ratio method in 1949. It was based on Archie's water saturation equation, but avoided the need to know porosity by using the ratio of deep and shallow resistivity readings.

From its earliest beginnings, the spontaneous potential log was interpreted by its curve shape. Since an SP voltage was developed across sandstones, and not along shale beds, it was relatively easy to identify sandstone from shale by the shape of the SP curve. Between 1943 and 1949, much work was done on the theory behind the spontaneous potential. Interpretation from this curve is still popular because it gives approximate values for formation water resistivity in clean (non-shaly) sandstone formations, or the shaliness of the formation in shaly sandstones.

Shale content calculations were enhanced by the appearance of the gamma ray log in 1934 because shale emitted natural gamma rays and clean sandstone and limestone did not. The log was calibrated to present a curve similar in shape to the spontaneous potential log. Although the gamma ray log has existed for seventy years, its appearance has not changed much. However, its resolution and accuracy have improved greatly due to more efficient and smaller gamma ray detectors.

The electrical, SP, and gamma ray logs all measured the average value of rock properties over eighteen inches to five feet of rock thickness. Beds thinner than this could not be detected or evaluated. The microlog was introduced in 1948 and allowed resistivity in beds as thin as two or three inches to be measured at a correspondingly shallow depth of investigation into the rock.

The curve shape approach to analysis was commonly used for microlog data, although laboratory derived charts allowed quantitative interpretation of formation factor, and as a result, porosity. The curve shape analysis for micrologs provided rapid visual identification of zones which were

invaded by drilling fluid, and were thus permeable to some small degree. The log is still used today for this purpose.

The structural dip of rock formations is an important piece of knowledge for geologists. The first dipmeter log using three simultaneous spontaneous potential measurements spaced equally around the perimeter of the borehole, was run in 1942. It was superceded in 1947 by three simultaneous resistivity measurements. The theory of interpretation was simple. Slight offsets in the depth of the bed boundaries recorded by each of the three curves, plus the tool geometry, hole diameter, and tool orientation in space, could be reduced to give the dip of the bed boundary. Initially this was done by hand comparison, later in manually operated optical comparators and now by computer cross-correlation. The work was tedious and fraught with difficult decisions when the curves wiggled too much or not enough.

The section gauge (or caliper log) also appeared in 1942 and made the application of borehole size corrections to all kinds of resistivity logs possible. The use of laboratory derived departure curves for this purpose, (between 1949 and 1955), was a common event in a log analyst's life. The corrections were seldom satisfying and may have been "gilding the lily" somewhat. Modern resistivity logs need little borehole correction if run in a well designed mud system in a reasonably good hole.

Additional logging tools have existed for a long time, and are used as aids to interpretation of other logs. One is the formation tester, which measures the formation pressure and obtains a fluid sample, usually of the invaded zone. It was first run in l957. Refinements with digital recording techniques proved very helpful in sorting out reservoir fluid content and reservoir continuity. The log made by the formation tester is of pressure versus time instead of a depth dependent log. Many such tests taken at different depths can provide a formation pressure versus depth log for analysis of pressure gradients.

The sidewall core gun (sample taker) was first used in l942. It used a large hollow bullet, tied to the tool by wires, to retrieve a small plug of rock from the well bore. The temperature log, used to detect entry of gas into the well bore, was made available about l936. It was also used to determine formation temperature and temperature gradient.

Much evolution was going on behind the scenes that the log analyst never really appreciated, but the logging engineer did. The rag-line logging cable gave way in l947 to steel armoured

multiconductor cable, which was far stronger and more reliable. Today, fiber optic cables are sometimes used. The tools evolved from purely electrical devices with ammeters and voltmeters, to vacuum tubes in the late forties, to transistors in the early sixties and finally integrated circuits and computers in the seventies and eighties.

Trucks changed radically from short wheel base, open cab flat decks with equipment bolted to the floor and shaded from the elements by an umbrella, to canvas covered vans in the early forties. Bread wagon style panel vans appeared in the late forties, to be superceded by the six and ten wheel "corn binders" of the fifties and sixties. The air conditioned behemoths of today, that look ever so much like space age garbage trucks, are the result of the computer revolution.

Figure 3.4: Early logging trucks c.1934 (Schlumberger photos)

3.1.2 The middle years (1949 - 1969)

All the logs mentioned so far, except the caliper, needed a conductive fluid in the borehole in order to operate. The induction log was introduced in 1949 to overcome this requirement in holes drilled with air or oil based drilling mud. The log was calibrated to read rock conductivity by inducing currents with electromagnetic coils. Prior to this invention, logging tools impressed currents into the formation by means of direct application of voltages from the logging tool electrodes. Over the next ten years, the induction log also became popular in wells drilled with fresh mud.

Interpretation of water saturation became more reliable because of reduced borehole effect on the resistivity measurements, compared to conventional electrical resistivity logs. To some degree,

bed boundary effects were more predictable and compensated for electronically. The induction log has evolved considerably over its fifty year life and is the most common log run today.

The laterolog was also introduced in 1948 - 1949. It was a multi-electrode electrical log designed to minimize borehole effects in salty drilling mud. Again, improved resistivity values led to better water saturation and porosity determinations, still using the Archie method.

The microlaterolog, to replace the microlog in salt mud, was first seen in 1952. Curve-shape analysis was not easy, but standard Archie methods worked well with this data. Other similar tools, such as the proximity log, and the micro-spherically focused log, are variations of the microlaterolog designed to improve shallow resistivity measurements in a variety of borehole conditions.

Neutron logs first appeared in 1938, but were not common until l946, when better sources of neutron radiation became more readily available. Neutrons emitted by the source, are absorbed by hydrogen atoms, which are common in water and petroleum. Qualitative interpretation of porosity (which contains water or oil) was possible by detecting the number of neutrons which were not absorbed but were scattered back to the detector. In some tools, the captured gamma rays created by the neutron bombardment were counted instead of the neutrons.

This was the first independent source of porosity information that did not rely on Archie's formation factor concept and the resistivity log data. The tool had, and has, its faults, but modern neutron logs are useful quantitative interpretation aids. Again, better detectors have increased the resolution and accuracy of the measurements. The modern version of the neutron log compensates for borehole size and a number of environment factors automatically.

The two-receiver acoustic travel time (sonic) log showed up in 1957. Laboratory work had demonstrated that the travel time of sound in a rock, after adjustments for fluid and matrix rock travel time values, was capable of estimating porosity. Thus, another independent source of porosity data was born.

The sonic-resistivity crossplot was invented shortly after the sonic log. It allowed visual as well as quantitative presentation of porosity and water saturation results on one piece of paper without the use of additional charts, nomographs, or slide rules (hand calculators had not yet been

invented). It was tedious work, but thousands of crossplots were made during the sixties, and a few less progressive analysts still use them today.

Quick look methods to differentiate hydrocarbon zones from water zones also followed the introduction of the sonic log. One such technique, the "Rwa Method", is still very popular. The principle used was to quickly calculate, from the Archie water saturation equation and the sonic log porosity value, the apparent water resistivity which would make the zone 100% water saturated.

Another quick look method is called the overlay method. The simplest approach was to overlay the resistivity log and the sonic log in such a way as to have the two curves fall on top of each other in the obvious water zones. Zones in which the resistivity log fell to the right of the sonic log were either potential pay zones or tight (non porous).

The invention of the logarithmic presentation for resistivity data, when the dual induction log was introduced in 1962, made quick look overlay methods even more popular and practical at the well site.

The density log was introduced in l959. It was another independent source of porosity data. With three sources of apparent porosity, (sonic, neutron and density), in addition to the resistivity methods, it was now possible to account for more variables. This led to cross plot or chart book methods which compared the apparent porosity values from two sources, to help identify lithology (shale content or limestone - dolomite ratio, for example). The sonic-density cross plot was common in the early sixties, with the density-neutron cross plot becoming more common in the late sixties, as the neutron logs became better calibrated and scaled in porosity units.

The late fifties and early sixties also saw a great deal of work in atomic physics and both the pulsed neutron (or atomic activation) log and natural gamma ray spectroscopy log were described. However, suitable tools did not become available until 1968, and were not common until 1971.

While the early years were clearly a period of invention of hardware and techniques, the middle years could be termed the period of understanding. Although significant new tools were developed, such as the sonic and density logs, the interpretation process required more

formidable effort. Customers wanted more reliable answers along with the more reliable logging tools.

3.1.3 The recent years (1969 - 1985)

Water saturation interpretation in shaly sands and porosity determination were both being studied in the late sixties. With several independent sources of data, and with more unknowns than measurements, a new style of interpretation was proposed. Instead of solving a fixed set of simultaneous equations, various iterative solutions were used to minimize the change in one or several computed results.

The primary goal was to correct for shale, light hydrocarbon effect, heavy mineral effect, and to solve for porosity and lithology at the same time. Success depended greatly on log data quality and on how well the calculation model actually fit the real geology. Much work is still being done in this area and new approaches appear in journals yearly.

During the seventies and early eighties, these methods were programmed on low cost sophisticated hand calculators. If large volumes of data were required, desktop computers with digitizers, plotters and printers could be obtained from several sources. Today, the ubiquitous personal computer does the work at a fraction of the cost and time.

The first truly portable stand-alone desktop system that did not require connection to a large mainframe computer was LOG/MATE, developed by the author and D. W. Curwen in l976. This was 5 years before IBM "invented" the PC. It has since been mimicked and improved upon by many others, so that a wide range of such systems are available.

Log analysis methods vary from crude to complex and the quality of results varies with the knowledge and experience of the analyst. The quality and age of input data is always a problem to consider. Simpler systems, with a good analyst at the controls, often provide better results, because of the personal input and knowledge of the analyst. More complex programs tend to do unexpected things and are not easy to control, even by expert log analysts.

While digital recording of well logs began in l965, early trials of digital computation at the well site did not begin until l972. After this date, the major service companies have almost completely replaced all their older analog logging units. This provided both log interpretation and calibration control by computer. The best known interpretation examples are Schlumberger's CYBERLOOK

and Dresser's PROLOG products. A number of new tools, revised uses of older tools, and significant advances in computer processing of log data have been introduced in the 1980's, and are gaining rapid acceptance by well operators.

Satellite transmission of log data from the well site to service company computer centers superceded the Telecopier and FAX machine in many areas, allowing faster decision making at the head office, somewhat to the detriment of local autonomy and egos.

The lithodensity log is an improved density log with reduced statistical variations on the density measurement, and a new curve, the photo electric capture cross-section curve, better known as the PE curve. Its' value depends on the rock lithology and is relatively unaffected by porosity and pore fluid type. Therefore, it can be used to assist in lithology identification in simultaneous equation solutions. The natural gamma ray spectrolog, is now also widely used to resolve lithology problems, such as radioactive dolomite or granite wash formations, or to help define clay types in shale.

One product, called FACIOLOG, by Schlumberger, was an attempt to reduce this data overload to a minimum. It provides a detailed electro-facies log which, when calibrated to rock sample and core data, can be very useful in understanding depositional environments and well to well correlations. It can also be presented on a seismic time scale to assist in correlating normal seismic data, or vertical seismic profiles taken in the same well. Its visual appearance mimics the type of shading used by geologists while drawing their geological sample logs. Unfortunately, such interpretive log displays have not received wide acceptance.

The recent years in well logging can be termed the era of digital data, giving tool designers and analysts the power of the computer to bring to the surface more data of higher quality than ever before.

3.1.4 The state of the art (1986 - Present)

The continuous evolution of logging tools to improve data quality, signal to noise ratio, bed resolution, and depth of investigation demonstrate the gradual, almost un-noticed, changes in our industry. This will no doubt continue; but how far can we go, or want to go, is an open question. We may already record more data than we can conveniently use. The question really is: Is it the right data to give the answers we need.

The introduction of digital image logs and signal processing theory to log data are dramatic improvements that have fundamentally altered how we use logs, for example in quantifying fracture porosity and intensity or in evaluating depositional environment. What could be the next great leap is not at all clear. We have exhausted most of the available frequencies of the electromagnetic spectrum (except maybe the infra-red) and have tested most physical principles.

Figure 3.5: Modern logging truck (Schlumberger photos)

We have come a long way since the Schlumberger brothers put the first electrical log onto paper in 1927.The incredible and unpredictable growth of other technologies outside our industry also had dramatic effects. Low-cost high-speed computers, powerful spreadsheet and graphics software, satellite data transmission, and group work via local area networks or the Internet have changed the way we do our work.

CHAPTER # 4

Wireline logging – A practical approach

4.1 Wire-line logging

Wire-line logging is the process of recording various physical, electrical, or other properties of the rock/fluid mixtures penetrated by drilling a well into the Earth. In its most usual form, an oil well log is a record displayed on a graph with the measured physical property of the rock on one axis and depth (distance from the surface) on the other axis. More than one property may be displayed on the same graph. None of the logs actually measure the physical properties that are of most interest to us, such as how much oil or gas is in the ground, or how much is being produced. Such important knowledge can only be derived, from the measured properties listed above (and others), using a number of assumptions which, if true, will give reasonable estimates of hydrocarbon reserves. Thus, analysis of log data is required. The art and science of log analysis is mainly directed at reducing a large volume of data to more manageable results, and reducing the possible error in the assumptions and in the results based on them. When log analysis is combined with other physical measurements on the rocks, such as core analysis or petrographic data, the work is called petrophysical analysis. The results of the analysis are called mapable reservoir properties. The petrophysical analysis is said to be "calibrated" when the porosity, fluid saturation, and permeability results compare favorably with core analysis data. Further confirmation of petrophysical properties is obtained by production tests of the reservoir intervals.

4.2 Generation of well logs

To perform a logging operation, the measuring instrument, often called a probe or sonde, is lowered into the borehole on the end of an insulated electrical cable. The cable provides power to the down-hole equipment. Additional wires in the cable carry the recorded measurement back to the surface. The cable itself is used as the depth measuring device, so that properties measured by the tools can be related to particular depths in the borehole.

Wire-line logging is done from a logging truck (shown in figure 4.1). The truck carries the downhole measurement instruments, the electrical cable and winch needed to lower the instruments into the borehole, the surface instrumentation needed to power the downhole instruments and to receive and process their signals, and the equipment needed to make a permanent recording of the "log."

The downhole measurement instruments are usually composed of two components. One component contains the sensors used in making the measurement, called the sonde. The type of sensor depends, of course, upon the nature of the measurement. Resistivity sensors use electrodes or coils; acoustic sensors use transducers; radioactivity sensors use detectors sensitive to radioactivity; etc. The sonde housing may be constructed of steel and/or fiberglass.

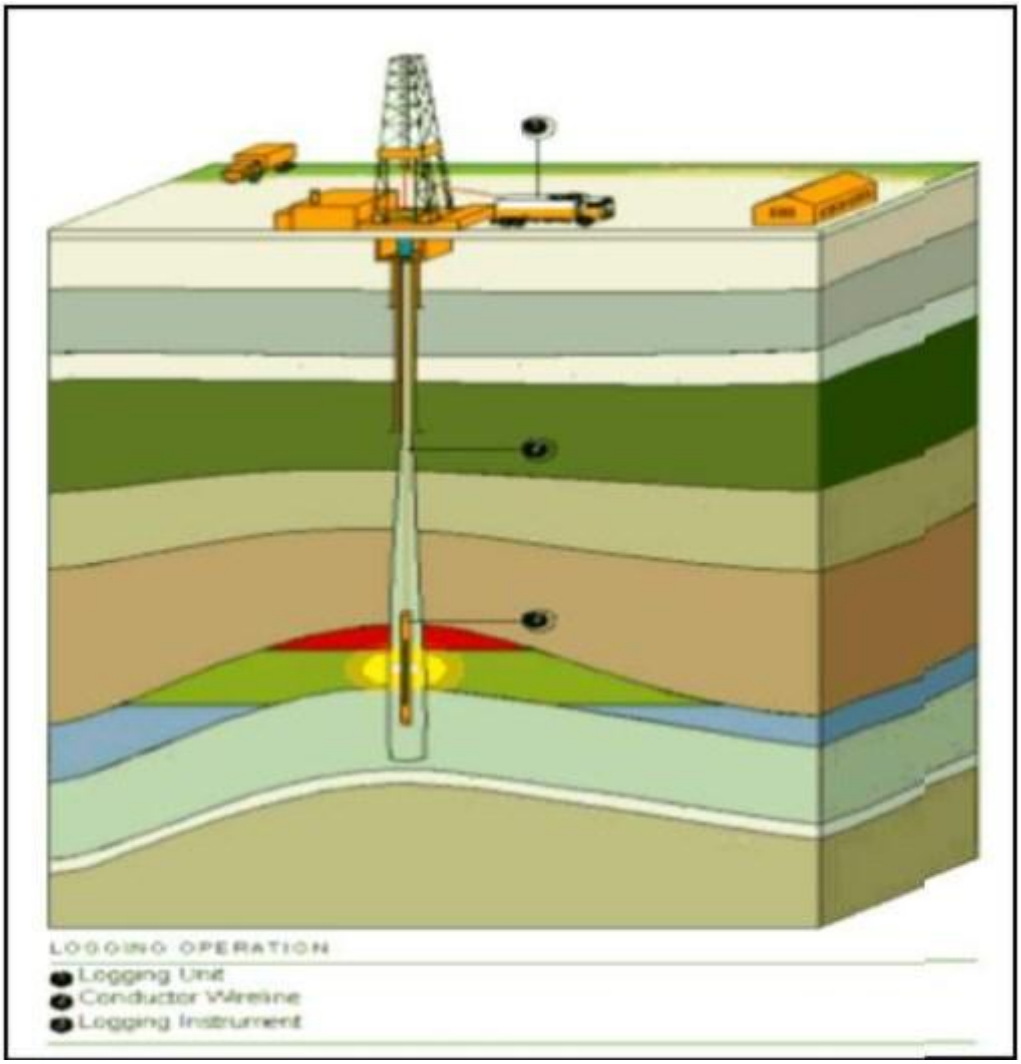

Figure 4.1: Diagram showing wire-line logging in progress

The other component of the downhole tool is the cartridge. The cartridge contains the electronics that power the sensors, process the resulting measurement signals, and transmit the signals up the cable to the truck. The cartridge may be a separate component screwed to the sonde to form the total tool, or it may be combined with the sensors into a single tool. That depends, of course,

upon how much space the sensors and electronics require and the sensor requirements. The cartridge housing is usually made of steel.

Today, most logging tools are readily combinable. In other words, the sondes and cartridges of several tools can be connected to form one tool and thereby make many measurements and logs on a single descent into and ascent from the borehole. The downhole tool (or tools) is attached to an electrical cable that is used to lower the tool into and remove from the well. Most cable used in open hole logging today contains seven insulated copper conductors. New cable developments include a fiber optics conductor in the center of six copper conductors. The cable is wrapped with a steel armor to give it the strength to support the tool weight and provide some strength to pull on the tool in case it becomes stuck in the borehole. The cable and tools are run in and out of the borehole by means of a unit-mounted winch. Well depths are measured with a calibrated measuring wheel system. Logs are normally recorded during the ascent from the well to assure a taunt cable and better depth control.

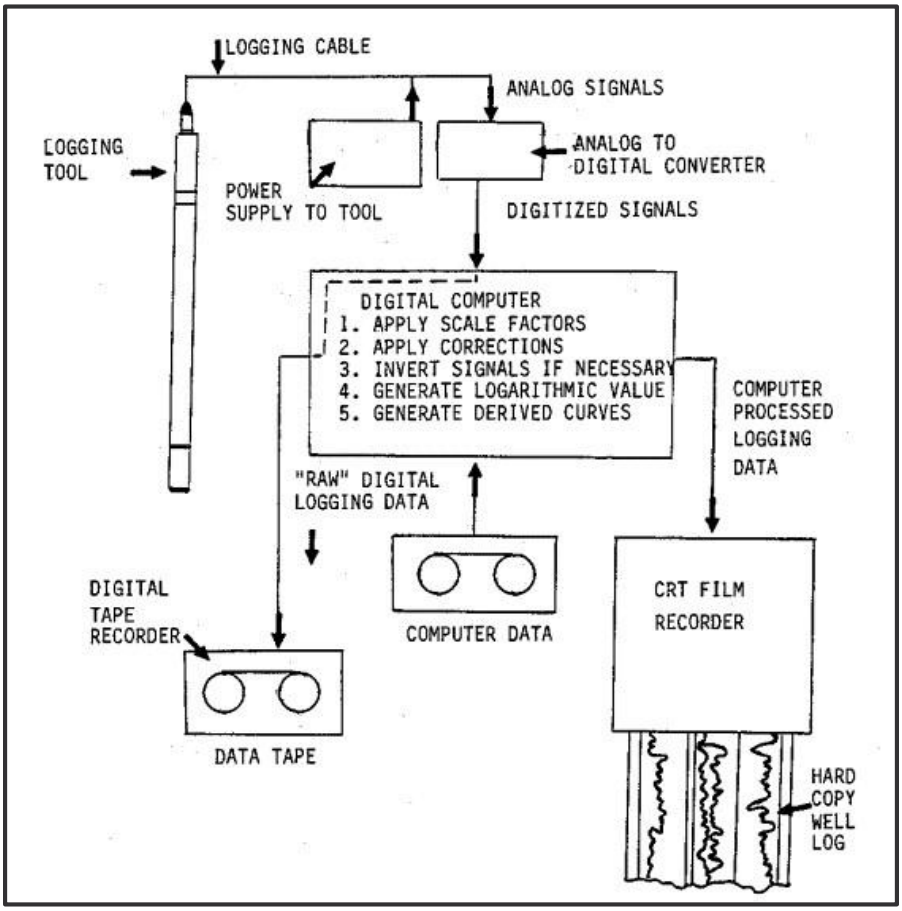

Figure 4.2: Diagram showing wire-line Logging procedure

Signal transmission over the cable may be in analog or digital form, modern trends favor digital. The cable is also used to transmit the electrical power from the surface to the downhole tools. The surface instrumentation provides the electrical power to the downhole tools.

More importantly, the surface instrumentation receives the signals from the downhole tools, processes and/or analyzes those signals, and responds accordingly. The desired signals are output to magnetic tape in digital form and to a cathode-ray tube and photographic film in analytical form. The photographic film is processed on the unit, and paper prints are made from the film. This continuous recording of the downhole measurement signals is referred to as the log (Shown in figure 4.3).

4.3 Representation of well logs

Well Logging is used as a relatively inexpensive method to obtain petrophysical properties down hole. Measurement tools are conveyed downhole using either wire-line or LWD method.

An example of wire-line logs is shown in figure 4.3. The first “track”, shows the natural gamma radiation level of the rock. The gamma radiation level “log” shows increasing radiation to the right and decreasing radiation to the left. The rocks emitting less radiation have more yellow shading. The detector is very sensitive and the amount of radiation is very low. In clastic rock formations, rocks that have smaller amounts of radiation are more likely to be coarser grained and have more pore space, rocks with higher amounts of radiation are more likely to have finer grains and less pore space (Poupon et.al, 1970).

The second track over in the plot records the depth below the reference point which is usually the Kelly bush or rotary table in feet, so these rocks are 11,900 feet below the surface of earth.

In the third track, the electrical resistivity of the rock is presented. The water in this rock is salty and the salt in the water causes the water to be electrically conductive such that lower resistivity is caused by increasing water saturation and decreasing hydrocarbon saturation (Brown, 1986).

The fourth track, shows the computed water saturation, both as “total” water (including the water bound to the rock) in magenta and the “effective water” or water that is free to flow in black. Both quantities are given as a fraction of the total pore space.

The fifth track shows the fraction of the total rock that is pore space, filled with fluids. The display of the pore space is divided into green for oil and blue for movable water. The black line shows the fraction of the pore space which contains either water or oil that can move, or be "produced." In addition to what is included in black line, the magenta line includes the water that is permanently bound to the rock.

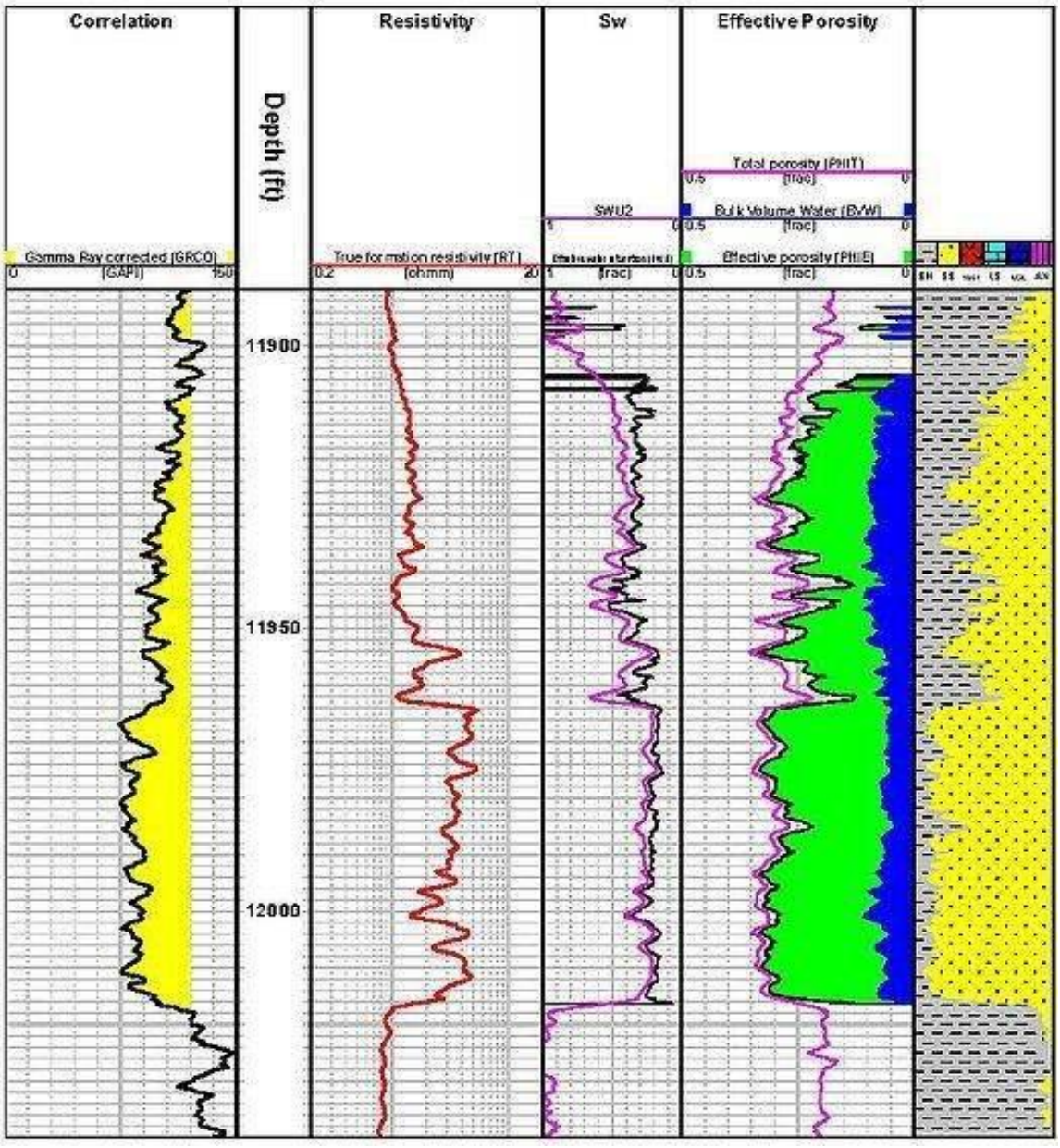

Figure 4.3: Representation of well log

The last track is a representation of the solid portion of the rock. The yellow pattern represents the fraction of the rock (excluding fluids) that is composed of coarser grained sandstone. The

gray pattern represents the fraction of rock that is composed of finer grained “shale.” The sandstone is the part of the rock that contains the producible hydrocarbons and water.

4.4 Borehole environment

When the borehole drilled in a formation, the rock and the fluid in the rock undergoes the alteration in the vicinity of the borehole. All logging measurements are then effected by the borehole and the altered rock around it. These include:

1. Borehole condition
2. Invasion of the drilling fluid

4.4.1 Bore hole condition

Borehole conditions effecting the log measurements are:

a. Bore hole size

b. Drilling mud

c. Mud Cake d.

Mud filtrate

a. Borehole size

The normal size of the hole is taken to be the outside diameter measurement of the drilling or coring bit used to make the hole. Borehole is seldom perfectly circular; it is usually elliptical due to removal of more material in the direction of least subsurface stress.

b. Drilling mud

The main functions of the drilling mud are:

1. To carry rock cuttings to the surface
2. To prevent the uncontrolled escape of the formation fluids
3. To cool and lubricate the drill string and the bit
4. To suspend cuttings during times when circulation is stopped.

The hydrocarbon static pressure of the drilling fluid must be greater than the formation fluid pressure, this overbalance system allows the entry of the mud fluid into the pore spaces of the

permeable rock, and this entry of the mud is called the invasion of the drilling mud that affects the logging tool response.

c. Mud cake

Mud Cake is formed within the few minutes of the formation being penetrated. Clay particles are caked against the size of the borehole and effectively seal off the formation to further invasion. Invasion takes place continuously as the hole is deepened because the mud cake becomes damaged or is removed by drilling, logging or testing tool. Thick mud cake affects the readings of the shallow investigation of the logging tool. The presence of mud cake is usually a good indication of the permeable rock.

d. Mud filtrate

Fluid which enters permeable zone from the mud is called the mud filtrate. The filtrate is usually the water in the normal mud system and its resistivity is dependent on the original salinity of the mud system. All logging tools are affected to some degree by the mud filtrate.

4.4.2 Invasion of the drilling fluid

Drilling fluid invasion is a process that occurs in a well being drilled with higher well bore pressure than formation pressure. The liquid component of the drilling fluid (known as the "mud filtrate") continues to "invade" the porous and permeable formation until the solids present in the mud, commonly bentonite, clog enough pores to form a mud cake capable of preventing further invasion. If invasion is severe enough, and reservoir pressures are unable to force the fluid and associated particles out entirely when the well starts producing, the amount of oil and gas a well can produce can be permanently reduced. This is especially true when a process called phase trapping.

This is when a fluid enters a formation that is below its irreducible saturation of that fluid. Once the fluid is present, it is held in place by capillary forces and usually cannot be removed. Invasion also has significant implications for well logging. In many cases the "depth of investigation" of a well logging tool is only a few inches (or even less for things like sonic logs), and it is quite possible that drilling fluid has invaded beyond this depth.

a. Depth of invasion

It is basically the distance from the borehole wall that the mud filtrate has penetrated into the formation. The depth of invasion affects whether a log measures the invaded zone, the undisturbed zone or part of each zone. The term is closely related to the diameter of invasion, the latter being twice the depth of invasion plus the borehole diameter. Depth of invasion is a more appropriate parameter for describing the response of pad and azimuthally focused measurements such as density and micro-resistivity logs.

The term is well-defined in the case of a step profile of invasion. In the case of an annulus or a transition zone, two depths must be defined, corresponding to the inner and outer limits of the annulus or transition zone. When the invasion model is not specified, the term usually refers to the outer limit of invasion. Depth of invasion depends upon several factors during logging like, filtration characteristics of the drilling mud and the differential pressure between the mud and the reservoir.

Invasion of the mud relates to the porosity, once the cake has started to built, its permeability becomes low relative to that of the average formation so that almost the entire pressure differential is across the mud cake and little is applied to the formation. The mud cake therefore controls the filtration rate. Depth of invasion will be minimum at higher porosity where plenty of the pore space available it is approximately inversely proportional to the porosity, other things being constant. Invasion depth will double as the porosity reduces from 36% to 9% etc.

b. Invasion profile

The process of invasion creates an invasion profile extending from the well bore into the formation. Three zones are recognized.

i. Flushed Zone ii. Transition Zone
iii. Undisturbed Zone

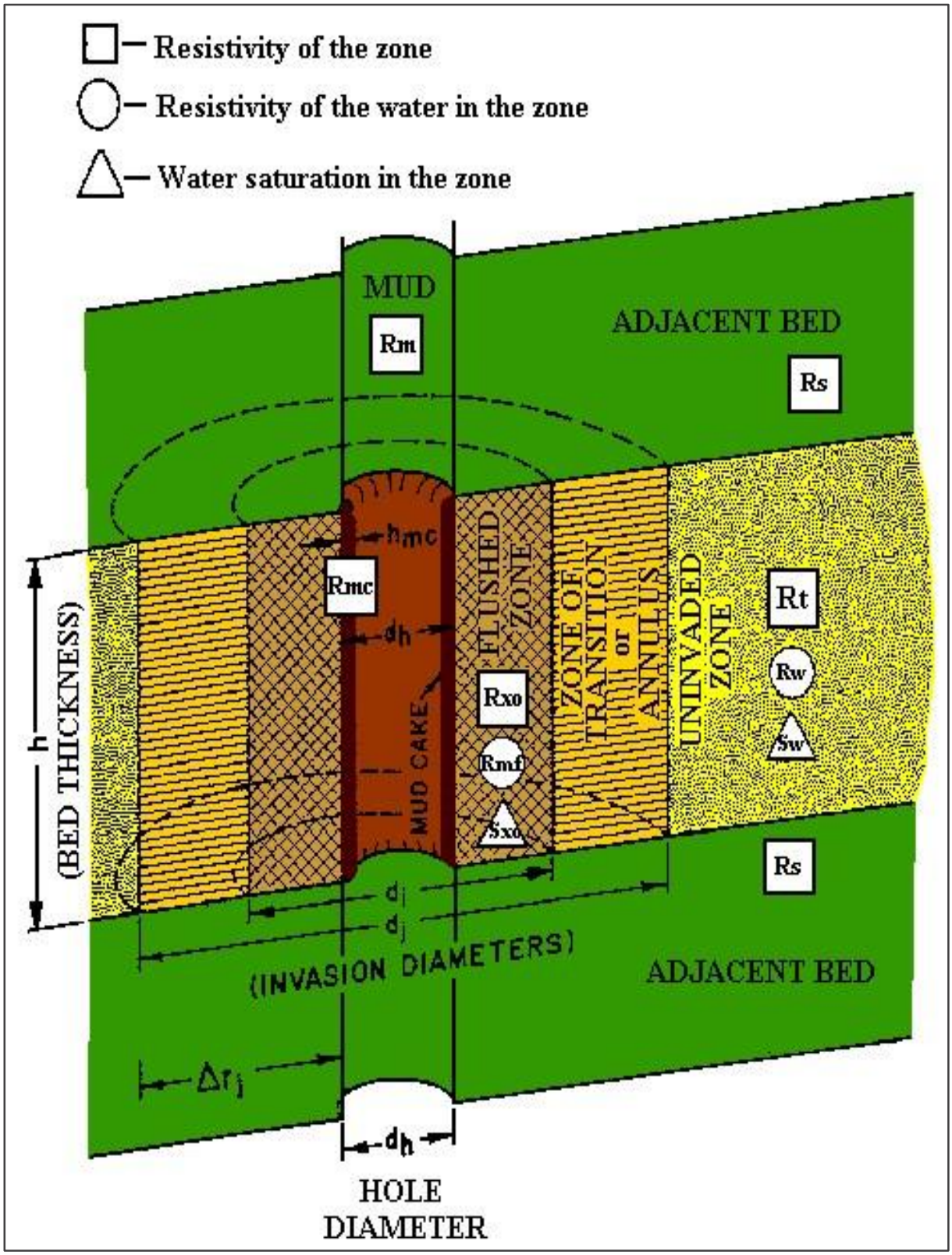

Figure 4.4: Borehole cross section showing its environment and the fluid invasion profile

i. Flushed zone

It is the volume close to the borehole wall in which all of the moveable fluids have been displaced by mud filtrate. The flushed zone contains filtrate and the remaining hydrocarbons, the percentage of the former being the flushed-zone water saturation, S_{xo}.

ii. Transition zone

It is the volume between the flushed zone and the undisturbed zone in which the mud filtrate has only partially displaced the moveable formation fluids.

iii. Undisturbed zone

It is the part of the formation that has not been affected by invasion.

c. Invasion resistivity profiles

The changes in water saturation combine with the changes in the fluid saturation and resistivity within the invaded zone create the invasion resistivity profile. The fluid distribution within the invaded zone of a porous and permeable formation can be represented by two idealized profiles:

i. Step profile
ii. Transition profile or Annulus profile

i. Step profile

With reference to invasion, an abrupt change from the flushed zone to the undisturbed zone, with no transition zone or annulus.

ii. Transition profile or annulus profile

It is a realistic profile in which the distribution of fluids in the invaded section beyond the flushed zone varies with increasing distance from the borehole.

CHAPTER # 5

Wireline Logging Tools

5.1 Introduction

The traditional wire line formation evaluation tool has been redesigned to provide a 'driller friendly' tool providing standard log readings. The new designs allows for more robust measurements with higher resolution to be logged at a much higher speed than was possible in the past. The new generation equipment is less than half the length and weight of the triple-combo equipment making setup and calibration of the tool much faster and safer.

5.2 Classification of logging tools

Since the development of wire-line logging tools for formation evaluation began in the 1920's, there have been a staggering number of logging tools produced. All of these having their own characteristics for measuring different parameters. Following is the table (table: 5.1) showing Information about logging modern logging tools and the physical parameters measured by these tools.

Measurement Type	Measuring Device	Measured Parameters
The Formation Resistivity	Laterolog type	Resistivity in invaded and uninvaded zones
	Induction type	Formation Resistivity in invaded and uninvaded zones
Flushed Zone Resistivity	MSFL type	Formation Resistivity in flushed zone
Lithology and Porosity	Neutron Log	Neutron formation porosity, Cased Hole Neutron Porosity
	Density Log	Density formation porosity
	Litho-Density	Formation density , porosity and PE (Photoelectric)
Porosity and Acoustic Logging	Standard BHC Sonic	Δtc and Sonic Porosity
	Digital Sonic	Δtc, Δts and Sonic Porosity
	Dipole Sonic	Δtc, Δts, Sonic Porosity and rock mechanics

	Borehole Acoustic Imaging	360 degree borehole image, fractures
Formation Dip	Dipmeter	Dip of formation, sedimentary features, fractures, and depositional environments.
	Formation Scanner	Borehole Image
Permeability	Magnetic Resonance	Magnetic Resonance Imaging, permeability, free water & irreducible water
Measurement of Natural Events	Spontaneous Potential (SP)	Sand-Shale differentiation and estimation of shaliness
	Gamma Ray (GR)	Clean zone –Shaly zone differentiation, Shale Volume from Gamma Ray (GR)
	Spectral Gamma-Ray	Clay Analysis (K,U Th concentrations)
	Temperature	Fractured zones, thief zones or water entrance
Borehole geometry	Caliper	Borehole diameter and geometry
Formation pressure, fluid	Formation Tester	Formation fluid sample, permeability and formation pressure

Table 5.1: Table showing information about logging tools and the physical parameters measured by these tools.

Broadly speaking these tools can be classified into three main categories:

1. Lithology logs 2.

Porosity logs 3.

Resistivity logs

5.2.1 Lithology logs

Two lithology logs are commonly used in formation evaluation, the Spontaneous Potential (SP) log and the Gamma Ray (GR) log. Both are recordings of naturally occurring phenomena in the formation.

These logs are designed to:

a. Identify permeable formations
b. Determine boundaries between permeable and non-permeable formations
c. Provide lithology data for correlation with other wells
d. Provide a degree of certainty for quantifying the formation lithology

5.2.2 Porosity logs

Conventional logging techniques for measuring porosity are the Density, Neutron and Sonic logs. All of these logs provide an indication of total porosity.

These logs are designed to:

a. Provide accurate lithologic and porosity determination
b. Provide data to distinguish between oil and gas
c. Provide porosity data for water saturation determination

5.2.3 Resistivity (Electrical) logs

Resistivity is one of the most useful physical properties measured in the borehole. The conventional resistivity logging techniques for measuring the resistivity of the formation are latero logging Induction logging and micro logging.

These logs are designed to:

a. Measure the formation resistivity measurements, in conjunction with porosity and water resistivity, are used to obtain values of water saturation and consequently, hydrocarbon saturation.
b. They are also used in conjunction with lithology logs to identify hydrocarbon bearing intervals and to estimate the net pay thickness.

5.3 The GR log

The GR log is a measurement of the natural radioactivity of the formations. This is also known as the shale indicator as it can be very useful for identifying shale beds.

5.3.1 Principle

In sedimentary formations, the log normally reflects the shale content of the formations. This is because the radioactive elements tend to concentrate in clays and shales. Clean formations usually have a very low level of radioactivity, unless radioactive contaminant such as volcanic ash or granite wash is present or the formation waters contain dissolved radioactive salts.

The GR log can be recorded in cased wells, which makes it very useful as a correlation curve in completion and work over operations. It is frequently used to complement the SP log and as a substitute for the SP curve in wells drilled with salt mud, air, or oil-based muds. In each case, it is useful for location of shales and non shaly beds and, most importantly, for general correlation.

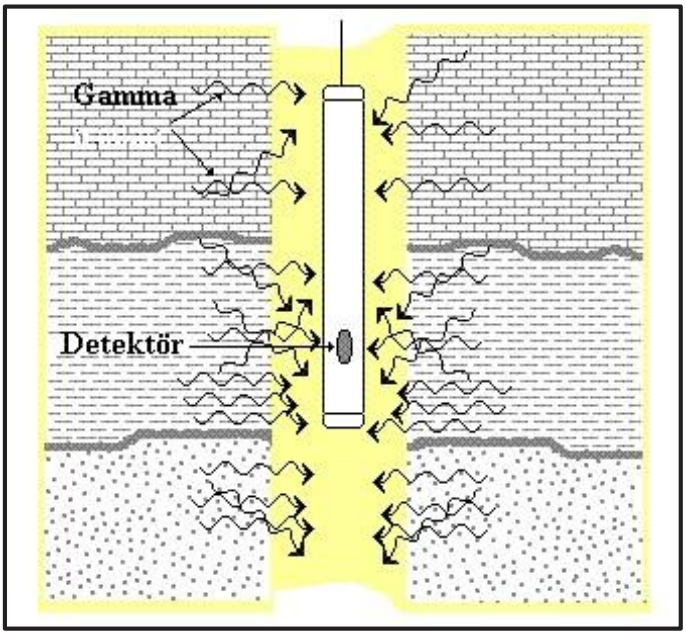

Figure 5.1: Diagram showing principle of GR log

5.3.2 Compton scattering and photoelectric effect

Gamma rays are burst of high energy electromagnetic waves that are emitted spontaneously by some radioactive elements. Nearly all the gamma radiation encountered in the earth is emitted by the radioactive potassium isotope of atomic weight 40 (K^{40}) and by the radioactive elements of

the uranium and thorium series. Each of these elements emits gamma rays; the number and energies of which are distinctive of each element. Fig. 3-8 shows the energies of the emitted gamma rays: potassium (K^{40}) emits gamma rays of a single energy at 1.46 MeV, whereas the uranium and thorium series emit gamma rays of various energies.

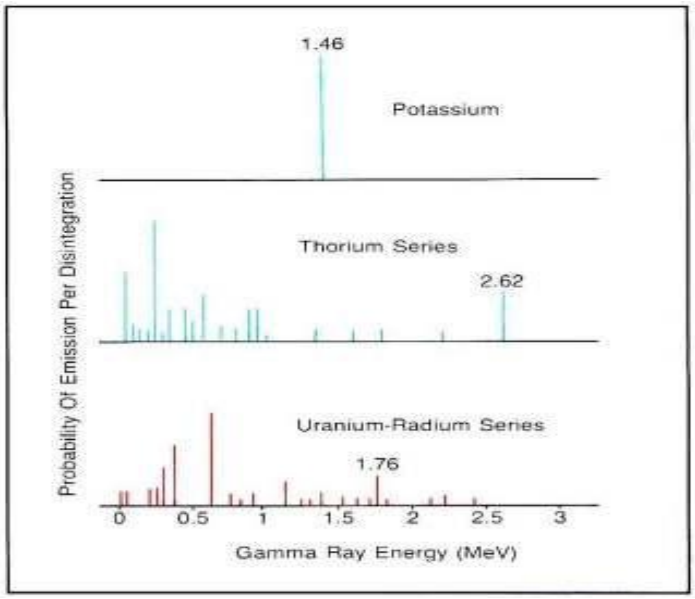

Figure 5.2: Gamma Ray emission spectra of radioactive minerals

In passing through matters, gamma ray experience successive Compton-scattering collisions with atoms of the formation material, losing energy with each collision. After the gamma ray has lost enough energy, it is absorbed, by the means of photo electric effect by the atom of the formation. The rate of absorption varies with formation density. The Gamma Ray log response after appropriate corrections for borehole etc. is proportional to the weight concentrations of the radioactive material in the formation.

$$GR = \frac{\Sigma \rho_i V_i A_i}{\rho_b}$$

Where,

ρ_i = Densities of the radioactive material

V_i = Bulk Volume Factors of the minerals

A_i = Proportionality factors corresponding to the radioactive of the minerals

ρ_b = Bulk Density of the Formation

5.3.3 Depth of the investigation

The depth of the investigation of the GR Log is about 1 foot.

5.3.4 Equipment

The GR sonde contains a detector to measure the gamma radiation originating in the volume of formation near the sonde. Scintillation counters are now generally used for this measurement. They are much more efficient than the Geiger-Mueller counters used in the past. Because of its higher efficiency, a scintillation counter need only be a few inches in length; therefore, good formation detail is obtained. The GR log may be, and usually is, run in combination with most other logging tools and cased hole production services.

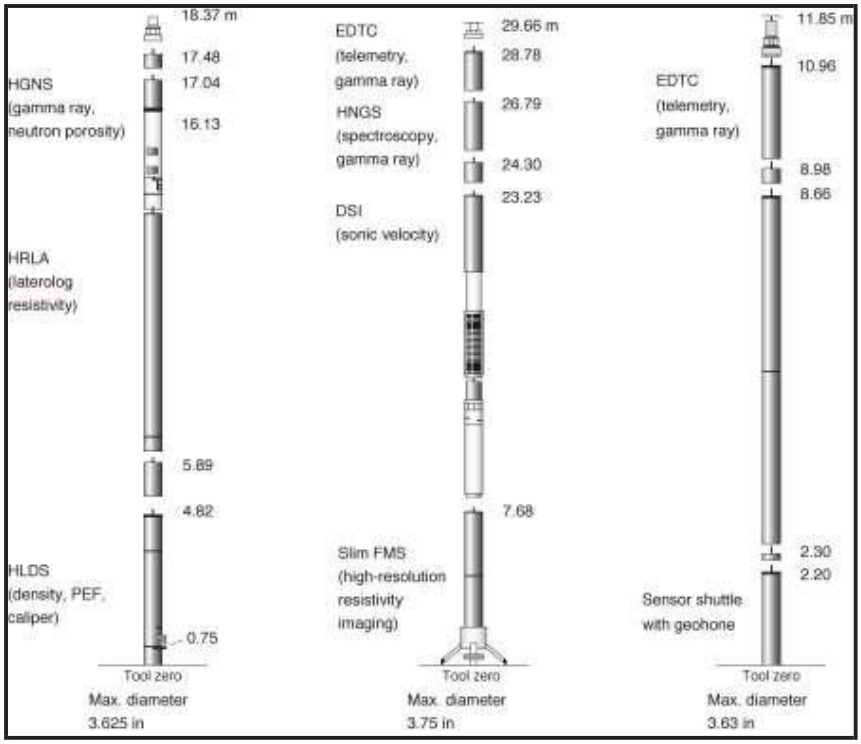

Figure 5.3: Diagram showing GR tool

5.3.5 Calibration

The primary calibration standard for GR tools is the API test facility in Houston. A field calibration standard is used to normalize each tool to the API standard and the logs are calibrated in API units. The radio activities in sedimentary formations generally range from a few API units in anhydrite or salt to 200 or more in shales. The GR log reflects the proportion of shale and, in

many regions, can be used quantitatively as a shale indicator. It is also used for the detection and evaluation of radioactive minerals, such as potash or uranium ore.

5.3.6 Log presentation

The gamma ray log, like other types of well logging, is done by lowering an instrument down the hole and recording gamma radiation at each depth. In the United States, the device most commonly records measurements at 1/2-foot intervals. A standard gamma ray curve is recorded & presented in track 1, it is in the API units. Gamma logs are affected by the diameter of the borehole and the properties of the fluid filling the borehole, but because gamma logs are most often used in a qualitative way, corrections are usually not necessary.

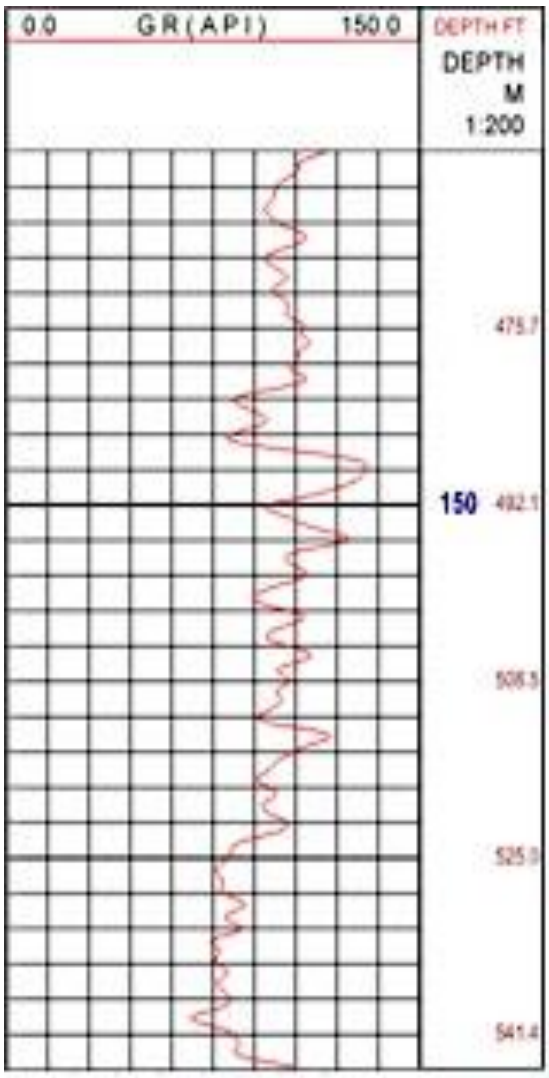

Figure 5.4: Diagram showing presentation of GR log

5.3.7 Applications

1. Gamma Ray Log is used for defining the shale beds.
2. Gamma Ray Log is used in non conductive muds, empty or air drilled holes, cased holes.
3. Gamma Ray Log is the quantitative indicator of the shale.
4. It is used for the detection & evaluation of the radioactive minerals (K, U)
5. It is also used for the detection of coal, halite, anhydrite and gypsum.
6. Gamma ray Log is applicable when $R_{mf} = R_w$

5.4 The Natural Gamma Ray Spectrometry log

Like the GR log, the NGS Natural Gamma ray Spectrometry log measures the natural radioactivity of the formations. Unlike the GR log, which measures only the total radioactivity, this log measures both the number of gamma rays and the energy level of each and permits the determination of the concentrations of radioactive potassium, thorium, and uranium in the formation rocks.

5.4.1 Measurement principle

The NGS Tool use a NaI Scintillation Detector contained in the pressure housing & it is in the skid mounted shape. Because of the interaction & the response of the NaI scintillation detector. The original spectrum is degraded to smeared spectra. The high energy part of the detected spectrum is divided into three energy windows Wl, W2, W3. Each covering a characteristic peak of the three radioactive series.

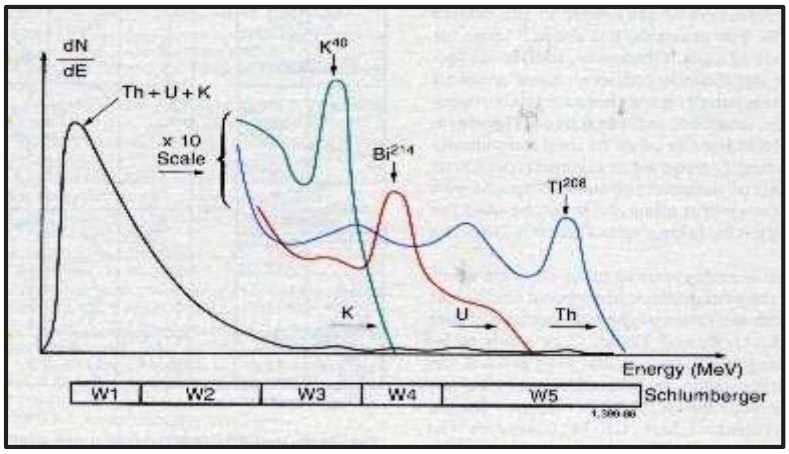

Figure 5.5: Spectral breakdown of total GR into its three major components.

Knowing the response of the tool and the number of counts in each window, it is possible to determine the amounts of thorium 232, uranium 238, and potassium 40 in the formation. By including the contribution from the high count rate, low energy part of the spectrum (Windows W4 and W5), these high statistical variations in the high-energy windows can be reduced by a factor of 1.5 to 2.

5.4.2 Log presentation

The NGS log provides a recording of the amount of potassium, thorium, and uranium in the formation. These are usually presented in Tracks 2 and 3 of the log (figure 5.6). The thorium and uranium concentrations are presented in part per million (ppm) and the potassium concentration in percent (%).

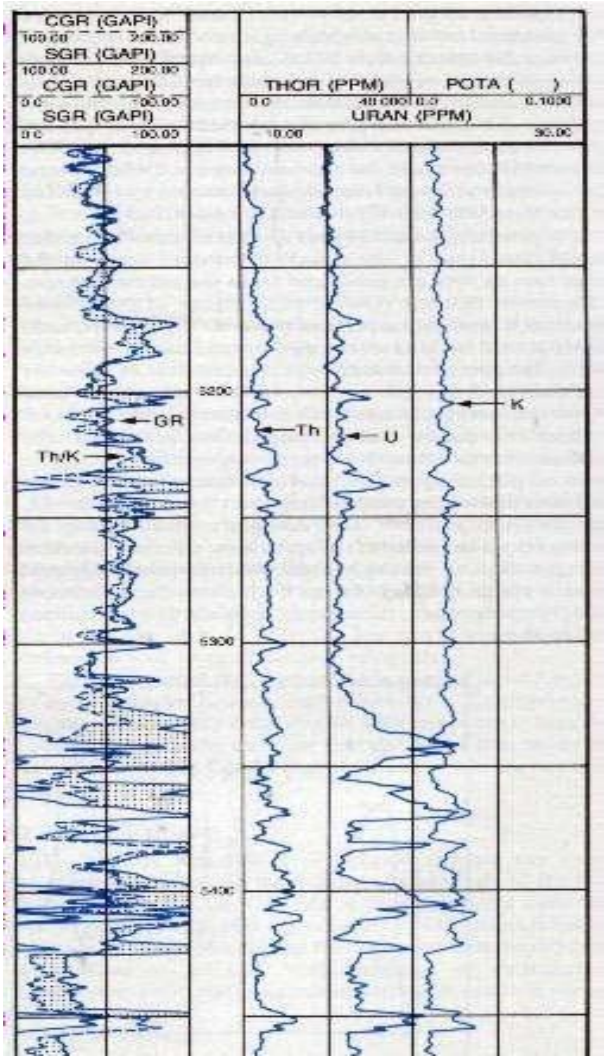

Figure 5.6: Diagram showing presentation of NGS log

5.4.3 Applications

1. It can be used to detect & evaluate the radioactive minerals.
2. It can be used to identify types of clay & to calculate clay volumes which further tell us the depositional environment, digenetic history, the petrophysical characteristics of the rocks.
3. In less complex mixtures it is used to identify minerals with greater certainty and volume to be calculated with greater accuracy.

5.5 Spontaneous Potential log

It is a log of the natural difference in electrical potential, in millivolts, between an electrode in the borehole and a fixed reference electrode on the surface. The most useful component of this difference is the electrochemical potential since it can cause a significant deflection opposite permeable beds. The magnitude of the deflection depends mainly on the salinity contrast between drilling mud and formation water, and the clay content of the permeable bed. The spontaneous potential (SP) log is therefore used to detect permeable beds and to estimate formation water salinity and formation clay content. The SP log cannot be recorded in nonconductive mud.

5.5.1 Principle

The SP curve is a recording versus depth of the difference between the electrical potential of a movable electrode in the borehole and the electrical potential of a fixed surface electrode.

Opposite shales the SP curve usually defines a more or less straight line on the log, called the shale baseline. Opposite permeable formations, the curve shows excursions from the shale baseline; in thick beds, these excursions (deflections) tend to reach an essentially constant deflection defining a sand line. The deflection may be either to the left (negative) or to the right (positive), depending primarily on the relative salinities-of the formation water and of the mud filtrate. If the formation water salinity is greater than the mud filtrate salinity, the deflection is to the left. For the reversed salinity contrast, the deflection is to the right. It is measured in milli volts (mV).

5.5.2 Origin of SP

The deflection of SP curve results from electric currents flowing in the mud in the borehole. These SP currents are caused by electromotive forces in the formations, which are of electrochemical and electrokinetic origins.

1. Electrochemical potential

a) Shale or membrane potential

Shale acts as ion selective membrane. It allows the cations only due to movement of ions the electromotive force is generated.

b) Liquid junction potential

The current flowing across the junction between the solutions of different salinity is produced by an electromagnetic force called Liquid junction potential. The magnitude of the liquid junction potential is only about the membrane potential.

2. Electro-kinetic potential

In the borehole, an electro kinetic emf is produced by the flow of mud into the formations due to difference in pressure, when mud cake is formed than no more electro kinetic potential is produced.

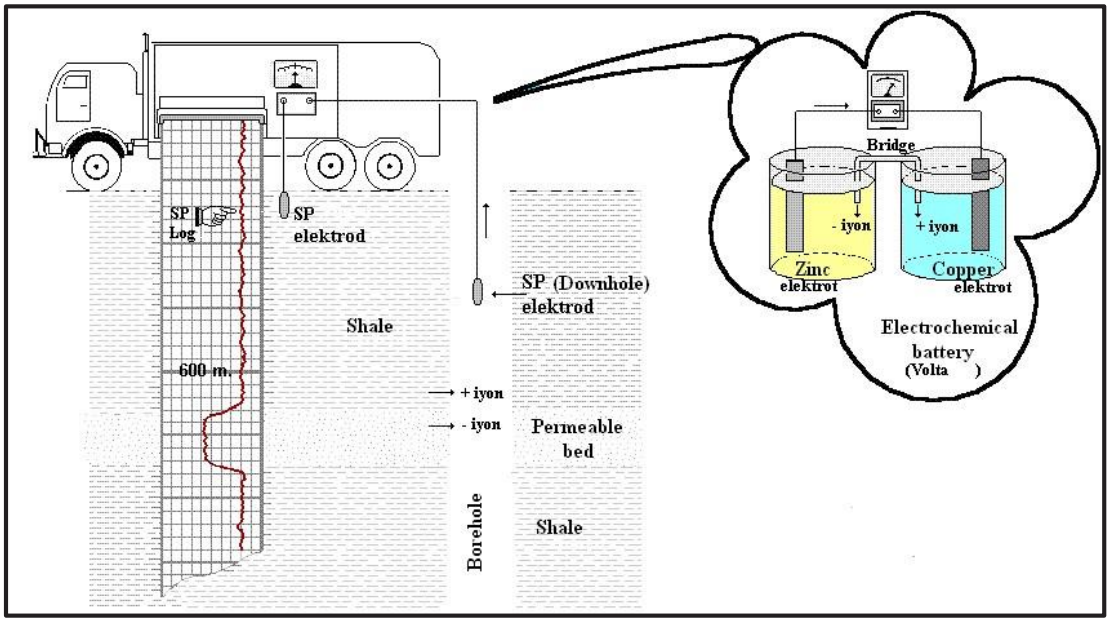

Figure 5.7: Diagram showing SP logging principle

5.5.3 Determination of SP from SP log

Total track of potential on sp log is 200 mV. Each division is of 20 mV. Sometimes it depends on the borehole conditions. First of all we mark the shale base line on the SP log. Then we draw the sand line at the maximum deflection of SP curve. The interval between the shale base line and sand base line is determined.

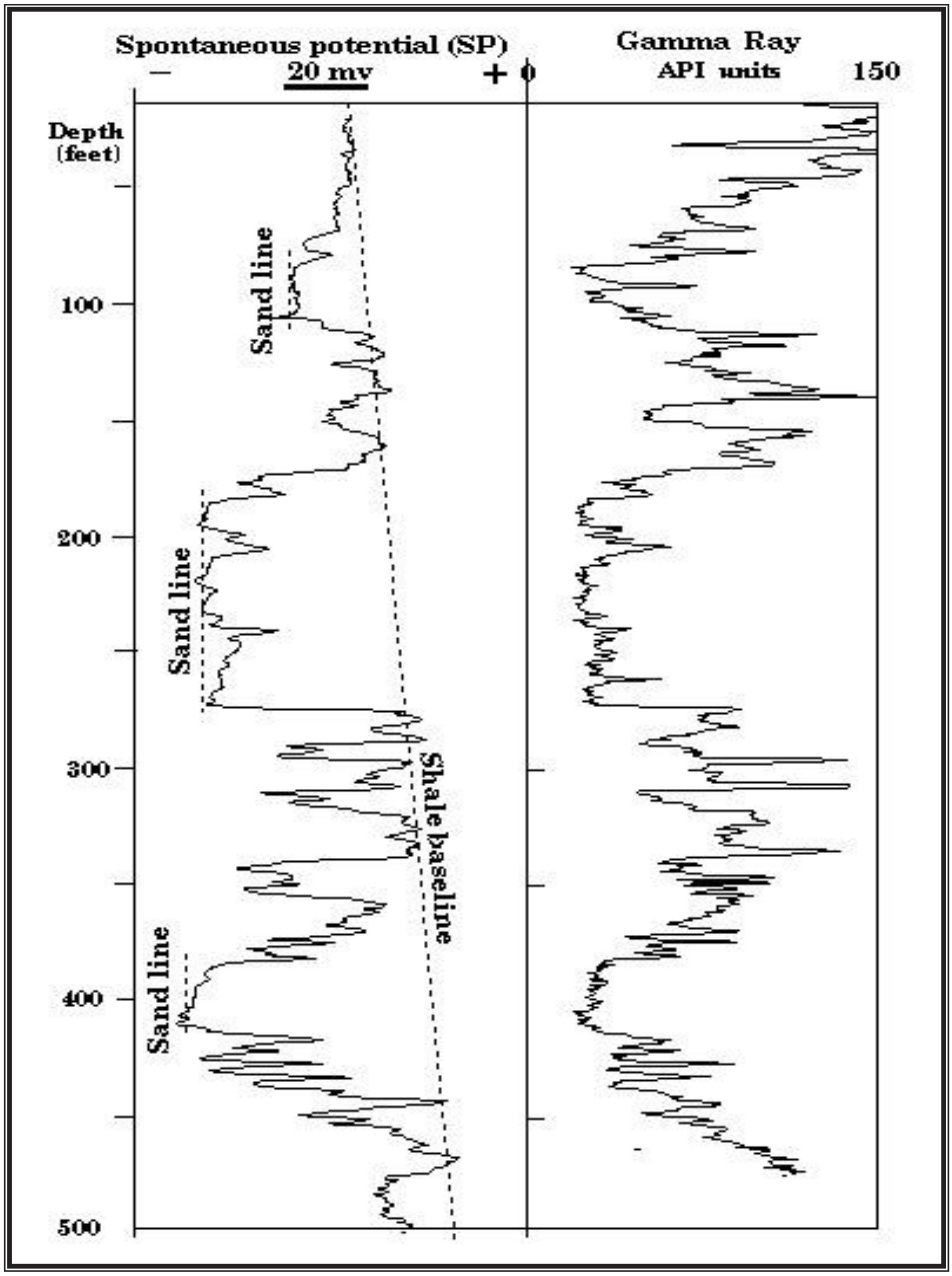

Figure 5.8: Diagram showing the trend of SP curve (Schlumberger log interpretation and applications by Schlumberger).

5.5.4 Factors affecting the shape and amplitude of SP curve

A number of factors affect the shape and amplitude of the SP including

1. Rmf/Rw
2. Bed thickness
3. Bed resistivity
4. Bore hole diameter
5. Invasion
6. Shaliness of porous and permeable bed

5.5.5 Tool calibration

No calibration is required for the SP electrodes, though electrical continuity and isolation checks are normally performed on the circuit prior to logging.

5.5.6 Log presentation

SP is presented in track 1 by a thin continuous line. SP is measured in mV (millivolts) and although there is no absolute scale, a relative scale of 10 mV per small division and usually -80 to 20 mV across track 1 is used.

5.5.7 Application of SP log

1. Differentiate shaly from non shaly formations
2. Detect permeable beds
3. Locate bed boundaries for correlation
4. Determine the value of formation water resistivity (R_w)

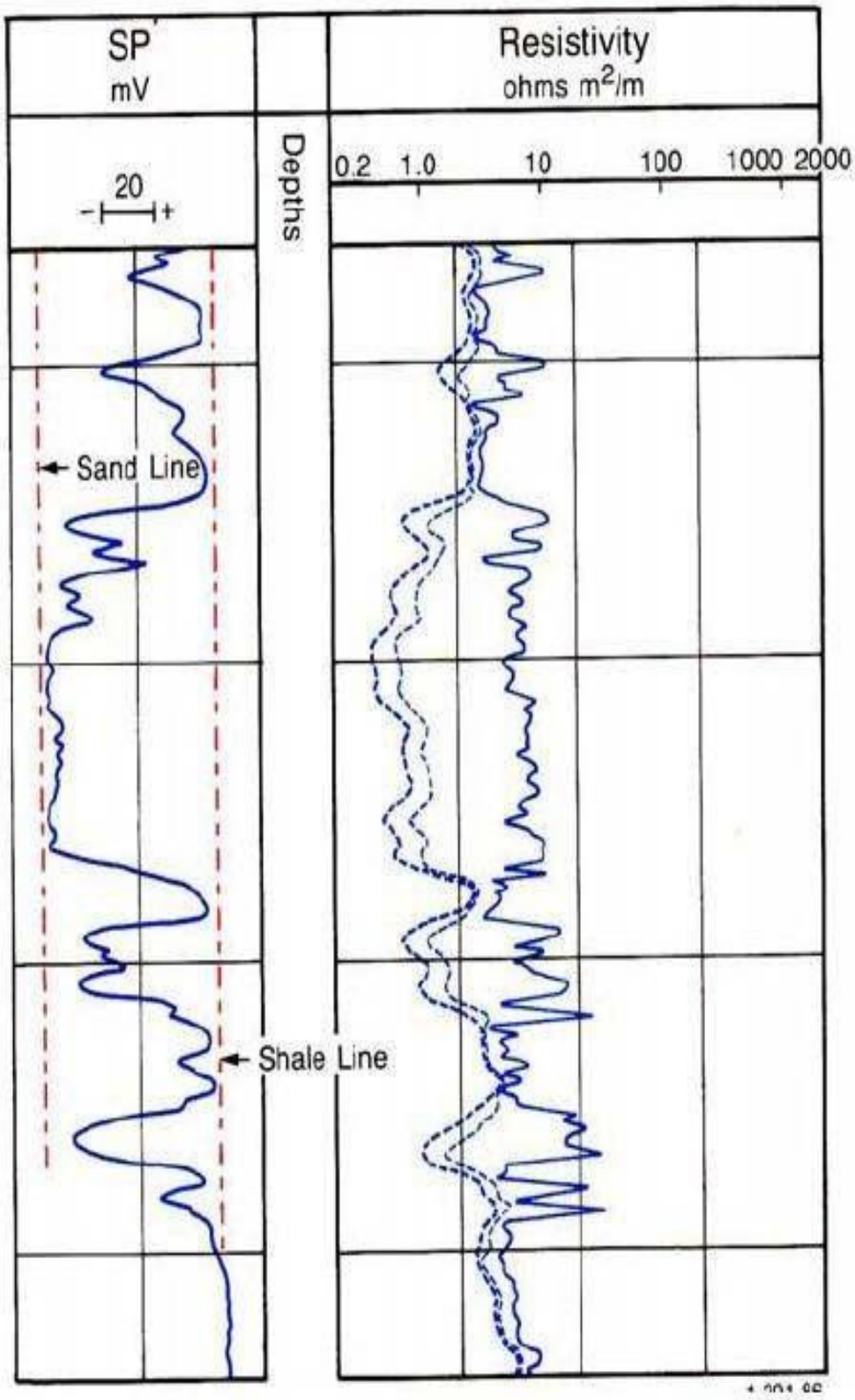

Figure5.9: Diagram showing presentation of an SP curve in a sand-shale sequence.

5.6 Sonic log

In its simplest form, a sonic tool consists of a transmitter that emits a sound-pulse and a receiver that picks up and records the pulse as it passes the receiver. The sonic log is simply a recording versus depth of the time, t, required for a sound wave to traverse 1 ft of formation known as the interval transit time, transit time, A_i or slowness, t is the reciprocal of the velocity of the sound wave. The interval transit time for a given formation depends upon its lithology and porosity. This dependence upon porosity, when the lithology is known, makes the sonic log very useful as a porosity log. Integrated sonic transit times are also helpful in interpreting seismic records. The sonic log can be run simultaneously with many other services.

MATERIAL	VELOCITY (ft/sec)	T (sec/ft)
Sandstone	18,000 – 19,000 21,000 –	55.5 – 51.0
Limestone	23,000 23,000 20,000	47.5 43.5
Dolomite	15,000 17,500 53,000	50.0 67.0
Anhydrite	54,000	57.0 189
Halite Casing		185
(Iron)		
Fresh Water Mud		
Salt Water Mud		

Table 5.2: Table showing velocities and interval transit times for common oil field materials.

5.6.1 Principle

The propagation of sound in a borehole is a complex phenomenon. It is governed by the mechanical properties of several separate acoustical domains. These include the formation, the borehole fluid column, and the logging tool itself. The sound emanated from the transmitter impinges on the borehole wal1. This establishes compressional and shear waves within the formation, surface waves along the borehole wall, and guided waves within the fluid column.

In the case of well logging, the borehole wall, formation bedding, borehole rugosity, and fractures can all represent significant acoustic discontinuities. Therefore, the phenomena of wave refraction, reflection, and conversion lead to the presence of many acoustic waves in the borehole when a sonic log is being run. It is not surprising, in view of these considerations, that many acoustic energy arrivals are seen by the receivers of a sonic logging tool. The more usual

energy arrivals are shown in the acoustic waveform displays of figure 5.10. These waveforms were recorded with an array of eight receivers located 8 to 11% ft from the transmitter.

The first arrival or compressional wave is one that has traveled from the transmitter to the formation as a fluid pressure wave, has been refracted at the borehole wall, has traveled within the formation at the compressional wave velocity of the formation, and has traveled back to the receiver as a fluid pressure wave.

The shear wave is one that has traveled from the transmitter to the formation as a fluid pressure wave, has traveled within the formation at the shear wave velocity of the formation, and has traveled back to the receiver as a fluid pressure wave.

The mud wave (not strongly evident in these wave trains) is one that has traveled directly from transmitter to receiver in the mud column at the compressional wave velocity of the borehole fluid.

The Stoneley wave is one of large amplitude that has traveled from transmitter to receiver with a velocity less than that of the compressional waves in the borehole fluid. The velocity of the Stoneley wave is dependent upon the frequency of the sound pulse, borehole diameter, formation shear velocity, densities of the formation and fluid, and fluid compressional wave velocity.

5.6.2 Equipment

There are currently three sonic tools in use: the BHC borehole compensated sonic tool, the LSS long-spaced sonic tool, and the Array-Sonic tool. Although the entire sonic waveform can now be recorded with any of these tools, only the Array-Sonic tool has been designed to provide full-waveform recording as a standard feature.

Nearly all BHC logs recorded in the past provide only a measurement of formation compressional interval transit time, t, accomplished through first motion detection at the receiver. In other words, the receiver triggers on the first arrival of compressional energy.

As shown in figure 5.11, the BHC system uses one transmitter above and one transmitter below two pairs of sonic receivers. This sonde substantially reduces the spurious effects of hole-size changes and errors from sonde tilt. When one of the transmitters is pulsed the time elapsed between detection of the first arrival at the two corresponding receivers is measured.

The speed of sound in the sonic sonde and in the drilling mud is less than that in the formations. Accordingly, the first arrivals of sound energy at the receivers correspond to sound travel paths in the formation near the borehole wall.

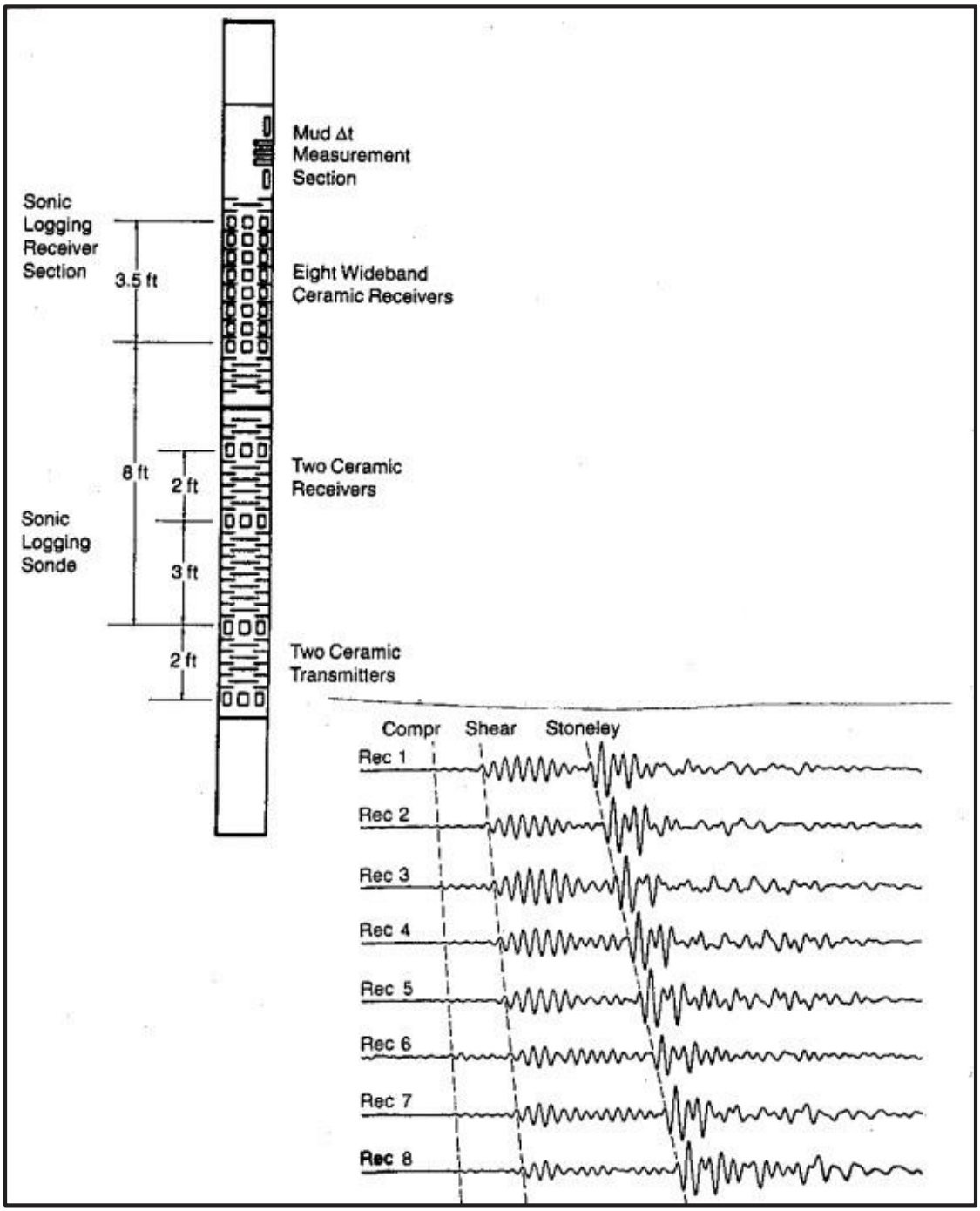

Figure 5.10: Multipurpose sonic sonde with waveforms from the eight-receiver Array-sonic tool

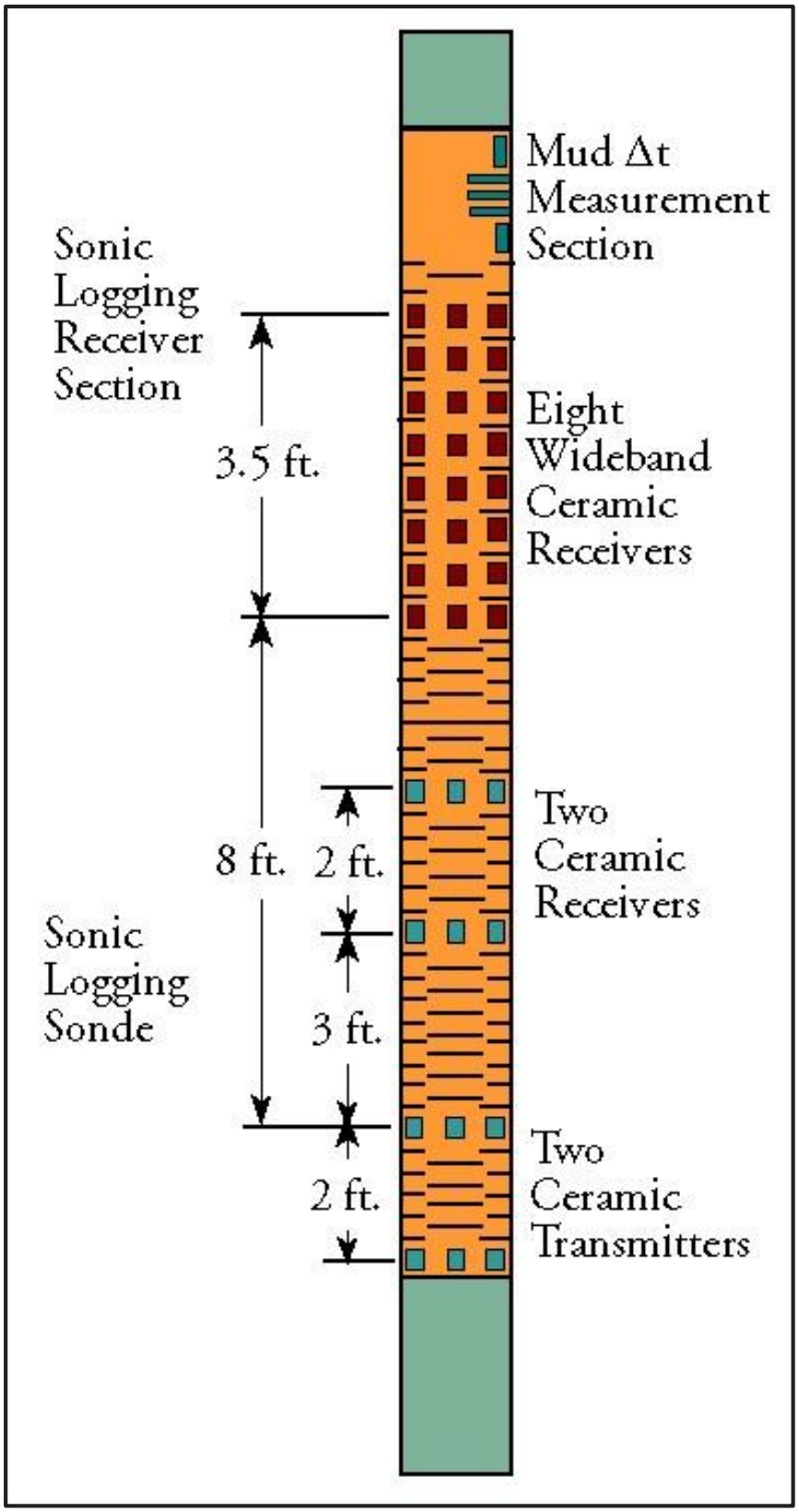

Figure 5.11: Diagram showing multipurpose Sonic sonde

5.6.3 Log presentation

Sonic velocities in common formation lithologies range from about 6,000 to 23,000 ft/sec. Presentation is usually 140-40 µs/ft (or 500-100 µs/m) across tracks 2 & 3.

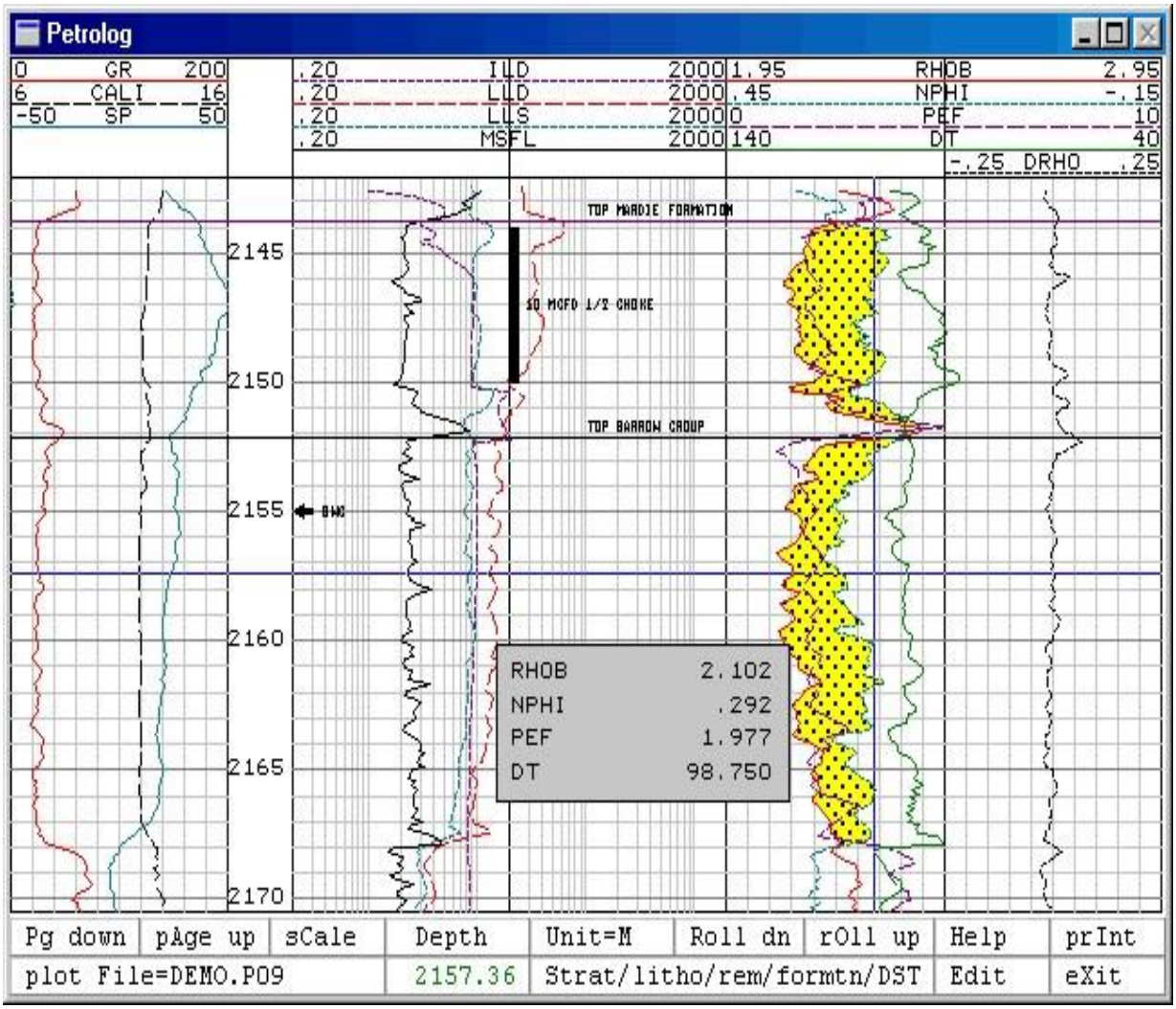

Figure 5.12: Typical sonic Log Presentation

5.6.4 Applications

1. Porosity determination
2. Lithology indicator
3. Seismic velocity calibration

5.7 Neutron log

Neutron logs, determine porosity by assuming that the reservoir pore spaces are filled with either water or oil and then measuring the amount of hydrogen atoms (neutrons) in the pores. The neutron log records counts of the collisions between neutrons that radiate from a tool source and hydrogen atoms within the rock of the borehole wall. So, the log is mainly a measure of hydrogen concentration (mostly contained by the pore fluids of the formation).

5.7.1 Basic concept

This log is a member of the porosity log family .Neutron Porosity tool use a radioactive source, such as Plutonium, Beryllium or Americium, to bombard the formation with high energy neutrally charged particles called neutrons (figure 5.13). When these high energy neutrons collide with the various atoms of both formation material and fluids, they begin to lose their energy, the amount of loss can be stated as

$$FEloss=4m/ (l+m)^2$$

Where,

FE = Represents the fractional energy loss

m = Mass of the struck nucleus in atomic mass unit

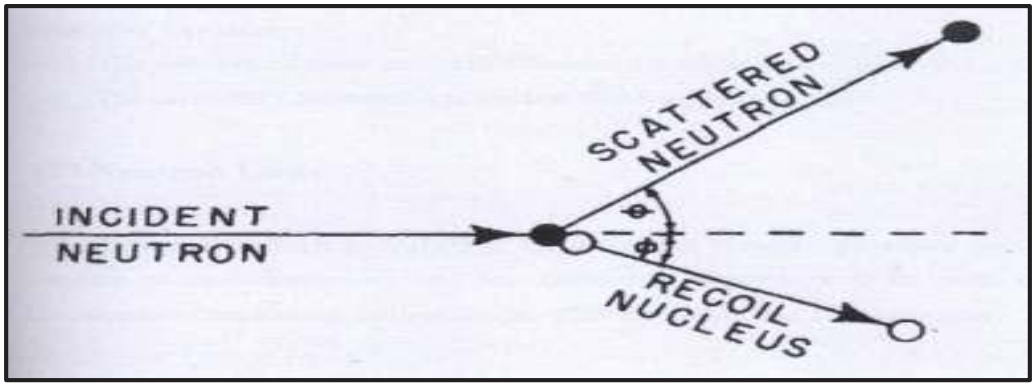

Figure 5.13: Diagram showing collision of neutrons

If the atom is small, the more energy the neutron will loss on collision. Collision depends on angle and mass. Energy is lost by neutrons due to collision. Hydrogen Index plays a vital role. Neutron have the same size as the Hydrogen atoms if there are more no of hydrogen atoms in the pore space, more neutrons collide, thereby losing their energy and become captured. The count

rate is consequently reduces. The pore space is usually filled with water, oil, gas. Water and oil have the same amount of hydrogen while gas has the lower hydrogen density. The neutron tool cannot differentiate between oil and water, but gas can be detected.

5.7.2 CNL tool

The CNL Compensated Neutron Log tool contains a radioactive source that bombards the formation with fast neutrons. These neutrons are slowed and then captured, primarily by hydrogen atoms in the formation. The slowed neutrons deflected back to the tool are counted by detectors. Since the tool responds primarily to the hydrogen content of the formation, the measurements are scaled in porosity units. Both epithermal (intermediate) neutrons and thermal (slow) neutrons can be measured depending on the detector design.

The CNT-H tool uses two thermal detectors for a borehole-compensated thermal neutron measurement. The CNT-G Dual-Energy Neutron Log (DNL) tool has two thermal and two epithermal detectors and provides separate energy measurements for gas detection and improved reservoir descriptions. The epithermal measurement can be made in air or gas-filled holes.

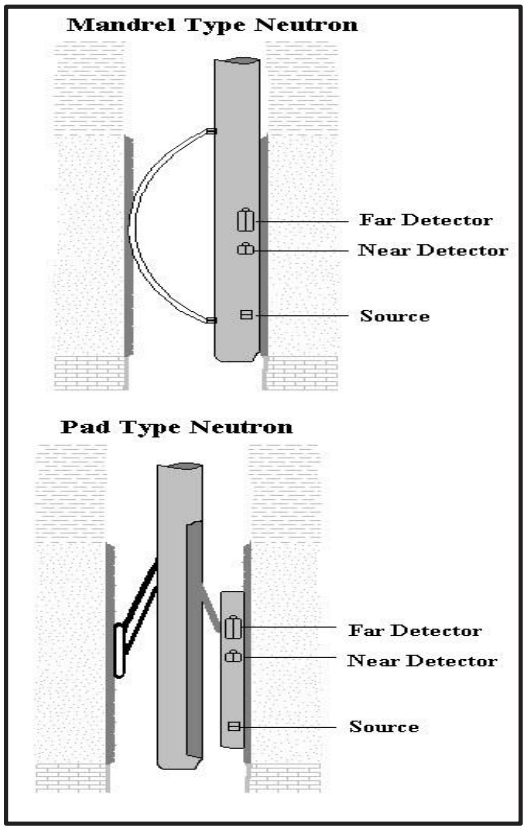

Fig 5.14: Diagram showing CNL tool

5.7.3 Calibration

Primary open hole calibration of the neutron instruments is carried out in fresh water filled pure laboratory formations. Fresh water also occupies the standard 7-7/8 in. borehole. No mud cake or instrument stand off from the borehole wall is present during calibration. Formations are at atmospheric pressure and 75 F. Standard formation lithologies include limestone, sandstone and dolomite. As a part of the initial calibration of instrument response, the laboratory limestone formation response is related to the API neutron calibration pit response.

5.7.4 Log presentation

The CNL is recorded in tracks 2 and 3 with a linear scale. The unit used is Neutron API unit. The caliper and the optional gamma ray log are recorded in track 1.

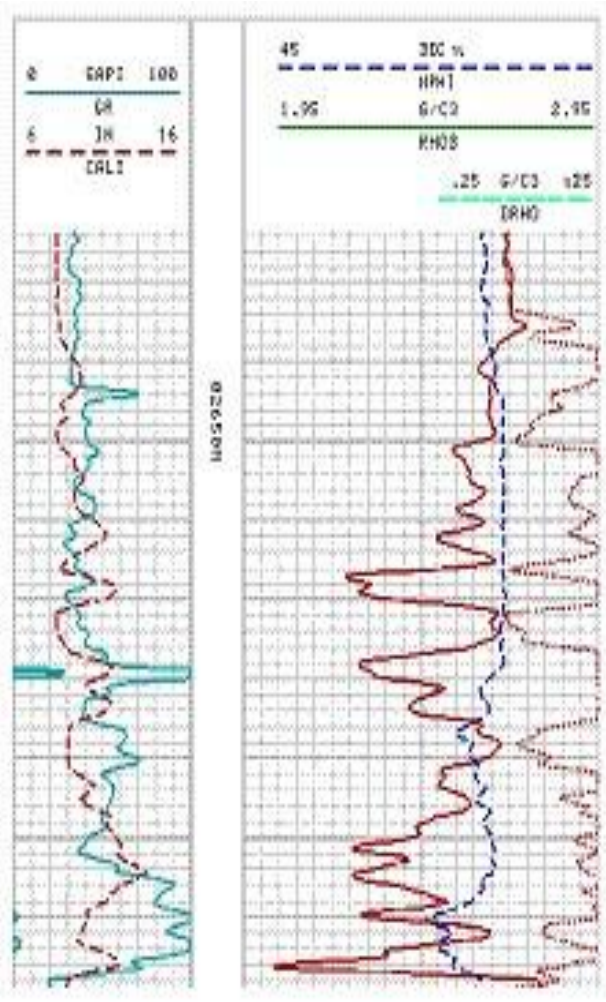

Figure 5.15: Diagram showing presentation od CNL log

5.7.5 Applications

1. Determine porosity
2. Identify lithology
3. Indicate shale and determine shale volume
4. Indicate gas and determine gas saturation

5.8 Density log

It is a continuous record of the variation in the density of the lithological column cut by the borehole. The density log is a measure of apparent density of the rock and is computed from the absorption of gamma rays emitted from a tool radioactive source by the formation. A Density Log when properly calibrated will provide reliable information about matrix bulk density. When density is known and a specific matrix is assumed then porosity of the matrix may be determined.

5.8.1 Bulk density

The term bulk density is applied to the overall or gross density of the unit volume of the rock. In the case of porous rock it includes the fluid density in the pore spaces as well as the grain density of the rock.

5.8.2 Neutron – bulk density cross-plot

Combination of data from a Neutron Porosity Log and Bulk Density log can be helpful in identification of lithology. A chart is used that has the known relationship between Neutron Porosity and Bulk Density for three matrices; Sandstone, Limestone, and Dolomite. It is possible to determine ratio of Sandstone/Limestone and obtain a more accurate porosity using the cross-plot chart. Results from the cross-plot chart should be correlated with known lithological information.

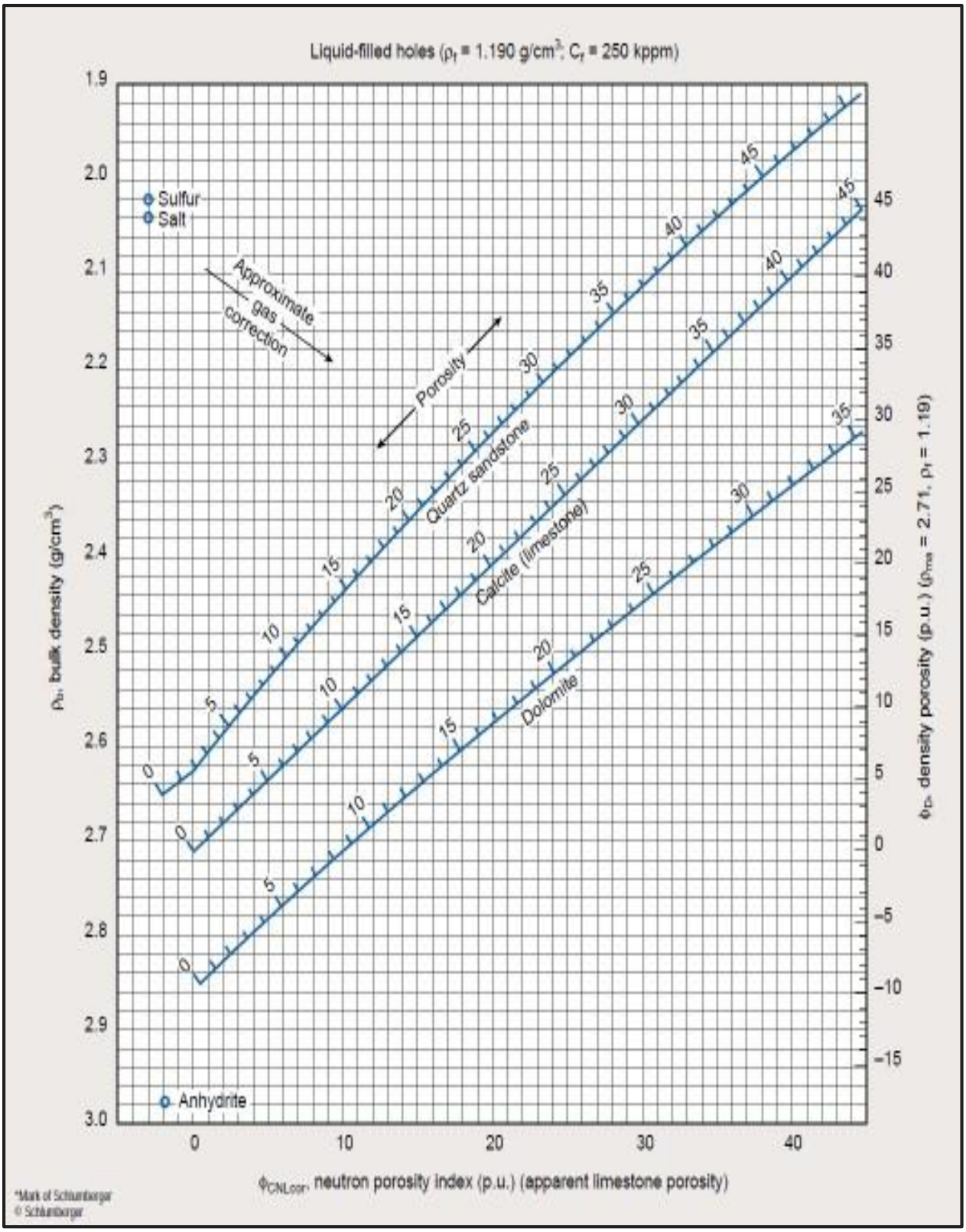

Figure 5.16: Diagram showing Neutron-density cross plot

5.8.3 Principle

A radioactive source, applied to the borehole wall in a shielded side wall skid, emits medium energy gamma rays into the formations. These gamma rays may be thought of high velocity particles that collide with the electrons of the formation. At each collision a gamma ray losses some, but not all of its energy to the electrons, and then continues with the diminished energy. This type of interaction is called Compton scattering.

5.8.4 Equipment

To minimize the influence of the mud column, the skid mounted source and detector are shielded. The openings of the shields are applied against the wall of the borehole by an eccentering arm. The force exerted by the arm, and the plow-shaped design of the skid, allow it to cut through soft mudcakes. Any mudcake or mud remaining between the tool and the formation is "seen" as part of the formation and must be accounted for.

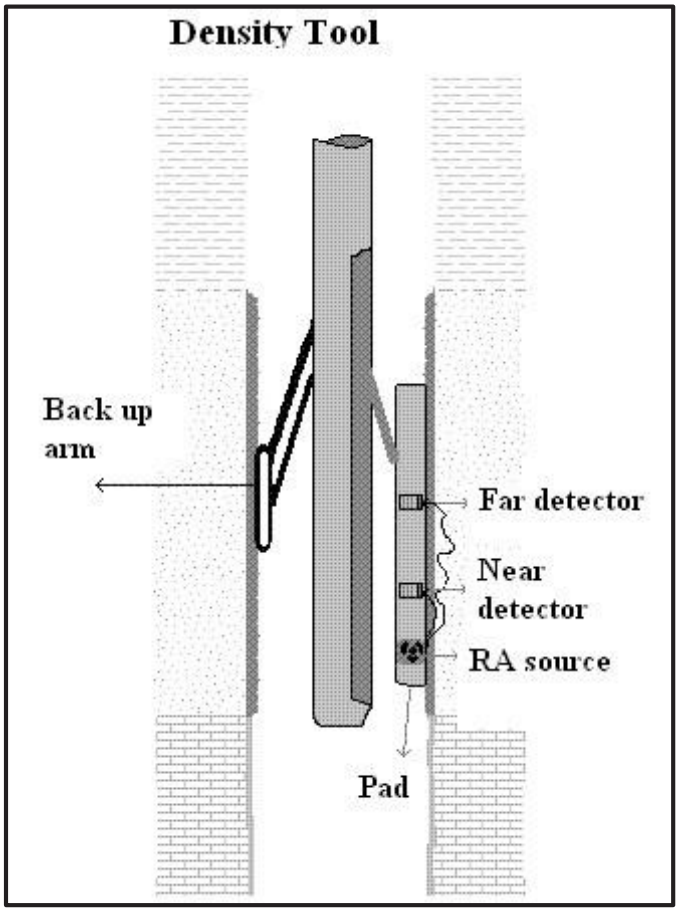

Figure 5.17: Diagram showing the Density tool

5.8.5 Log presentation

Log information is presented as shown in figure 5.18. The bulk density curve is recorded in Tracks 2 and 3 with a linear density scale in grams per cubic centimeter.

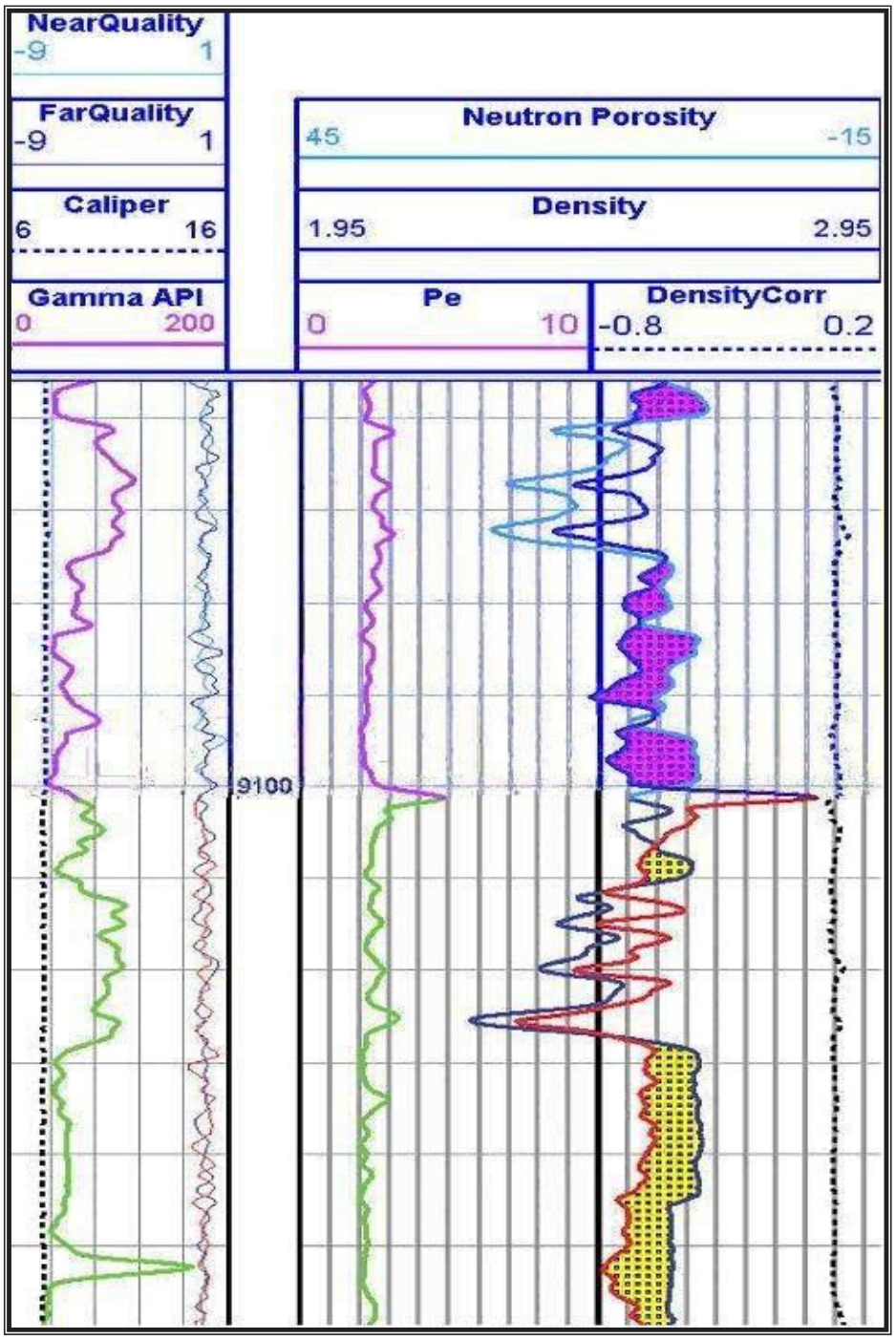

Figure 5.18: Diagram showing Density curve (Schlumberger log interpretation and applications by Schlumberger).

5.8.6 Applications

The Formation Density log has a number of applications:

1. Measuring density of the formation
2. Calculation of porosity
3. When combined with sonic travel times, the density data gives the acoustic impedance, which is important for calibration of seismic data
4. Identification of evaporites
5. Gas detection in reservoirs when used in combination with the neutron log
6. The Pe curve is a good lithology indicator. The influence of reservoir porosity and fluid content (including gas) on the Pe is minor.

5.9 Litho-Density log

The Litho-Density log is an improved and expanded version of the FDC log. In addition to the bulk density measurement, the tool also measures the photoelectric absorption index of the formation, P_e Photoelectric absorption can be related to lithology; whereas the e_b, measurement responds primarily to porosity and secondarily to rock matrix and pore fluid, the P_e, measurement responds primarily to rock matrix (lithology) and secondarily to porosity and pore fluid.

5.9.1 Principle and theory

At a finite distance from the source, such as the far detector, the energy spectrum might look as illustrated in (figure 5.19). The number of gamma rays in the higher energy region (region of Compton scattering) is inversely related only to the electron density of the formation (i.e. an increase in the formation density decreases the number of gamma rays). The number of gamma rays in the lower energy region (region of photoelectric effect) is inversely related to both the electron density and the photoelectric absorption. By comparing the counts in these two regions, the photoelectric absorption index can be determined.

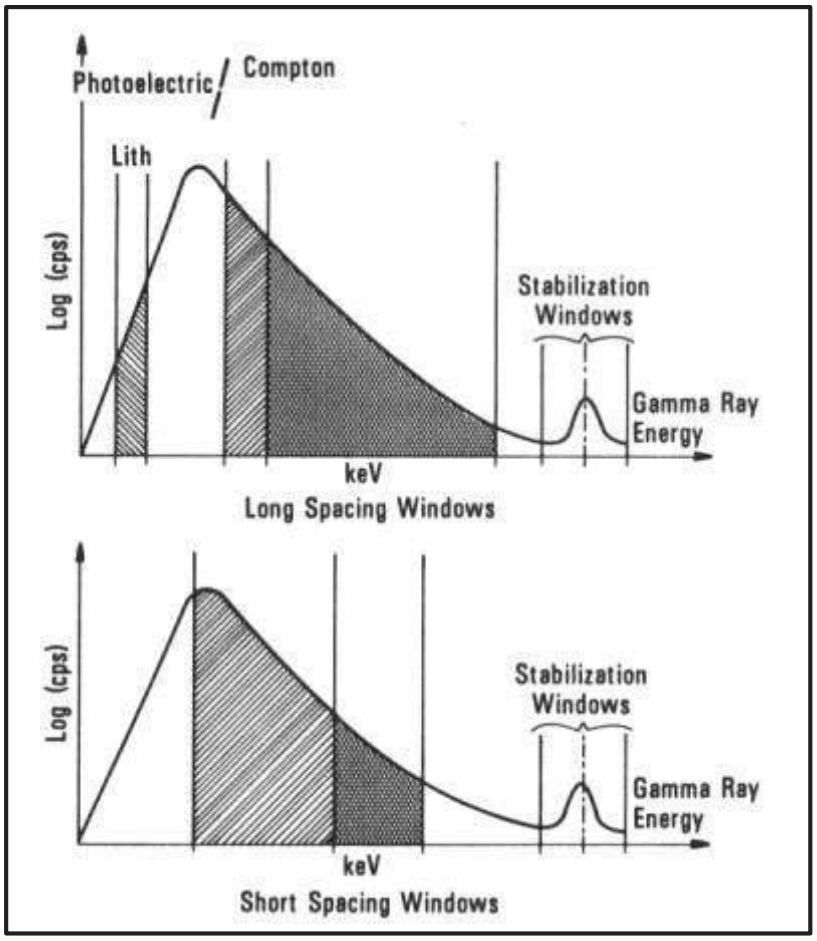

Figure 5.19: Diagram showing measurement of Gamma Rays with Litho-Density System (Courtesy of Schlumberger)

5.9.2 Litho-density tool

In appearance and operation, the Litho-Density tool is similar to the FDC tool. The tool has a pad, or skid, in which the gamma ray source and two detectors are located. This skid is held against the borehole wall by a spring-activated backup arm. Gamma rays, emitted by the source at energy of 662 keV, are scattered by the formation and lose energy until absorbed through photoelectric effect.

5.9.3 Tool response

The Litho-Density tool 'skid and detector system have been designed so that greater counting rates are obtained than with the FDC tool and result in lower statistical variations and better repeatability of the measurements. The geometry of the skid has also been altered so that the density reading has a greater vertical resolution than that of the FDC measurement. The P_e,

measurement exhibits an even better vertical resolution; this has applications in identifying fractures and laminar formations. The procedure for mudcake and borehole rugosity compensation with the Litho-Density tool uses “spine and rib” as done with the FDC tool. Because of the fixed radius of curvature of the measuring device surface, borehole size also influences the measurement.

5.9.4 Log presentation

The log is commonly referred to as the Photo-Electric Factor log (PEF). It is shown in tracks 2 and 3 together with the formation density and neutron curves. Scales running from 0 to 10 or 0 to 15 or 0 to 20 barns/electron are most often used. As the PEF for most common rock forming minerals is low, this log usually sits to the left hand side of track 2.

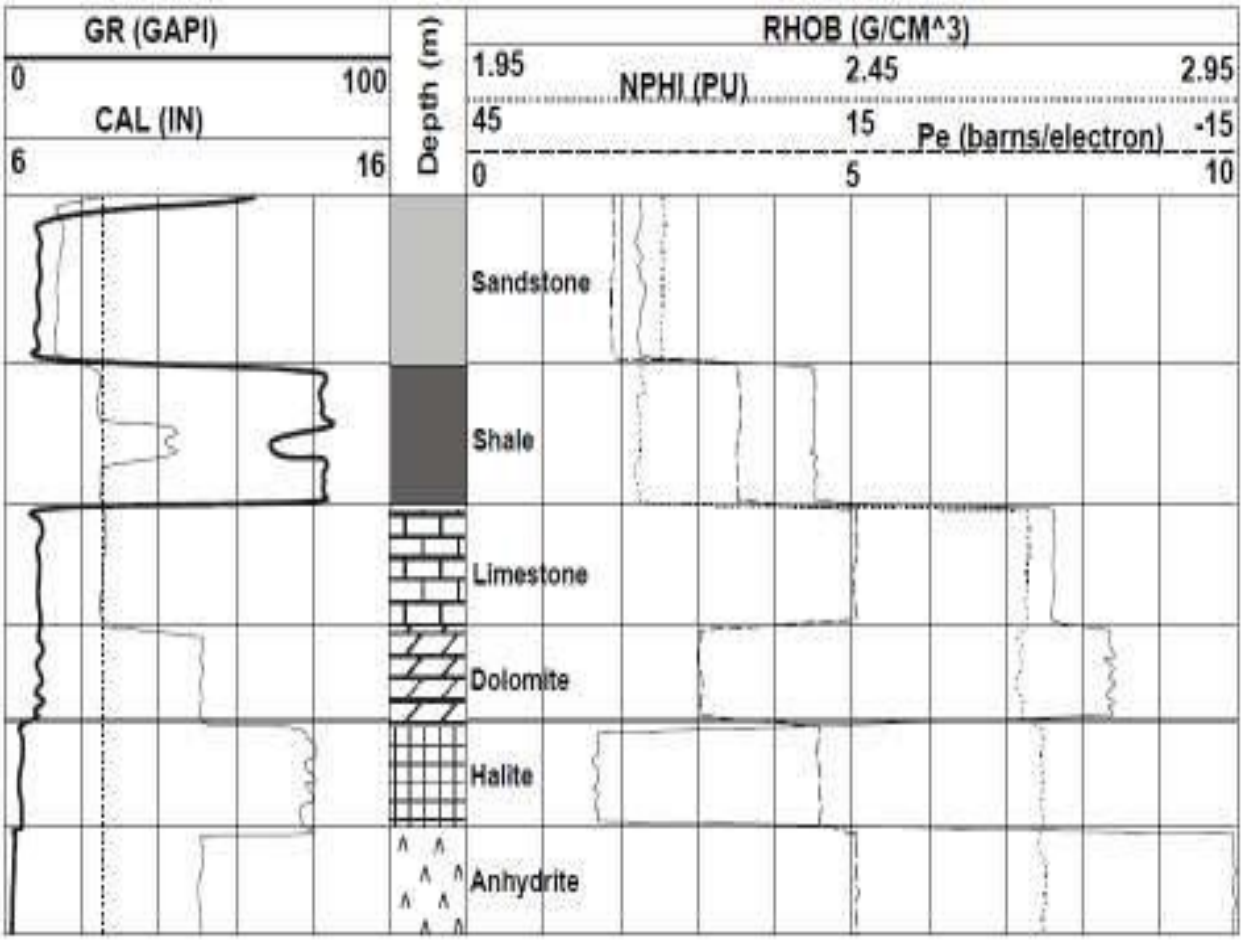

Figure 5.20: Diagram showing presentation of litho-density log

5.10 Caliper log

A Caliper log is a set of measurements of the size and shape of a bore hole commonly made when drilling oil and gas wells. This can be an important indicator of cave in or shale swelling in the bore hole.

5.10.1 Principle

The Caliper tool measures the variation in bore hole diameter as it is withdrawn from the bottom of the hole. It is constructed with two or more articulated arms that push against the bore hole wall to take measurements. The arms show variable movements of the cursor by measuring electrical resistance, creating electrical variation. The variation in output is translated into changes of diameter after a simple calibration. The Caliper log is printed as a continuous series of values of hole diameter with depth.

5.10.2 Equipment

In the two arm tool (figure 5.21), the bore hole diameter is measured. Borehole diameters larger and smaller than the bit size are possible. Many bore holes can attain an oval shape after drilling. This is due to the effect of the pressures in the crust being different in different directions as a result of tectonic forces. In oval holes the two arm caliper will lock into the long axis of the oval cross section giving larger values of borehole diameter than expected. In this case tools with more arms are required.

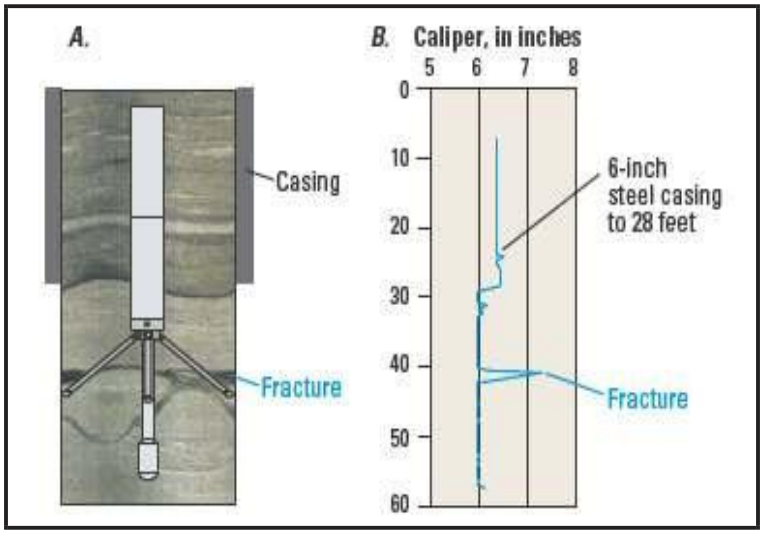

Figure 5.21: Diagram showing Caliper tool in the borehole and its corresponding log curve

In the 4 arm (dual caliper) tool the two opposite pairs work together to give the borehole diameter in two perpendicular directions. An example of an arm tool is the Borehole Geometry Tool (BGT). This has 4 arms that can be opened to 30 inches (40 inches as a special modification) and give two independent perpendicular caliper readings. The tool also calculates and integrates the volume of the bore hole and includes sensors that measure the direction and dip of the bore hole which is useful in plotting the trajectory of the borehole.

In the multi-arm tools up to 30 arms are arranged around the tool allowing the detailed shape of the borehole to be measured.

5.10.3 Log presentation

The Caliper logs with the drilling bit size for comparison or as a differential caliper readings, where the reading represents the caliper value minus the drill bit diameter. The scale is generally given in inches, which is standard for measuring bit sizes. The ticks represent borehole volume. This formation is useful to estimate the amount of drilling mud in the borehole and to estimate the amount of cement required to case the hole. There are engineering approximation formulae to calculate both of these from caliper data.

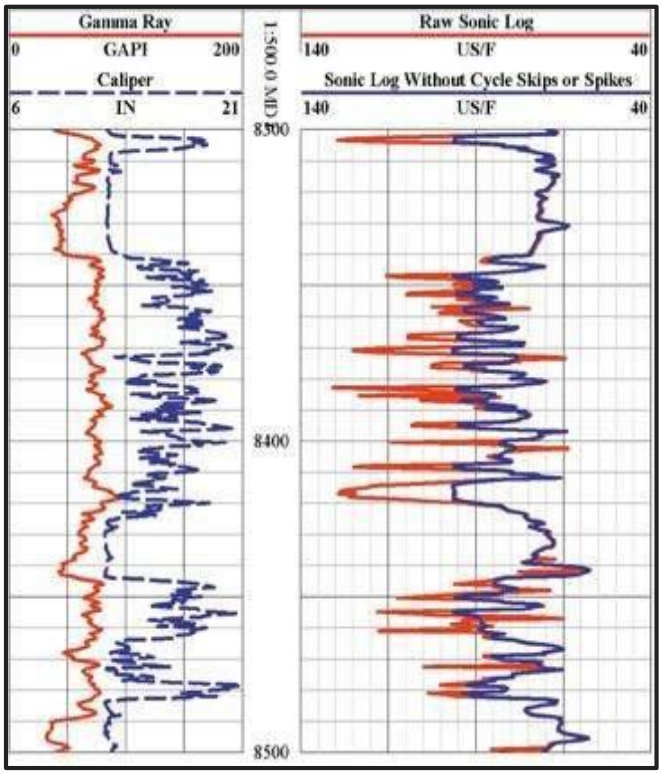

Figure 5.22: Log presentation of Caliper log

5.11 Dual Laterolog (DLL)

The objective of any deep reading resistivity device is to measure the true formation resistivity, R. Deep reading resistivity tools were designed so that, as much as possible, their response is determined by the resistivity of the virgin formation beyond the invaded zone. Unfortunately, no single measurement as yet succeeded in entirely eliminating the effects of the invaded zone.

A solution is to measure the resistivity with several arrays having different depths of investigation. Measurements responding to three appropriately chosen depths of investigation usually approximate the invasion profile well enough to determine R. For best interpretation accuracy such a combination system should have certain desirable features:

1. Borehole effects should be small and/or correctable.
2. Vertical resolutions of the devices should be similar.
3. Radial investigations should be well distributed; i.e. one &ding as deep as practical, one reading very shallow, and the third reading in between. This need resulted in the development of the DLL dual Laterolog. The DLL consists of two laterologs, a deep laterolog and a shallow investigating device recorded simultaneously.

a. The Deep Laterolog (LLD)

The LLD is the deepest investigation laterolog available. This tool is needed to extend the range of formation conditions in which reliable determinations of R_t are possible. At the same time it is necessary to obtain good vertical resolution, for which very long guard electrodes are needed (28 feet measured between ends of the guard electrodes).

The same electrode array is used for deep laterolog and shallow laterolog, but the current flows are different. The symmetrical electrodes are shorted except for the small voltage sensing electrodes.

b. The Shallow Laterolog (LLS)

The Shallow Laterolog (LLS) has the same vertical resolution as the deep laterolog i.e. 2 feet, but the response more strongly to the region affected by invasion.

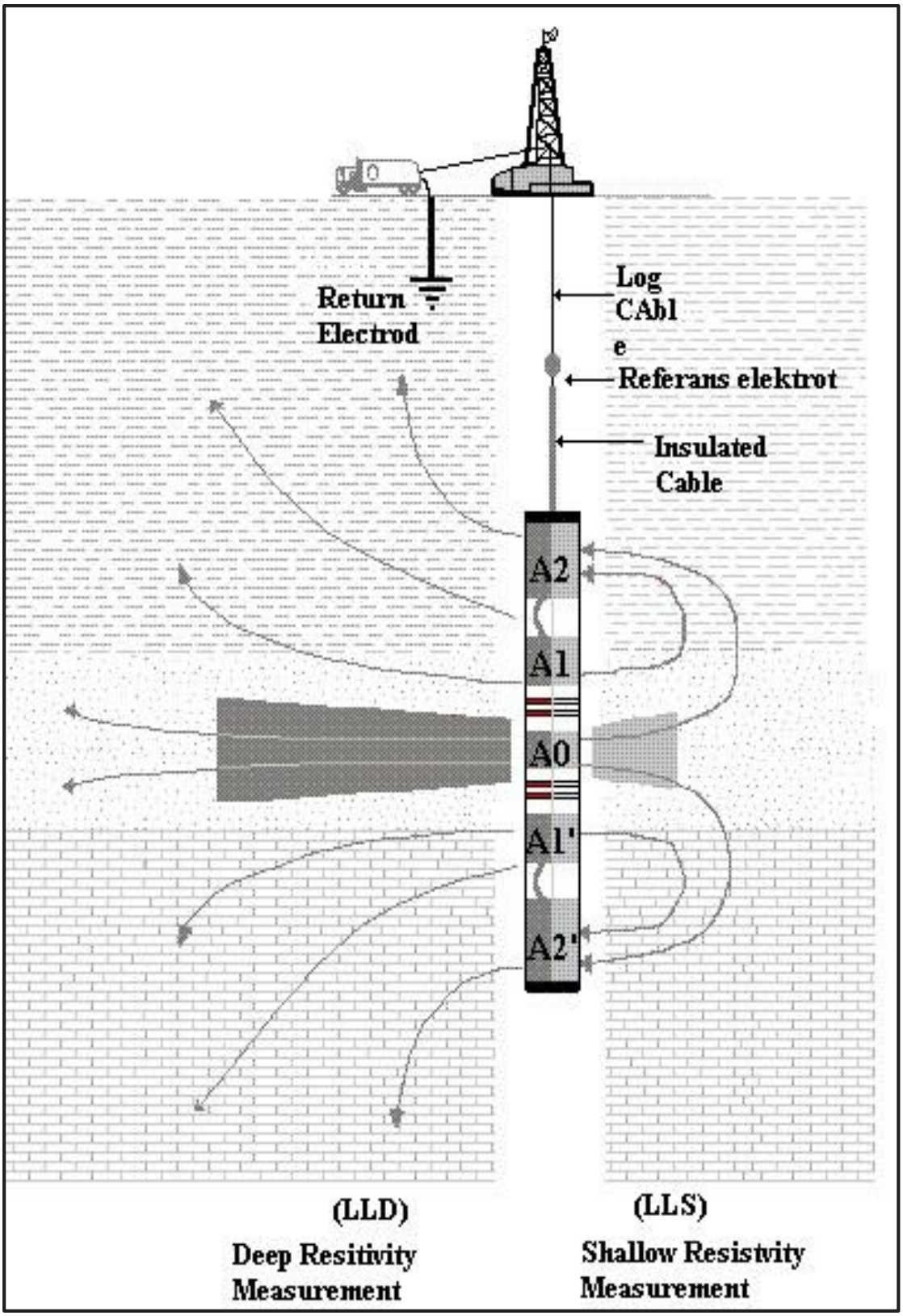

Figure 5.23: Diagram showing DLL in progress

5.11.1 Equipment

The Dual Laterolog consists of two advance laterolog tools which share the same electrodes on the primary sonde. One laterolog is used for deep investigation of the undisturbed zone (R_t), and the other for the shallow investigation of transition zone (R_i). The laterolog electrode arrangement consists of a center current electrode placed symmetrically between three short-circuited pairs of electrodes. A controlled current is emitted from the short-circuited outer pair of electrodes in such a manner that the voltage difference between the two inner short-circuited pairs of electrodes is essentially zero. As in the guard system, these electrode arrangements focus the formation current into a thin disc, which flows perpendicularly to the borehole.

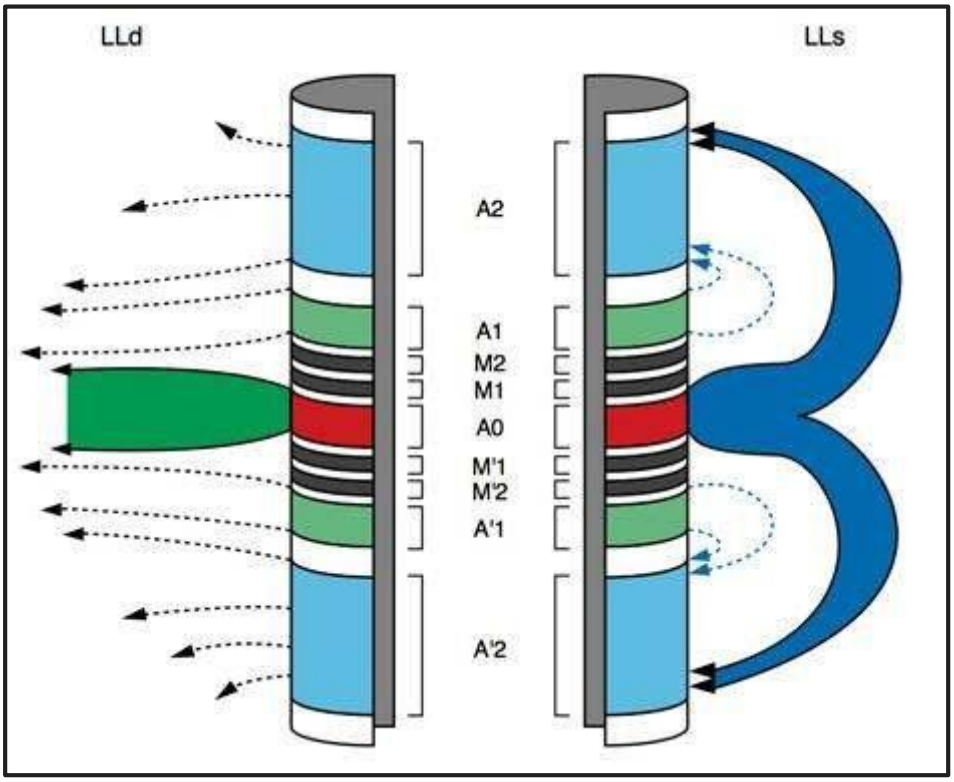

Figure 5.24: Diagram showing Dual Laterolog sonde electrode distribution and current path shape

5.11.2 Tool calibration

Current emitting devices such as the Dual Laterolog, SFL and MSFL or MLL, are calibrated electronically before and after logging surveys in the well is made. This can be done while the tool is down hole by using precision resistors in the tool, no shop calibration is required.

5.11.3 Log presentation

The LLD and LLD curves are usually displayed on a resistivity logarithmic scale, along with the gamma ray log. These are recorded in track 2 with scale running from 0.2 to 2000 ohm-m.

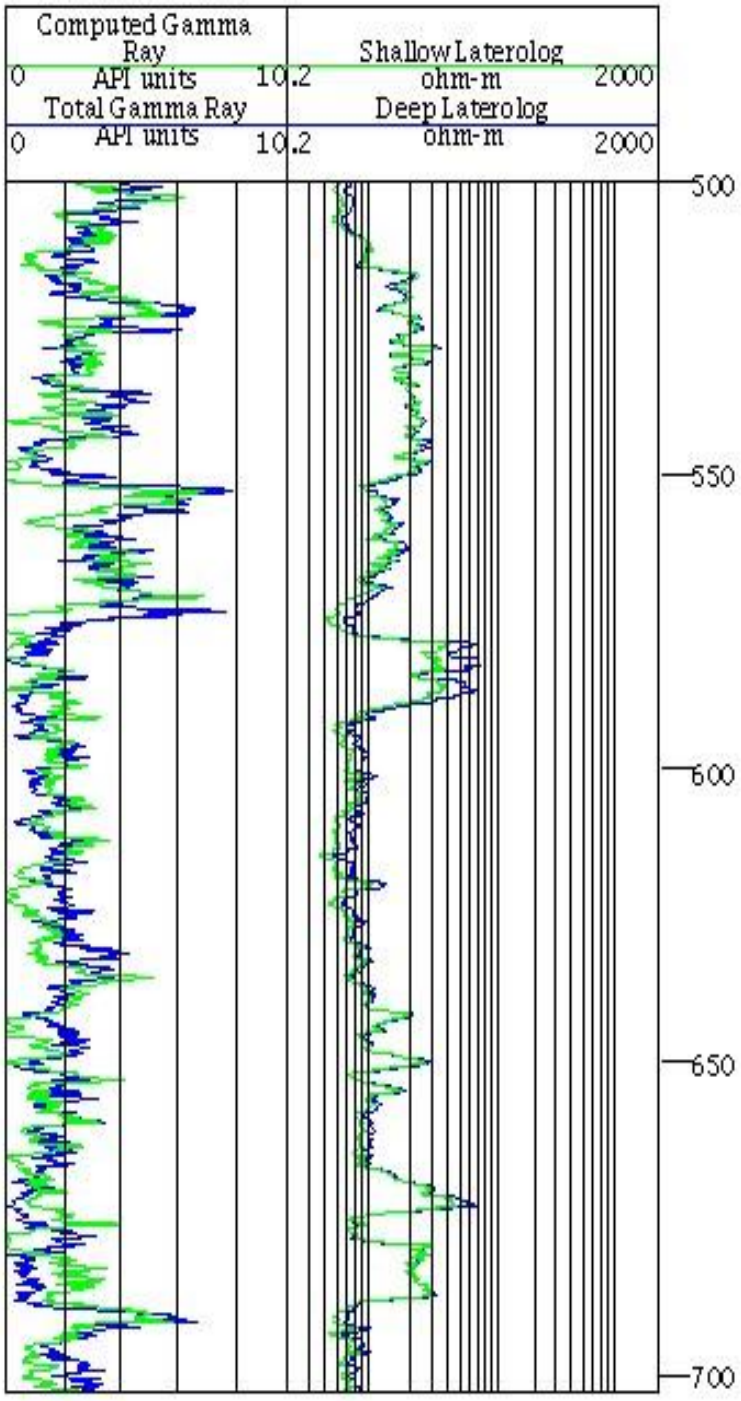

Figure 5.25: Diagram showing presentation of DLL log

5.11.4 Applications

1. Because of the inverse relationship between resistivity and porosity, the dual laterolog can be used to compute the porosity of the rock from Archie's equation.
2. Fracture Porosity Estimate can be estimated from the separation between the deep and shallow measurements based on the observation that the former is sensitive to the presence of horizontal conductive features only, while the latter responds to both horizontal and vertical conductive structures.

5.12 Micro Spherically Focused Log (MSFL)

Microresistivity tools are designed to measure the resistivity of the flushed zone (R_{xo}). Since the flushed zone could be only 3 or 4 inches deep, R_{xo} tools have very shallow readings, with depths of investigation approximately 1 to 4 inches. The MicroSFL is a pad-mounted spherically focused logging device that has replaced the microlaterolog and Proximity tools. It has two distinct advantages over the other R_{xo} devices. The first is its combinability with other logging tools, including the DIL and DLL tools. This eliminates the need for a separate logging run to obtain R_{xo} information. The second improvement is in the tool's response to shallow R_{xo} zones in the presence of mudcake.

5.12.1 MSFL Tool

Figure 5.26 shows the MSFL array. Five rectangular electrodes mounted on an insulating pad that is forced to ride the side of the borehole survey current I_o flows from A_o and bucking current I_a flows between A_1. The latter current is adjusted to maintain zero voltage between the monitor electrodes indicated. This forces the survey current directly into the formation, where it bells out quickly and returns to a nearby electrode. The voltage V between electrode M_o and the monitor electrodes is measured. Resistivity is proportional to V/i_o With this system the MicroSFL has sufficiently shallow penetration to read flushed-zone resistivity, R_{xo}, directly, even in the presence of mud cakes up to 3/4 inch thick.

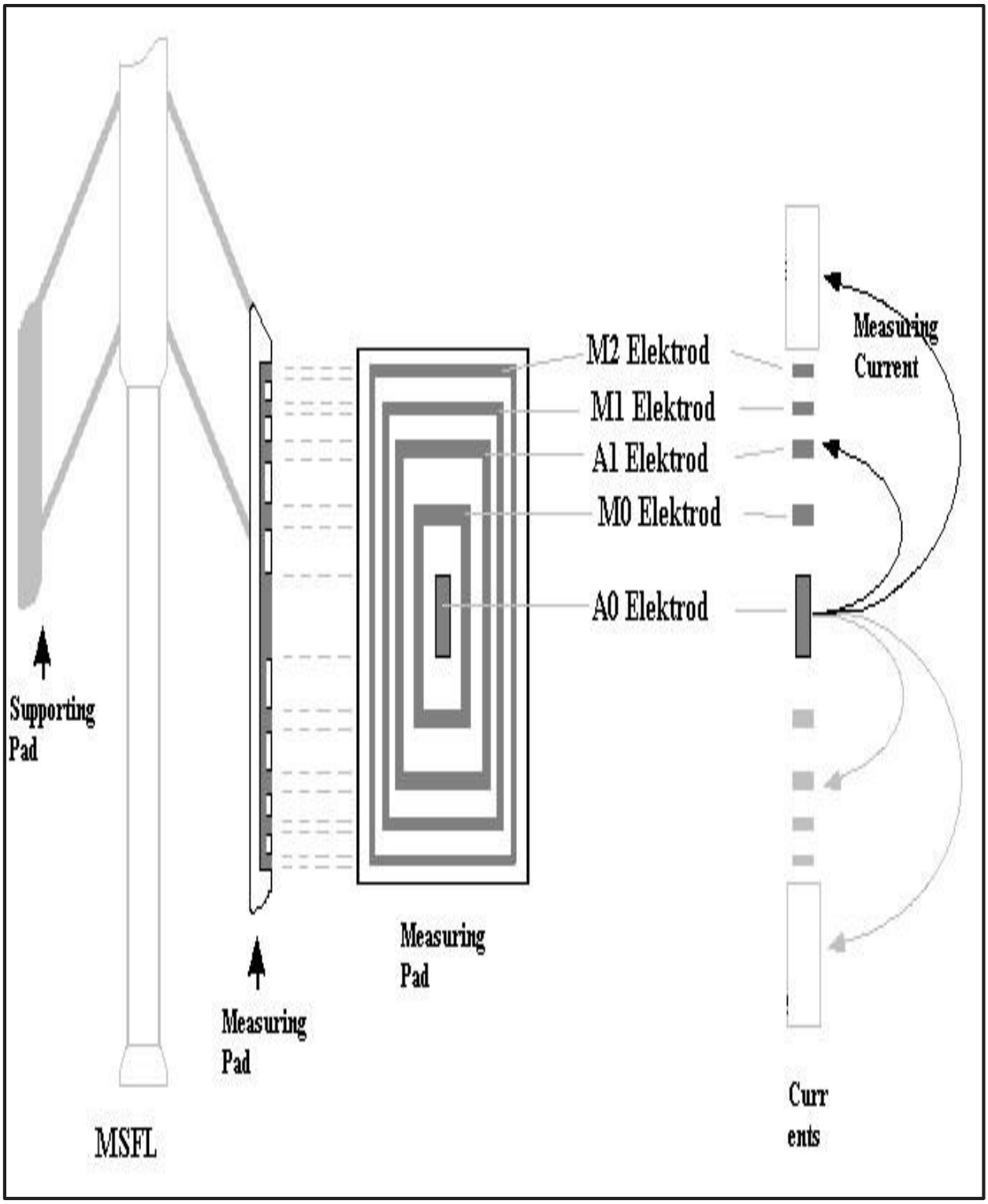

Figure 5.26: Diagram showing MSFL tool

5.12.2 Log presentation

Figure 5.27 is an example of the DLL-MSFL log in salt mud. A GR curve, which can be run simultaneously, is presented in Track 1 since the SP is poor in salt mud. These three resistivity curves are recorded in Tracks 2 and 3 on the several-decade logarithmic scale. Normal presentation is LLD heavy dashed, LLS light dashed, and MSFL solid. With salt mud the shallowest curve reads lowest resistivity and the deepest curve reads highest in water bearing zones, which is the reverse of the fresh-mud situation.

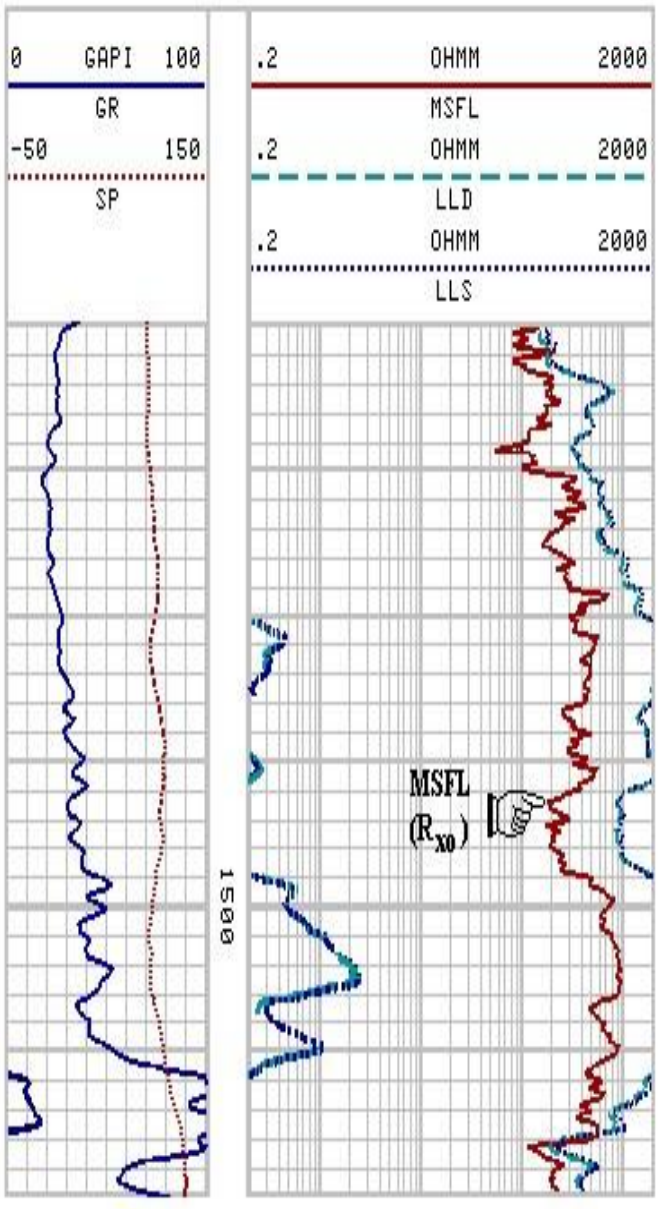

Figure 5.27: Diagram showing DLL-MSFL logs

5.12.3 Applications

1. It is used in measuring the resistivity of the flushed zone.
2. Bed resolution of the MSFL and other R_{xo} tools is extremely good, on the order of 6 inches. In fact, there is so much detail, the curve is often averaged over 2 ft during recording to make it more compatible with the LLD and LLS curves.
3. Borehole corrections for MSFL are negligible.

CHAPTER # 6

Tectonics & Stratigraphy of the study area

6.1 Tectonics of the Central Indus Basin

The Central Indus Basin is separated from Upper Indus Basin by the Sargodha high and Pezu uplift in the north. It is bounded by Indian shield in the east, marginal zone of Indian plate in the west, and Sukkur rift in the South (figure 6.1). The oldest rocks exposed in this basin are of Triassic age (Wulgai Formation) while the oldest rocks penetrated through drilling are of Precambrian Range formation on Punjab Platform. The depth to the basement is about 15,000 meters in the trough areas. Pre-Himalayan non organic movements have resulted in prolonged uplift to sea regression causing unconformities which have led to the large gaps in succession.

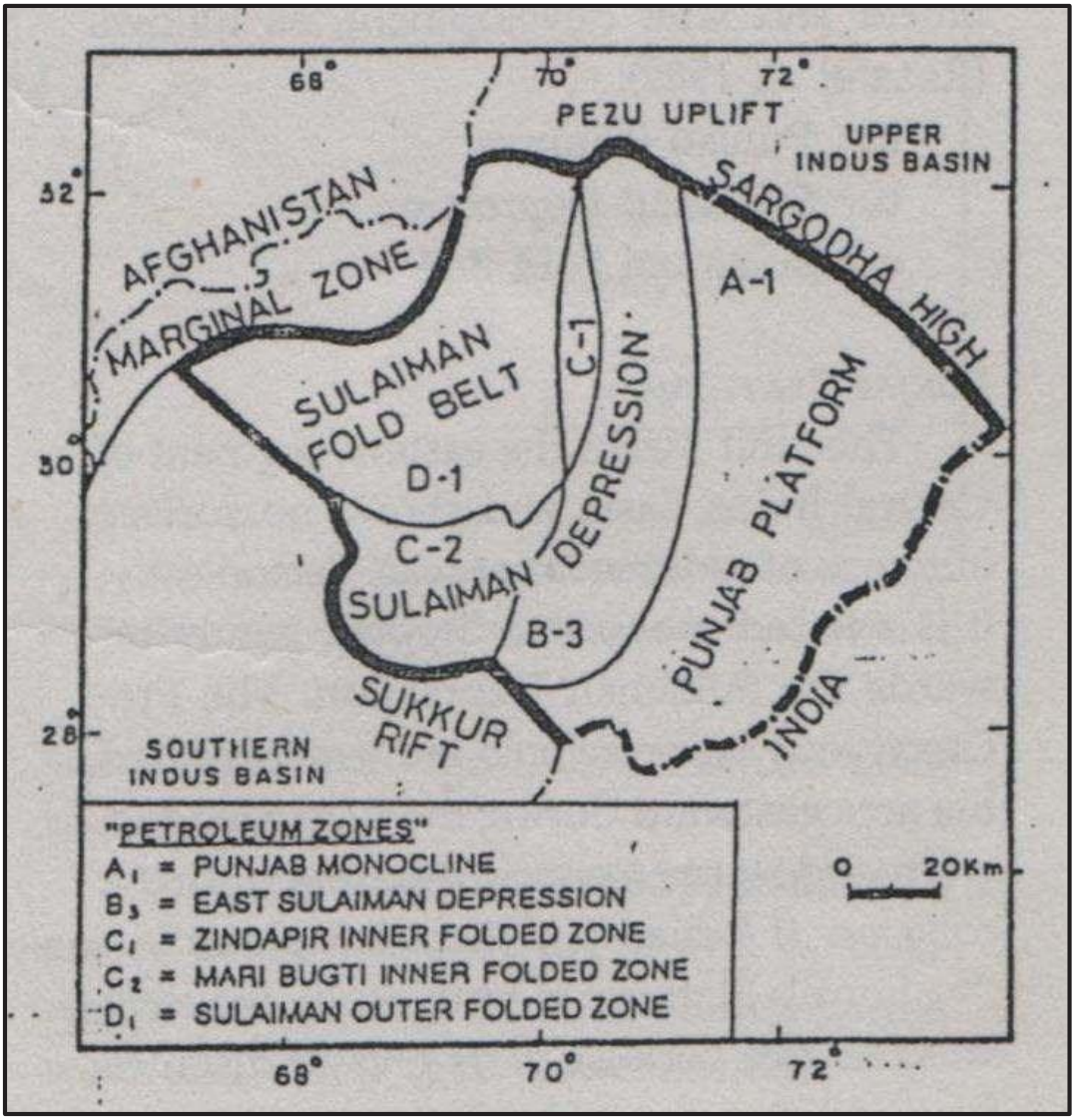

Figure 6.1: Central Indus Basin and the subdivision into petroleum zones. (After Raza et.al, 1989)

Precambrian rocks are largely missing from the basin, although Precambrian shield rocks are evident along the rim of the Indian Plate. Cambrian aged shallow marine rocks are recorded in Karampur well (Shell, 1958). The basin comprises, from east to west, three main units (figure 6. 2) on the basis of the topography of Indian Shield and later development, as follows (Raza et.al, 1989)

1. Punjab platform
2. Sulaiman depression
3. Sulaiman fold belt

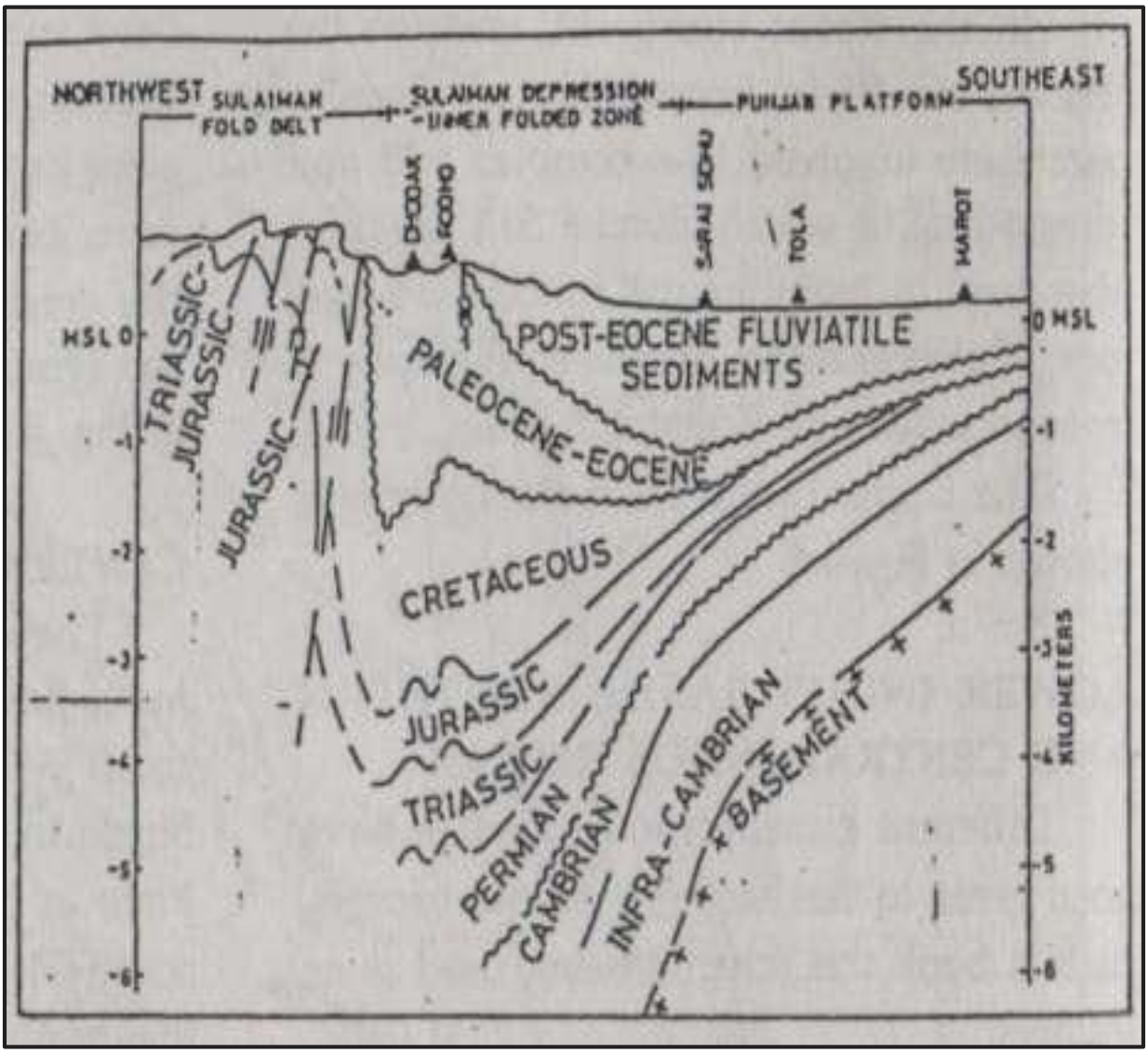

Figure 6.2: Regional cross section, Central Indus Basin (After Raza et all, 1989)

6.1.1 Punjab platform

This unit marks the eastern segment of Central Indus Basin and shows no surface outcrops of sedimentary rocks. Tectonically, it is a broad monocline dipping gently towards the Sulaiman depression. The Pre-Cretaceous non-organic movements tilted the area eastward during the Paleozoic and westward since Mesozoic resulting from the collision of Indian and Eurasian plates.

Punjab platform is tectonically the least affected area because of its greater distance from collision zone. However this presents larger stratigraphic variations. A number of wells have been drilled on this platform. The stratigraphic sequence established on the basis of these wells revealed some of the most significant stratigraphic pinch outs in Pakistan.

6.1.2 Sulaiman depression

This depression is clearly indicated on gravity data and is a longitudinally oriented area of subsidence; it becomes arcuate and takes up a transverse orientation along its southern rim. Like many other features, this depression was also formed as a result of the collision between two plates. The western flank of the depression includes Zindapir inner folded zone lies in the south; to the east it merges into Punjab Platform. On Seismic evidence the area shows some buried anticlines (e.g Ramak) which may have been formed at the expense of flow of Eocene shales. The stratigraphy in the depression area is more complete.

6.1.3 Sulaiman Fold Belt

This is a major tectonic feature in the proximity of collision zone and, therefore, contains a large number of disturbed anticlinal features. Unlike the Upper Indus Basin, the decollement zone in this part was possibly provided by shales. In the Lower Indus Basin the oldest rocks (Triassic-Wulgai Formation) are exposed in this region.

The most important litho-stratigraphic variations observed in Sulaiman depressions and the fold belt are in Paleocene/Eocene. This period marks the facies changes from north to south and east to west. The reason for this variation is believed to be the presence of a number of new basins at that time, created due to the collision of plates and their irregular and non-uniform coalescence.

6.2 Structures of Central Indus Basin

The Central Indus Basin is very important in terms of its natural gas yield. The structures present in this basin were formed as a result of basement uplift (e.g. gentle domal structures like Khairpur, Kandhkot, Mari etc) and compressional tectonics (e.g Inner and Outer Sulaiman folded zone). These ranges from simple dome (Sui) to very complex duplex types (outer folded zones).

6.2.1 Sulaiman fold belt

Similar to Kirthar fold belt, Sulaiman fold belt represents the thin skinned tectonics where the rigid basement is not playing any major role. The sedimentary cover becomes imbricated due to severe compression and its intensity increases northwards of Sui.

West of Sulaiman depression the wrench component also becomes significant in the north-south oriented Sulaiman range. Similar to Kirthar fold belt, duplex structures are expected in the northern part of Sulaiman range.

The arcuate nature of Sulaiman range and the large fold wave length in the south (i.e Sui, Uch, Zin etc) indicate that this range slid over a decollement in a similar way as its analogue in the north; the Salt Range structures in Sulaiman fold belt become simpler and younger towards the periphery of the arcuate belt. It can be summarized that the Sulaiman fold belt represents compressional and strike-slip tectonics.

6.2.2 Punjab platform

In the seventies the Punjab platform area was explored on the basis of the so-called ‘Oman Model’ which envisaged salt related dynamics, affecting Paleozoic strata, for structural closure.

This argument was based on the fact that in Precambrian time, the Indian shield along with African/Arabian shields was part of the super-continent, Pangaea, located much to the south. Reconstruction of Pangaea during the Precambrian indicates that the northern and north-western margins of these shields were characterized by evaporitic (salt/anhydrites) basins. This is confirmed by the presence of Precambrian evaporitic sequence (Salt Range Formation) in Potwar and Punjab platform and a similar evaporitic sequence (Huqf Group) of the same age with suitable combination of source and reservoir rocks in the oil producing basin of Oman.

6.3 Stratigraphy of the Central Indus Basin

The stratigraphic section in the Central Indus Basin consists of rocks ranging from Cretaceous up to Oligocene age. Following diagram shows the General stratigraphy of the Punjab Platform, Central Indus Basin (After Raza and Ahmed 1990). The detailed description of these formations is given below.

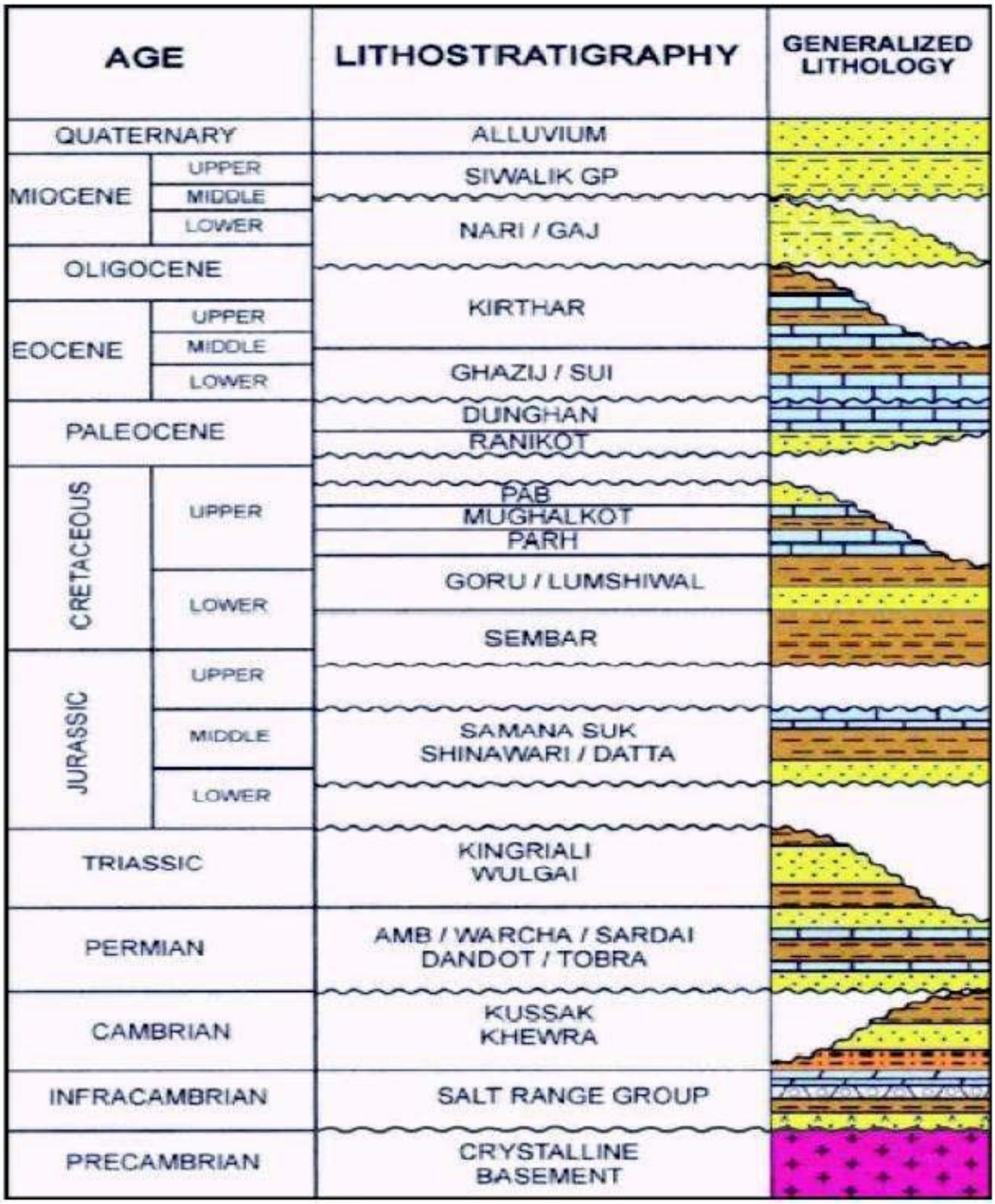

Figure 6.3 General stratigraphy of the Punjab Platform, Central Indus Basin (After Raza and Ahmed 1990)

6.3.1 Sembar Formation

Type locality

The type locality of the formation is Sembar pass.

Lithology

The Sembar Formation consists of black shale interbedded with siltstone and nodular, argillaceous limestone. The shale and siltstone are commonly glauconitic.

Thickness of the formation

The thickness of the Sembar Formation at the type locality is 133 m.

Contact relationship

The lower contact of Sembar Formation with various Jurassic Formations is unconformable while upper contact with Goru Formation is gradational.

Fossil content

The most common fossils found in Sembar Formation are belemnites and foraminifera.

Age of the formation

The age of the Sembar Formation is Early Cretaceous.

6.3.2 Goru Formation

Type locality

The type locality of the formation is Goru Village.

Lithology

This formation is composed of interbedded limestone, shale and siltstone. The lower part is more shaly and consists of very thin bedded, light colored limestone interbedded with thin to irregularly bedded, calcareous, hard, splintery grey to olive green shale. The upper part is largely thin bedded, light colored porcellaneous limestone with subordinate shale.

Thickness of the formation

The thickness of the Goru Formation at the type locality is 536 m.

Contact relationship

The lower contact Goru Formation with Sembar and upper contact with Parh Limestone both are conformable.

Fossil content

The Goru Formation containsbelemnites (Hibolithes sp.) and foraminifera (Fritz and Khan 1967).

Age of the formation

The age of the Goru Formation is Early Cretaceous.

6.3.3 Parh Limestone

Type locality

The type locality of the Parh Limestone is at Parh Range.

Lithology

The Parh Limestone consists of shale, marl and limestone and the limestone is dominant unit.

Thickness of the formation

The Parh limestone is 268 m thick.

Contact relationship

The lower contact of Parh limestone with Goru Formation is conformable and upper contact with Mughal Fort Formation is unconformable.

Fossil content

The Parh Limestone is rich in foraminifers; two important species are Pseudotextulari species and Globotruncana species (Kazmi 1955, Gigon 1962).

Age of the formation

The age of the Parh Limestone is Late Cretaceous.

6.3.4 Mughal Kot Formation

Type locality

The type section exposed along the Fort Sandeman to Dera Ismail Khan road between 2 and 5 km west of Mughal Kot post.

Lithology

It consists mainly of calcareous shale and mudstone with intercalation of sandstone and limestone are the gradient of this formation.

Thickness of the formation

The thickness of the Formation is 150 m.

Contact relationship

The lower contact with Parh Limestone is unconformable while upper contact is conformable with Fort Pab Sandstone.

Fossil content

The foraminifera have been reported from this formation.

Age of the formation

The age of the Mughal Kot Formation is Late Cretaceous.

6.3.5 Pab Sandstone

Type locality

The type section is west of Wirahab Nai in the Pab range.

Lithology

It consists mainly of quartzose, sandstone with intercalations of subordinate argillaceous limestone and shale.

Thickness of the formation

The thickness of the Pab sandstone ranges from 240 m to 1000 m.

Contact relationship

The lower contact with Mughal Kot Formation is conformable while upper contact is unconformable with Khadro, Rakshan and Dungan Formation.

Fossil content

The foraminifera have been reported from this Formation.

Age of the formation

The age of the Pab Sandstone is Late Cretaceous.

6.3.6 Ranikot Group

Ranikot Group has three main Formations.

a. Khadro Formation
b. Bara Formation c.
Lakhra Formation

Lithology

In the lower part the group consists of olive, yellowish brown sandstone and shale with interbeds of limestone (Khadro Formation) followed by variegated sandstone and shale of mainly fluviatile origin (Bara Formation). The upper part consists of grey limestone, weathering brown, and some grey to brown sandstone and shale of estuarine origin (Lakhta Formation).

Thickness of the formation

The thickness of the Ranikot Group ranges from 540 m to 660 m.

Contact relationship

The lower contact with the Pab sandstone is unconformable, while the upper contact with the Dungan Formation is confirmable.

Fossil content

The formations in the Ranikot groups are richly fossiliferous and contain foraminifera, corals, molluscs, and echinoids. Some reptile remains are also reported from some formations.

Age of the group

A Paleocene age has been assigned to this group.

a. Khadro Formation

Type locality

The type locality of the Khadro Formation is Bara Nai in northern Lakhi Range.

Lithology

The formation consists of sandstone and shale with some limestone. The sandstone is olive, yellowish brown, grey and green, soft, medium grained, and calcareous. The shale is olive, bluish grey and gypsiferous and contain thin interbeds of argillaceous limestone.

Thickness of the formation

The thickness of the Khadro Formation at the type locality is 67 m.

Contact relationship

The lower contact of Khadro Formation with Pab sandstone is unconformable whereas its upper contact with Bara Formation is conformable.

Fossil content

A long list of foraminifera has been designated from Khadro Formation.

Age of the formation

The age of Khadro Formation is Early Paleocene.

b. Bara Formation

Type locality

The type locality of the Bara Formation is Bara Nai northern Lakhi range.

Lithology

The formation consists of dominant sandstone with lesser shale and minor volcanic debris. The sandstone is in different color and fine to coarse grained.

Thickness of the formation

The thickness of the Bara Formation at the type locality is 120 m.

Contact relationship

The lower contact with Khadro Formation and upper contact with Lakhara Formation both are conformable.

Fossil content

The formation contains oestrous, reptile remains and leaf impressions.

Age of the formation

The age of the Bara Formation is Middle Paleocene.

c. Lakhra Formation

Type locality

The type locality of the formation is Lakhra Bholari section on the southern flank of the Lakhra anticline Laki range.

Lithology

The Lakhra Formation consists of thin to thick bedded, nodular, sandy argillaceous, fossiliferous limestone with interbeds of sandstone and shale in the upper part of the formation.

Thickness of the formation

The thickness of the Lakhra Formation is 242 m.

Contact relationship

The lower contact with Bara Formation is conformable while upper contact with Lakhi Formation is unconformable.

Fossil content

The Lakhra Formation contains foraminifera, corals, molluscs, and echinoids.

Age of the formation

The age of the Lakhra Formation is Middle Paleocene.

6.3.7 Dunghan Formation

Type locality

The type section of the Dunghan Formation is in the Mehrab Tangi 8 km northeast of Harnai.

Lithology

The formation consists largely of thick to medium to massive nodular limestone with subordinate marl, shale and sandstone.

Thickness of the formation

The thickness of Dunghan Formation is 100 m.

Contact relationship

The lower contact of the Dunghan Formation with Ranikot Formation is gradual and normal while upper contact with Ghazij Group is conformable.

Fossil content

The formation contains a rich fossil assemblage of foraminifera, gastropods, bivalves and algae.

Age of the formation

The age of Dunghan Formation is Paleocene to Early Eocene.

6.3.8 Sui Main Limestone

Lithology

The Sui Main Limestone contains traces of shale. Limestone is off white to creamy in color, medium to hard with calcite vein and marl. Traces of shale are laminated and light greenish grey to light grey in color.

Contact relationship

The upper contact of the Sui Main Limestone with the Sui Shale and lower contact with the Dunghan Formation both are conformable.

Fossil content

The Sui Main Limestone is highly fossiliferous.

Age of the formation

The age of the Sui Main Limestone is Lower Eocene.

6.3.9 Ghazij group

Ghazij group has five main formations.

a. Marap Conglomerate
b. Shaheed Ghat Formation
c. Drug Formation
d. Toi Formation
e. Baska Formation

Type locality

The Ghazij group crops out extensively in the Sulaiman Range and the northern part of the Kirthar Range. The type locality of the Ghazij group is at spintangi.

Lithology

The Ghazij group dominantly consists of shale, interbedded with layers and lenses of clay stone, mudstone, sandstone, limestone, conglomerates and alabaster (Kazmi 1962). It contains deposits of coal which are being mined.

Thickness of the group

The thickness of Ghazij group varies from 160 m to 1300 m.

Contact relationship

The lower contact of Ghazij group with Dungan Formation is conformable and upper contact with the Habib Rahi Formation is also conformable.

Fossil content

The Ghazij group contains foraminifera, gastropods, bivalves, echinoids, algae and plant remains (Eames 1952, HSC 1960, Latif 1964, Iqbal 1969a).

Age of the group

The age of the Ghazij group is Early Eocene.

a. Marap conglomerate

Type locality

It crops out in the Kalat Plateau area and forms the basal part of the Ghazij Group. The type locality is at Marap Valley.

Lithology

It consists of well rounded and poorly sorted pebbles and boulders of limestone, shale, and sandstone derived from the underlying formations including the Jurassic rocks. The conglomerate is interbedded with sub-ordinate shale, sandstone, and less commonly limestone.

Thickness of the formation

The Marap Valley is the type locality where it is about 910 m thick.

Age of the formation

The age of the Marap conglomerate is Early Eocene.

b. Shaheed Ghat Formation

Type locality

The type locality is at Shaheed Ghat 5 km southwest of Zinda Pir.

Lithology

The Shaheed Ghat Formation consists of grey to olive green, laminated shale with marl. At places the shale contains layers with nummulites, gastropods and lamellibranchs.

Thickness of the formation

The thickness of the formation ranges from about 340 m at Moghal Kot to over 680 m at Shaheed Ghat.

Fossil content

At some places in the Shaheed Ghat Formation the shale contains layers with nummulites, gastropods, and lamellibranches.

Age of the formation

The Shaheed Ghat Formation is Early Eocene in age.

c. Drug Formation

Type locality

The type locality of the Drug Formation is at Drug Tangi 3 km northeast of Drug Village.

Lithology

The formation consists of largely of limestone interbedded with subordinate shale. The limestone is orange, pale-olive, and grey green to creamish white in color. It is thin bedded, hard, pebbly and nodular, crystalline, argillaceous and commonly has marly partings. The lower part of formation is mostly shale which is greenish grey to dark grey, calcareous, at places pyritic or with minor limestone.

Thickness of the formation

The thickness of the Drug Formation ranges from 40 to 340 m.

Age of the formation

The Drug Formation is Early Eocene.

d. Toi Formation

Type locality

The type section of the Toi Formation is in Toi Nala.

Lithology

The Toi Formation consists mainly of interbedded sand stone and mudstone, siltstone, shale and conglomerate with locally developed coal seams. The sandstone is coarse grained, pebbly, poorly sorted and cross bedded, at places containing freshwater bivalves, gastropods and calcareous. The mudstone and siltstone are brown to reddish brown, soft, blackish and calcareous.

Thickness of the formation

The thickness of the Toi Formation is about 1196 m at the Mughal Kot section.

Contact relationship

The lower contact of the Toi Formation with Drug Formation is conformable and where the Drug Formation missing it overlies the Shaheed Ghat Formation.

Fossil content

The Toi Formation contains freshwater bivalves, gastropods and calcareous at some places.

e. Baska Formation

Type locality

The type locality of the Baska Formation is 2 km east-northeast of Baska Village.

Lithology

The formation consists of green to grey shale and clay stone interbedded with alabaster, gypsiferous limestone and marl. At places the shale is interbedded with thin limestone beds.

Thickness of the formation

The thickness of Baska Formation ranges from about 160 m to about 820 m.

Fossil content

The formation contains foraminifera, bivalves and gastropods.

Age of the formation

The age of Baska Formation is Early Eocene.

6.3.10 Kirthar Formation

Type locality

The type section in the Kirthar Range is Gaj River section.

Lithology

The formation is mainly fossiliferous limestone inter bedded to massive, nodular in some areas, grey to white in color. The upper part of the formation is massive cliff-forming limestone. The shale is olive, orange, yellow or grey, soft, earthly and calcareous.

Thickness of the formation

The thickness of the Kirthar Formation is 15 to 1270 m.

Contact relationship

The lower contact of the Kirthar Formation with Laki Formation and upper contact with the Nari Formation is conformable.

Fossil content

The formation contains abundant foraminifera, gastropods, bivalves, echinoids and vertebrate remains (Oldham 1890, Vredenburg 1906, 1909a. Pilgrim 1940, Eames 1952, HSC 1960)

Age of the formation

The age of the Kirthar Formation is Middle Eocene to Early Oligocene.

6.3.11 Habib Rahi Formation

Type locality

The type section of the Habib Rahi Formation is proposed north of Zampost, along the Zhob Dera Ismail Khan road.

Lithology

The formation consists of largely grayish brown, thin to thick bedded or massive, hard argillaceous, fossiliferous limestone with nodules and cherty beds.

Thickness of the formation

The thickness of the Habib Rahi Formation ranges from 15 m to 150 m.

Contact relationship

The lower contact of the Habib Rahi Formation with Baska formation and upper with Domanda Formation both are conformable.

Fossil content

The Habib Rahi Formation contains foraminifera, echinoids, astrocods, bivalves and bryozoans.

Age of the formation

The Age of the Habib Rahi Formation is Middle Eocene.

6.3.12 Domanda Formation

Type locality

Its type locality is west of Domanda.

Lithology

The formation consists of brown to grey clay stone with intercalation of limestone at some places, and with subordinate grey to brown, fine to medium grained thick bedded to massive calcareous sandstone in the upper part of the formation.

Thickness of the formation

The thickness of the Domanda Formation ranges from about 130 to 330 m.

Contact relationship

The lower contact of Domanda Formation with Habib Rahi Formation and upper contact with Pirkoh Formation both are conformable.

Fossil content

The formation contains foraminifera, gastropods, bivalves, echinoids, and rare vertebrate fossils.

Age of the formation

The age of the Domanda Formation is Middle Eocene.

6.3.13 Pirkoh Formation

Type locality

The type locality of the formation is Pirkoh anticlines.

Lithology

The Pirkoh Formation consists of brown, grey to white, thin bedded limestone with subordinate fossiliferous marls and brown fossiliferous limestone inter beds. At places it is inter bedded with grey, calcareous sandstone in the middle part of the formation.

Thickness of the formation

The thickness of the Pirkoh Formation ranges from 110 m to 170 m.

Contact relationship

The lower contact of the Pirkoh Formation with the Domanda Formation and upper contact with Drazinda Formation both are conformable.

Fossil content

The formation is highly fossiliferous and contains foraminifera, bivalves, bryozoans, and echinoids.

Age of the formation

The age of the Pirkoh Formation is Middle Eocene.

6.3.14 Drazinda Formation

Type locality

The type locality of the formation is northeast of Drazinda.

Lithology

The Drazinda Formation consists of brown to grey clay with subordinate fossiliferous marls and brown fossiliferous limestone inter beds. At some places it is inter bedded with grey, calcareous sandstone in the middle part of the formation.

Thickness of the formation

The thickness of the Drazinda Formation ranges from 15 m to 500 m.

Contact relationship

The lower contact of the Drazinda Formation with the Pirkoh Formation is conformable and upper contact with the Nari Formation is unconformable.

Fossil content

The Drazinda Formation contains a rich fauna of foraminifera, bivalves, bryozoans, and echinoids.

Age of the formation

The age of the Drazinda Formation is Middle Eocene.

6.3.15 Nari Formation

Type locality

The type section of the Nari Formation is in the Gaj River gorge in the Kirthar Range.

Lithology

The lower part of the Nari Formation consists of inter bedded grey to brown, fossiliferous sandy limestone, calcareous sandstone and shale. At many places the lower part of the formation is a grey to brown shaly, nodular, and thick bedded to massive limestone which has been named the Nal Member (HSC 1960).

Thickness of the formation

The thickness of the Nari Formation ranges from 1045 m to 1820 m in the Kirthar area.

Contact relationship

The lower contact of the Nari Formation is unconformable and upper contact is conformable.

Fossil content

The Nari Formation contains a rich fauna including echinoids, molluscs, corals, foraminifera, and algae (Duncan et al. 1963, Khan 1968, Iqbal 1969b).

Age of the formation

The age of the Nari Formation is Oligocene to Early Miocene.

CHAPTER #7

Petrophysical Analyses

7.1 Introduction

Petrophysical analysis is the study and interpretation of the wire-line logs, generated by the downhole logging. In this, petrophysist generally follow the sequence of task in order to evaluate the hydrocarbon potential of the formation. In order to do so, they calculate different parameters to find out the saturation of hydrocarbons in the reservoir. The complete interpretation workflow is shown in figure 7.1.

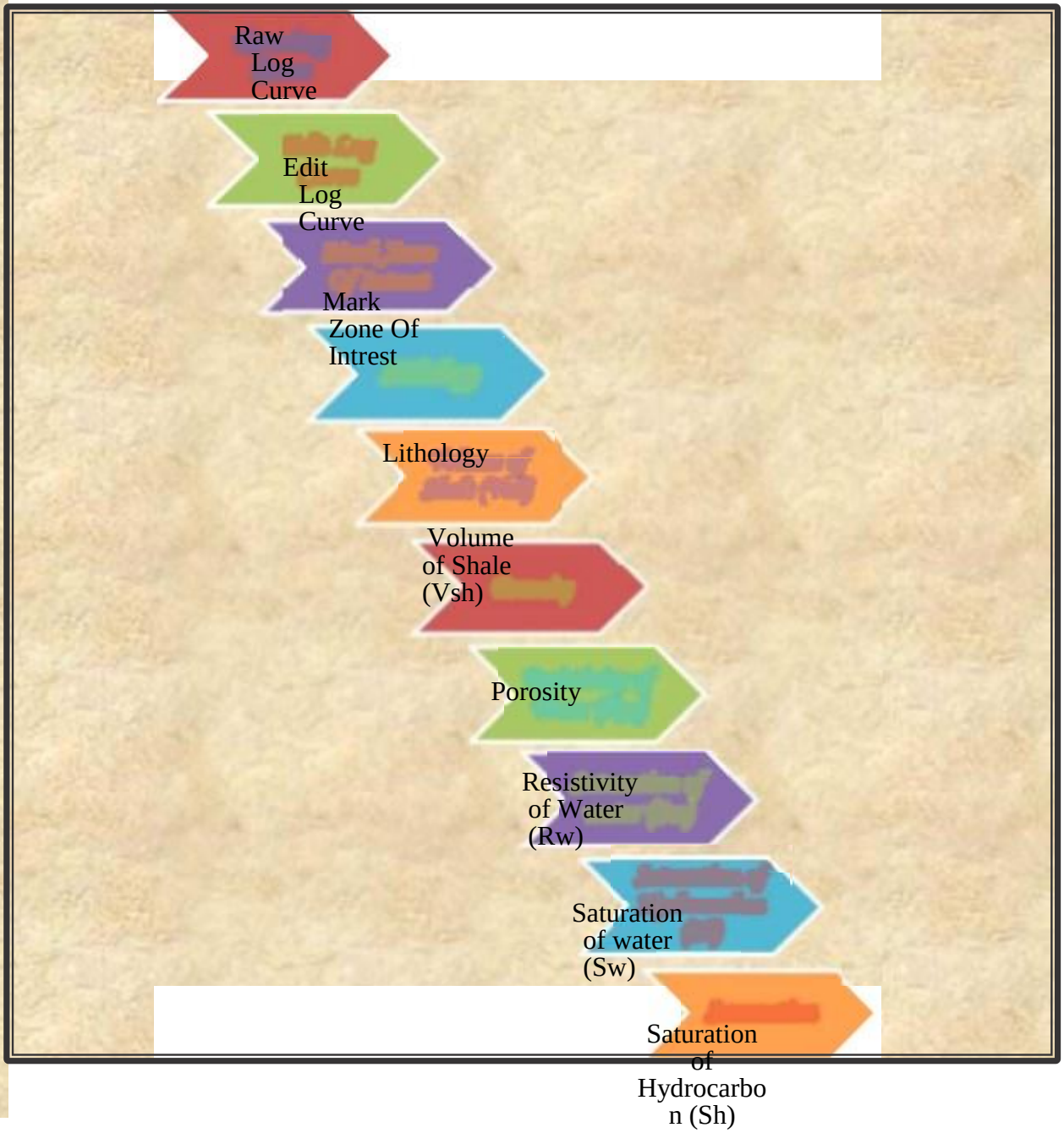

Figure 7.1: Diagram showing Interpretation work Flow

The interpretation involves, first of all the editing of the newly generated raw log curve. After the log has been edited, zones of interest are marked. Now we are ready to calculate different parameters from the different log curves like volume of shale (V_{sh}), porosity (φ), Saturation of Water (S_w), Saturation of Hydrocarbon (S_{hc}), Permeability and Lithology. During the calculation of these parameters, one thing should be kept in mind that all the relevant logs are being studied side by side rather separately in order to get the accurate measurement. In addition to this, make sure that the scale of all the logs is the same.

7.2 Methodology adopted

In evaluating two of the wells in the Central Indus Basin, namely Mari Deep 6 and Mari Deep 9, the method for the formation evaluation adopted was that first we marked the zones of interest in the logs, where we observed gas effect, after that we calculated volume of shale with the help of GR log. Porosity was calculated with the help of Neutron log, Bulk Density log and Dual Lateral Log. And finally permeability, saturation of water, saturation of hydrocarbon and lithology were calculated by using different techniques. The methodology adopted for the determination of these petrophysical parameters is discussed in detail below:

7.2.1 Determination of volume of shale (V_{sh})

Volume of Shale was calculated with the help of GR log. In this, we first note down the maximum and the minimum values of the GR curve in that particular zone and then we note down the GR readings at different intervals in each zone marked. Then we apply all these data gathered into the following formula in order to get the volume of shale or gamma ray "shale index" I_{GR} at different depths.

$$\mathbf{I_{GR}} = \frac{GR_{Log} - GR_{Min.}}{GR_{Max.} - GR_{Min.}}$$

Where,

GR_{log} = log response in the zone of interest, API units

GR_{min} = log response in the clean beds, API units

GR_{max} = log response in the shale beds, API units

7.2.2 Determination of Lithology

The lithology was determined with the help of "M-N Plot for mineral identification" cross plot shown in figure 7.2 below. This cross plot is used to identify mineral mixtures from sonic, density and neutron logs. The values of "M" and "N" have been determined with the help of formula given below:

$$\mathbf{M} = \frac{t_f - t}{\rho_b - \rho_f} \times 0.01$$

Where,

T_f = Time of fluid

ρ_b = Bulk density

ρ_f = Fluid density

$$\mathbf{N} = \frac{(\varphi_N)_f - \varphi_N}{\rho_b - \rho_f}$$

Where,

$(\varphi_N)_f$ = NPHI of fluid = 1

φ_N = NPHI

ρ_b = Bulk density

ρ_f = Fluid density

By plotting the values of M and N on cross plot we get the lithology.

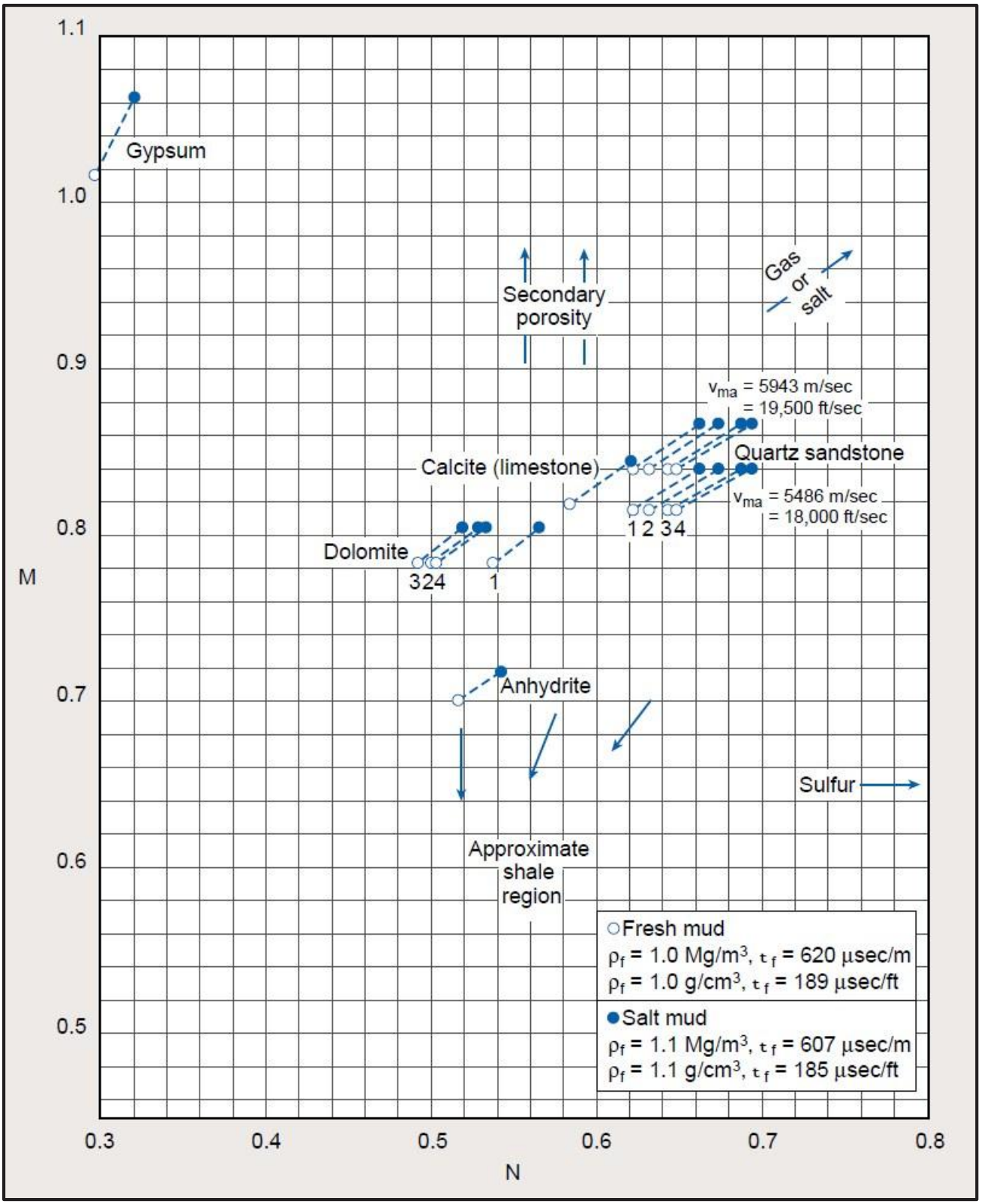

Figure 7.2: M-N Plot for mineral identification

7.2.3 Calculation of Porosity

Porosity was calculated by using cross plot between bulk density (RHOB) and Neutron porosity Hydrogen Index (NPHI) shown in figure 7.3 below. Both of these were noted down from the log at different depth intervals and then plotted in the cross plot with bulk density on the Y – axis and the neutron porosity index on the X – axis. We plot these values and eventually get to a point where these two lines meet then we drop this point vertically to the lithology at that particular depth where we get the porosity of the rocks at that depth. Following is the cross plot used for calculating the porosity of the formation.

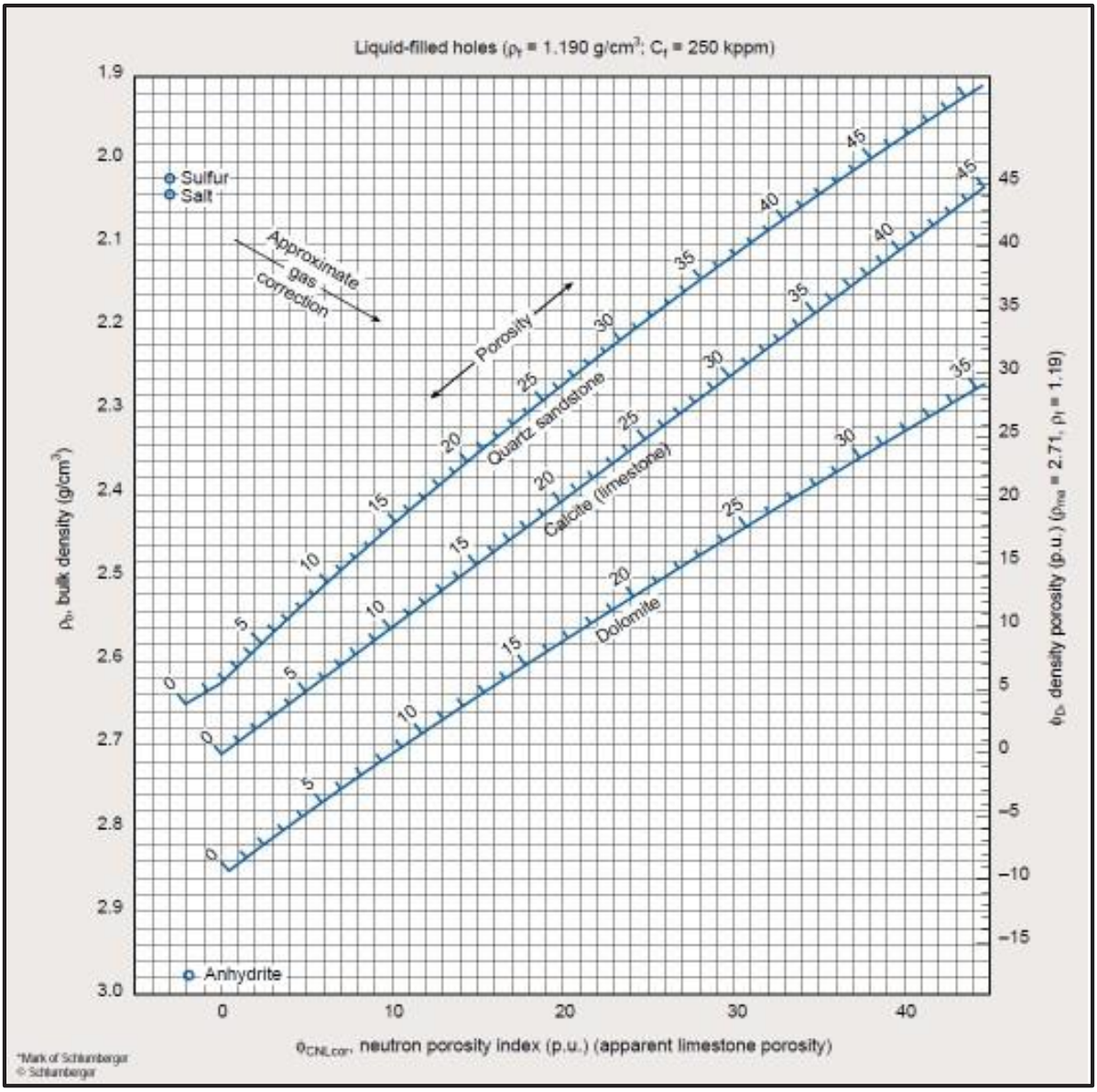

Figure 7.3: Bulk density (RHOB) and Neutron porosity Hydrogen Index (NPHI) cross plot.

7.2.4 Calculation of Water Saturation (S_w)

Water saturation was calculated with the help of Archie's equation:

$$S_w = \sqrt{\left(\frac{a}{\varphi^m}\right) \times \left(\frac{R_w}{R_t}\right)}$$

Where,

S_w = Water Saturation

φ = Porosity

R_w = Formation water resistivity

R_t = Observed LLD curve

a = A constant (often taken to be 1)

m = Cementation factor (varies around 2)

In calculating porosity, we first calculated the formation water resistivity R_w from the water zone in that formation, by using following formula:

$$R_w = \frac{\varphi^m \times R_t}{a}$$

Where,

R_w = Formation water resistivity

R_t = Observed LLD curve

φ = Porosity

m = Cementation factor (varies around 2)

Above calculated R_w is kept constant throughout the formation along with the values of other two constants a and m. These are put into the Archie's equation, along with the value of R_t, which is the resistivity of the formation at different depth intervals.

7.2.5 Calculation of Hydrocarbon Saturation (S_{hc})

Hydrocarbon saturation was calculated by a simple formula given below:

$$S_{hc} = 1 - S_w$$

Where,

S_{hc} = Saturation of hydrocarbon

S_w = Saturation of water

7.2.6 Calculation of Permeability

Permeability was calculated by utilizing a cross plot between porosity (φ) at X – axis and water saturation (S_w) at Y – axis, shown in figure 7.4 below. In this we take the porosity values and the value of water saturation at a certain depth and plot them against their respective axis. The point where these two lines meet is the permeability of the rocks at that particular depth. Below is the cross plot used to determine the permeability of the formations at different depths. The scale ranges from 0 – 60 in % for water saturation and 0 – 40 in % for porosity, any value beyond this scale cannot be calculated.

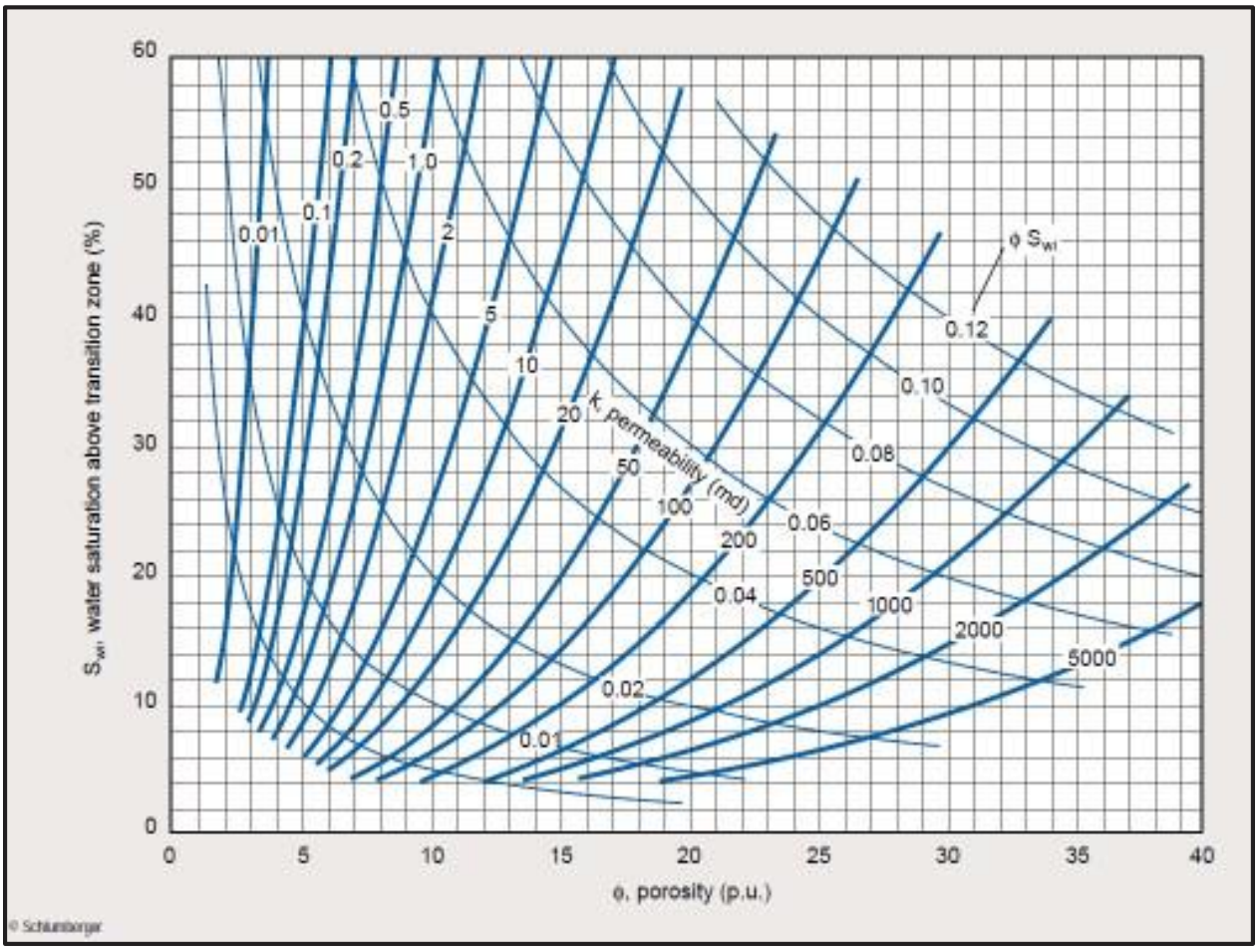

Figure 7.4: Porosity (φ)and water saturation (S_w) cross plot for calculating permeability

CHAPTER # 8

Interpretation of Mari Deep 6 and Mari Deep 9, Central Indus Basin

8.1 Interpretation of Mari deep 6, Central Indus Basin

In Mari deep 6, we encountered six zones which were interpreted in order to evaluate the hydrocarbon potential of this well. Different parameters calculated, which were discussed in previous chapter, are given below:

Zone 1

Depth (ft)	Volume of Shale (V_{sh}) (%)	Porosity (Φ) (%)	Water Resistivity (R_w) (Ωm)	Water Saturation (S_w) (%)	Saturation of Hydrocarbons (S_{hc}) (%)	Permeability	Lithology
1712	27.27273	22.5	0.473	72.04632	27.95368	N/A	Limestone
1714	36.36364	24.8	0.473	74.11649	25.88351	N/A	Limestone
1716	72.72727	23.5	0.473	73.16489	26.83511	N/A	Limestone
1718	54.54545	21	0.473	79.43041	20.56959	N/A	Limestone
1720	27.27273	20	0.473	85.96874	14.03126	N/A	Limestone
1722	81.81818	21.2	0.473	83.76239	16.23761	N/A	Limestone
1724	45.45455	25	0.473	86.99425	13.00575	N/A	Limestone
1726	54.54545	21.5	0.473	82.59362	17.40638	N/A	Limestone
1728	27.27273	20.5	0.473	96.84698	3.153019	N/A	Limestone
1730	63.63636	24.5	0.473	100	0	N/A	Limestone
1732	0	25	0.473	97.26253	2.737469	N/A	Limestone

Table 8.1: Table showing interpretation of zone 1, Mari deep 6, Central Indus Basin

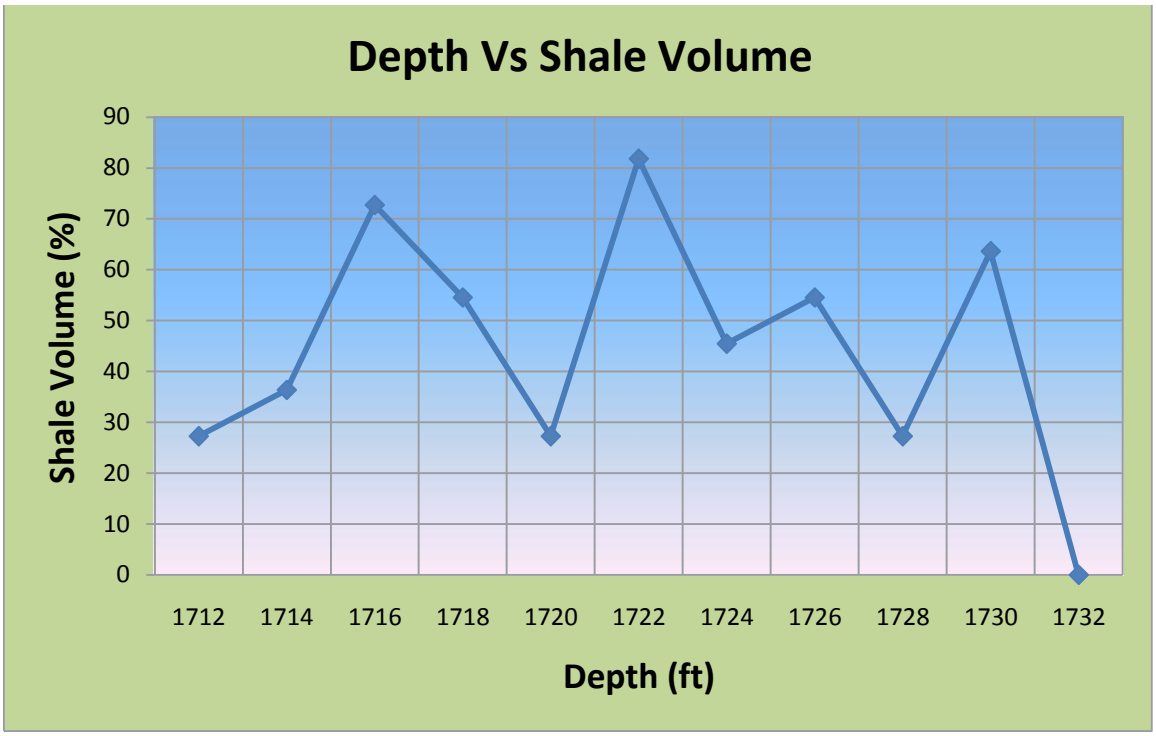

Graph 8.1: Graph showing relationship of shale volume with depth in zone 1, Mari deep 6, Central Indus Basin

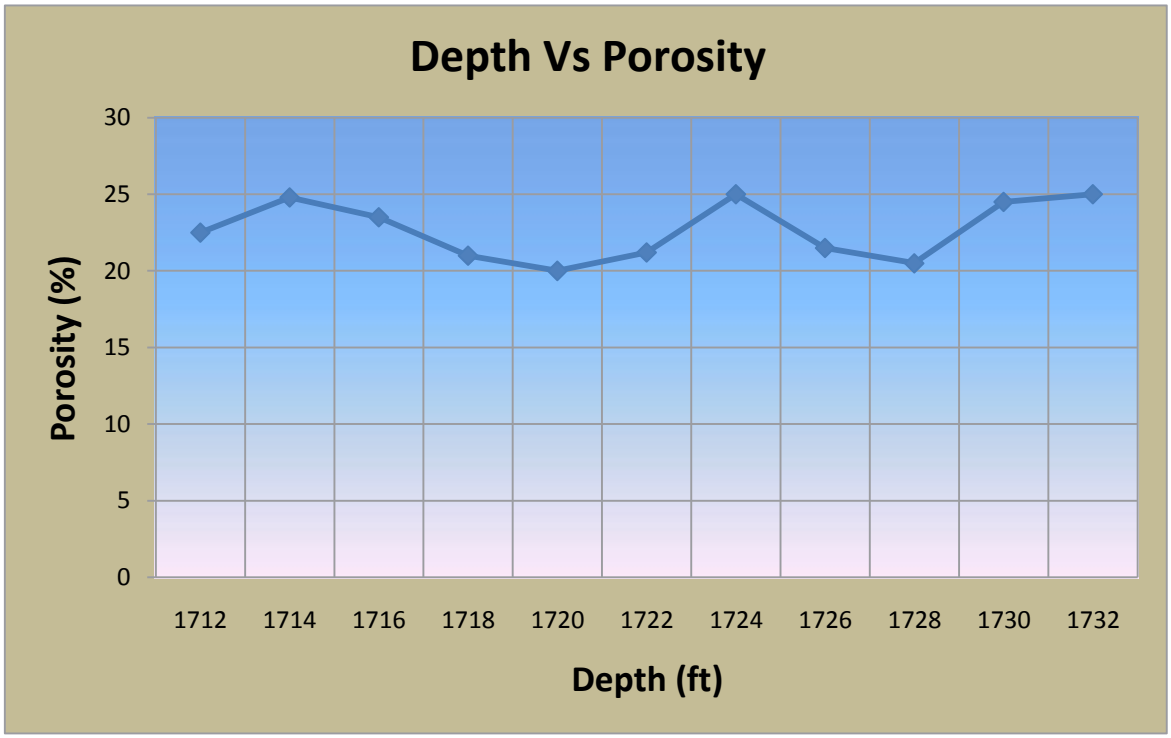

Graph 8.2: Graph showing relationship of porosity with depth in zone 1, Mari deep 6, Central Indus Basin

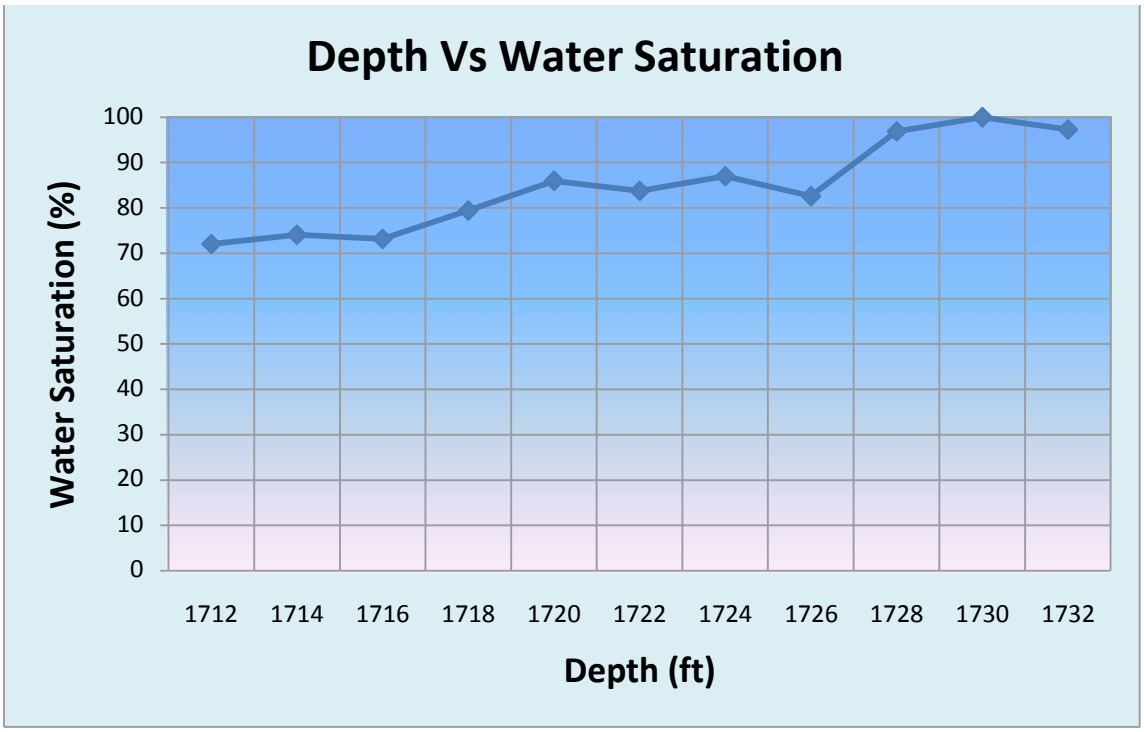

Graph 8.3: Graph showing relationship of water saturation with depth in zone 1, Mari deep 6, Central Indus Basin

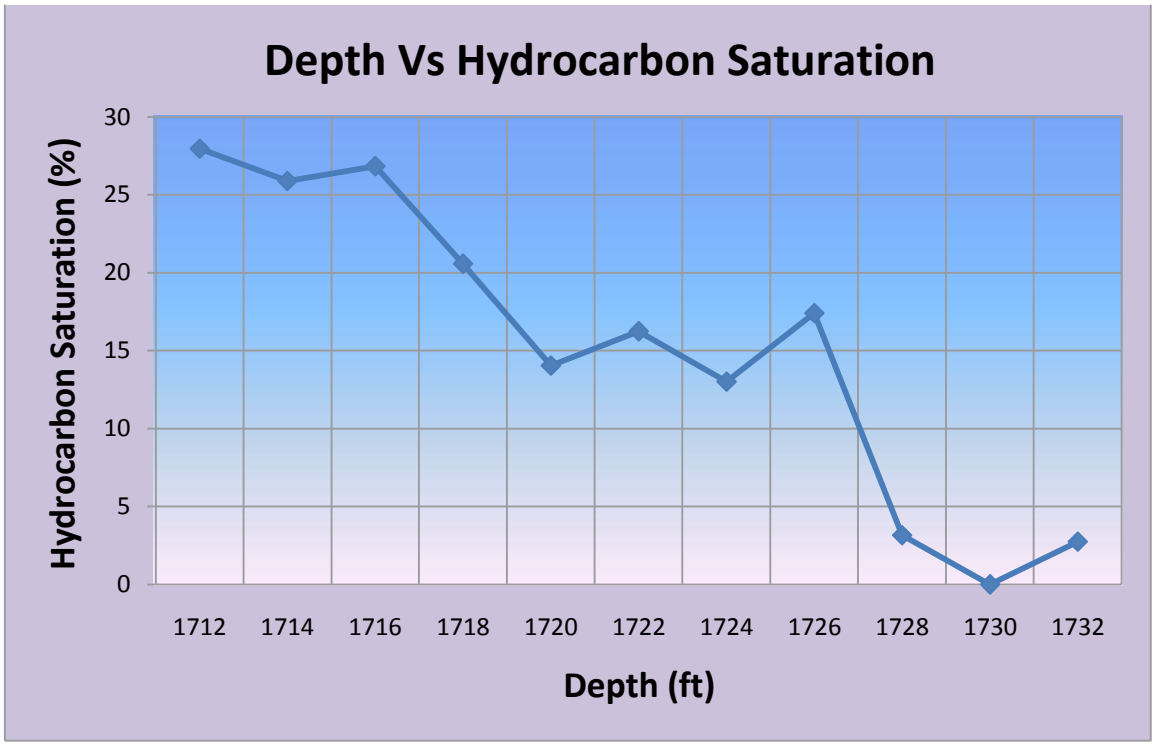

Graph 8.4: Graph showing relationship of hydrocarbon saturation with depth in zone 1, Mari deep 6, Central Indus Basin

Zone 2

Depth (ft)	Volume of Shale (V_{sh}) (%)	Porosity (Φ) (%)	Water Resistivity (Rw) (Ωm)	Water Saturation (S_w) (%)	Saturation of Hydrocarbons (S_{hc}) (%)	Permeability	Lithology
2250	30.43478	24.2	0.18	78.40358	21.59642	N/A	Limestone
2260	14.49275	23.5	0.18	42.55319	57.44681	80	Limestone
2270	8.695652	17	0.18	26.30668	73.69332	50	Limestone
2280	11.5942	15.3	0.18	22.64119	77.35881	47	Limestone
2290	15.94203	20	0.18	15.38968	84.61032	320	Limestone
2300	7.246377	16.1	0.18	26.35181	73.64819	40	Limestone
2310	10.14493	20.8	0.18	12.18972	87.81028	600	Limestone
2320	10.14493	19.8	0.18	7.824209	92.17579	1200	Limestone
2330	8.695652	15.5	0.18	17.31149	82.68851	80	Limestone
2340	7.246377	20.3	0.18	13.21814	86.78186	500	Limestone
2350	5.797101	19.6	0.18	15.30612	84.69388	340	Limestone
2360	8.695652	23	0.18	12.16311	87.83689	900	Limestone
2370	10.14493	18	0.18	16.66667	83.33333	180	Limestone
2380	13.04348	19.5	0.18	21.75713	78.24287	150	Limestone
2390	7.246377	20.8	0.18	17.88963	82.11037	320	Limestone
2400	1.449275	17.5	0.18	23.11542	76.88458	75	Limestone
2410	11.5942	24.2	0.18	20.95424	79.04576	400	Limestone
2420	7.246377	22.2	0.18	24.67219	75.32781	170	Limestone
2430	14.49275	27	0.18	18.78121	81.21879	800	Limestone
2440	18.84058	26	0.18	18.24391	81.75609	750	Limestone
2450	14.49275	26	0.18	26.47105	73.52895	350	Limestone
2460	1.449275	25	0.18	30.98387	69.01613	200	Limestone
2470	4.347826	24	0.18	45.64355	54.35645	80	Limestone
2480	11.5942	27	0.18	78.56742	21.43258	N/A	Limestone
2490	5.797101	27	0.18	95.62922	4.370782	N/A	Limestone

Table 8.2: Table showing interpretation of zone 2, Mari deep 6, Central Indus Basin

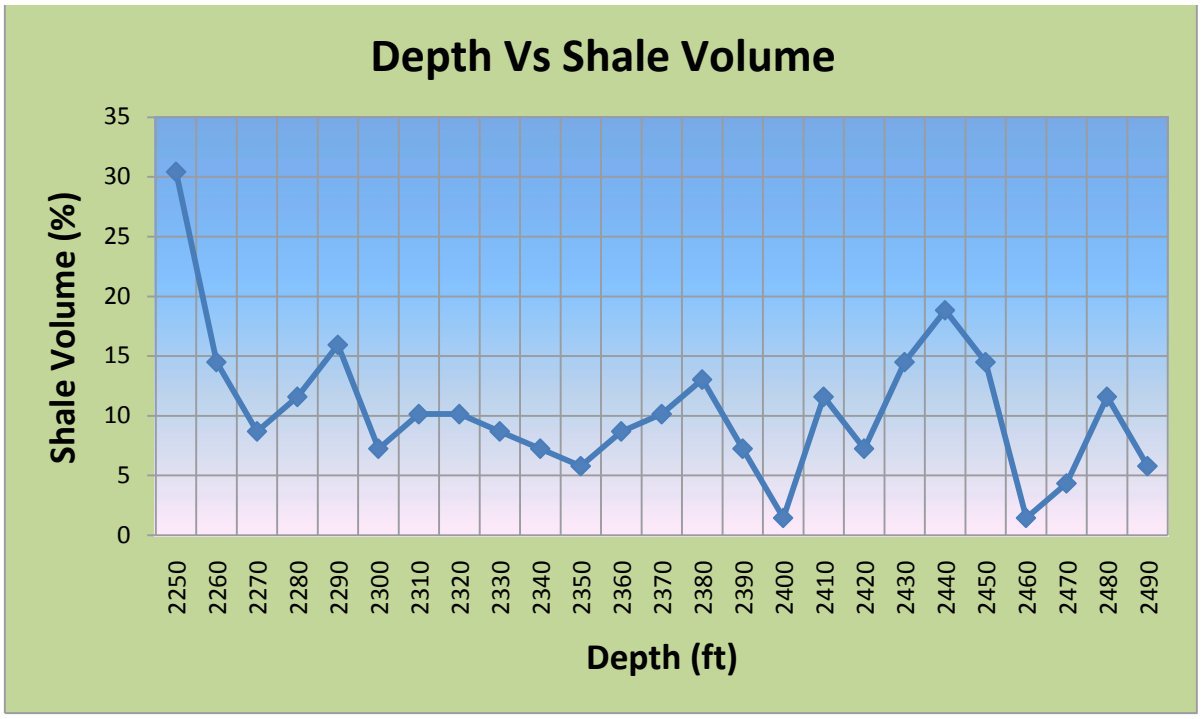

Graph 8.5: Graph showing relationship of shale volume with depth in zone 2, Mari deep 6, Central Indus Basin

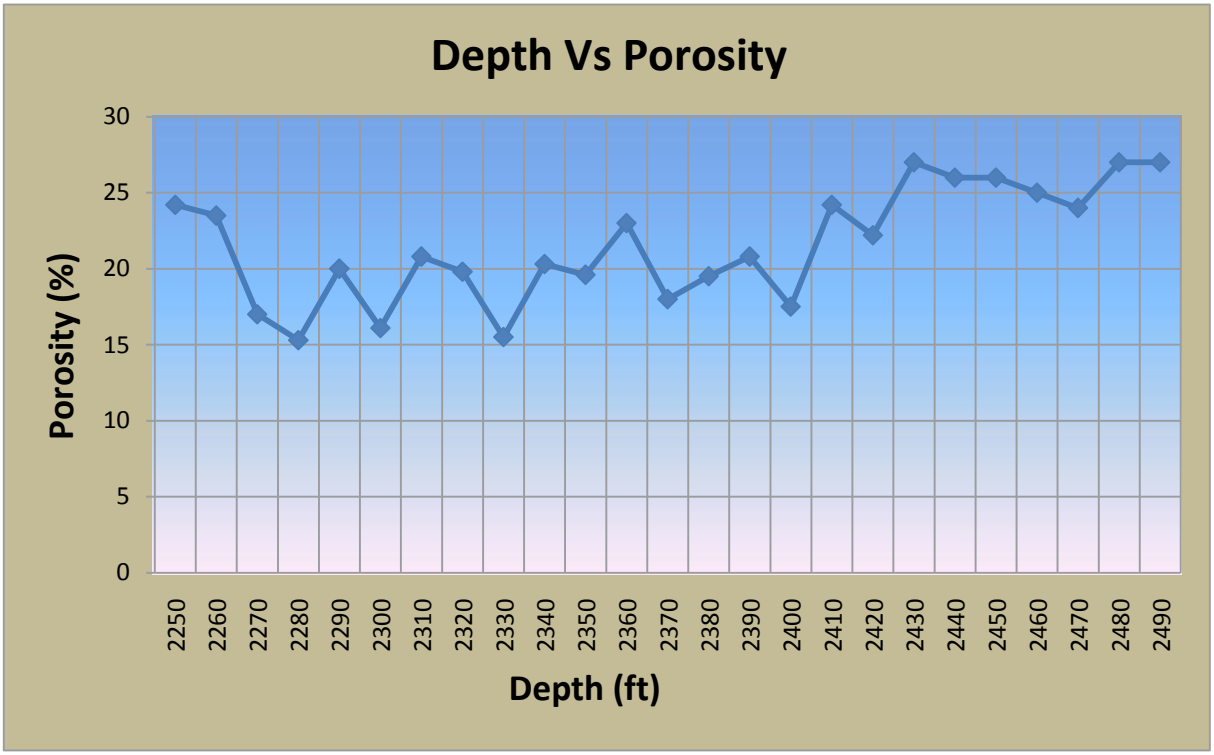

Graph 8.6: Graph showing relationship of porosity with depth in zone 2, Mari deep 6, Central Indus Basin

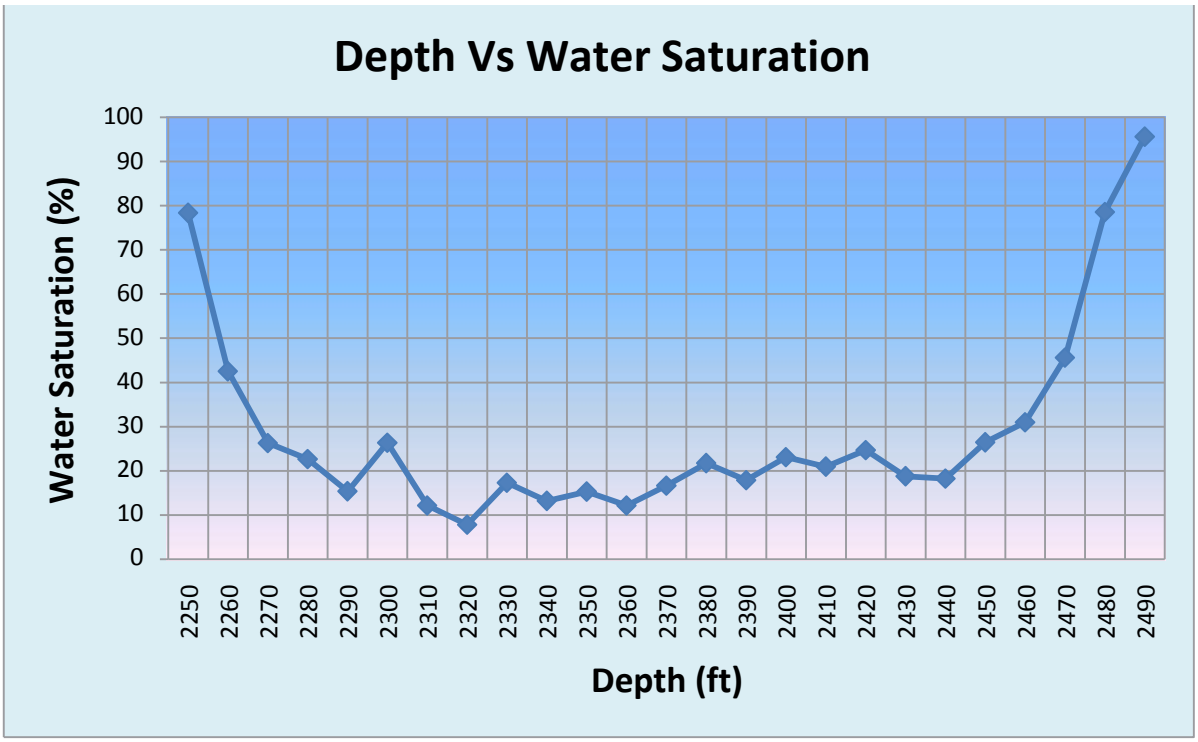

Graph 8.7: Graph showing relationship of water saturation with depth in zone 2, Mari deep 6, Central Indus Basin

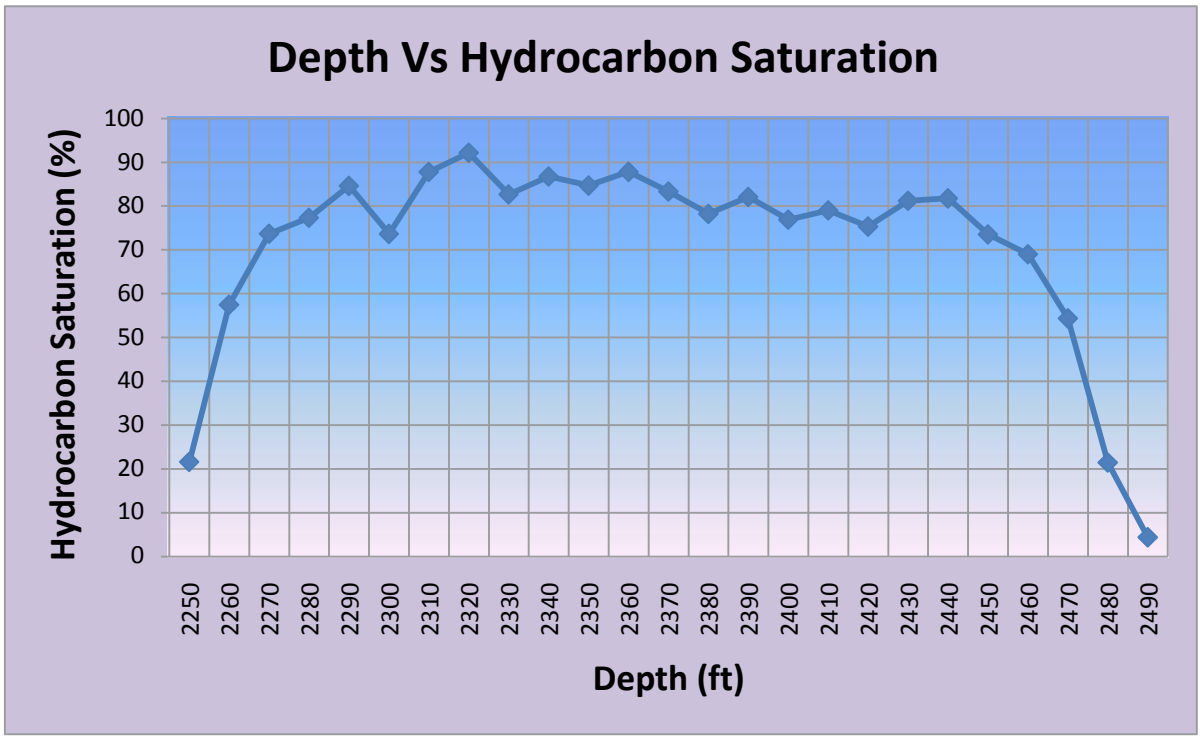

Graph 8.8: Graph showing relationship of hydrocarbon saturation with depth in zone 2, Mari deep 6, Central Indus Basin

Zone 3

Depth (ft)	Volume of Shale (V_{Sh}) (%)	Porosity (Φ) (%)	Water Resistivity (Rw) (Ωm)	Water saturation (S_w) (%)	Saturation of Hydrocarbons (S_{hc}) (%)	Permeability	Lithology
8744	17.64706	9	0.121	86.42416	13.57584	N/A	Sandstone
8746	3.921569	8	0.121	64.81812	35.18188	N/A	Sandstone
8748	3.921569	9	0.121	61.11111	38.88889	N/A	Sandstone
8750	2.941176	11	0.121	40.82483	59.17517	4	Sandstone
8752	3.921569	11	0.121	57.73503	42.26497	1.5	Sandstone
8754	4.901961	10	0.121	63.50853	36.49147	N/A	Sandstone
8756	5.882353	12	0.121	52.92377	47.07623	3	Sandstone
8758	18.62745	10	0.121	89.81462	10.18538	N/A	Sandstone
8760	97.05882	19	0.121	57.89474	42.10526	18	Sandstone

Table 8.3: Table showing interpretation of zone 3, Mari deep 6, Central Indus Basin

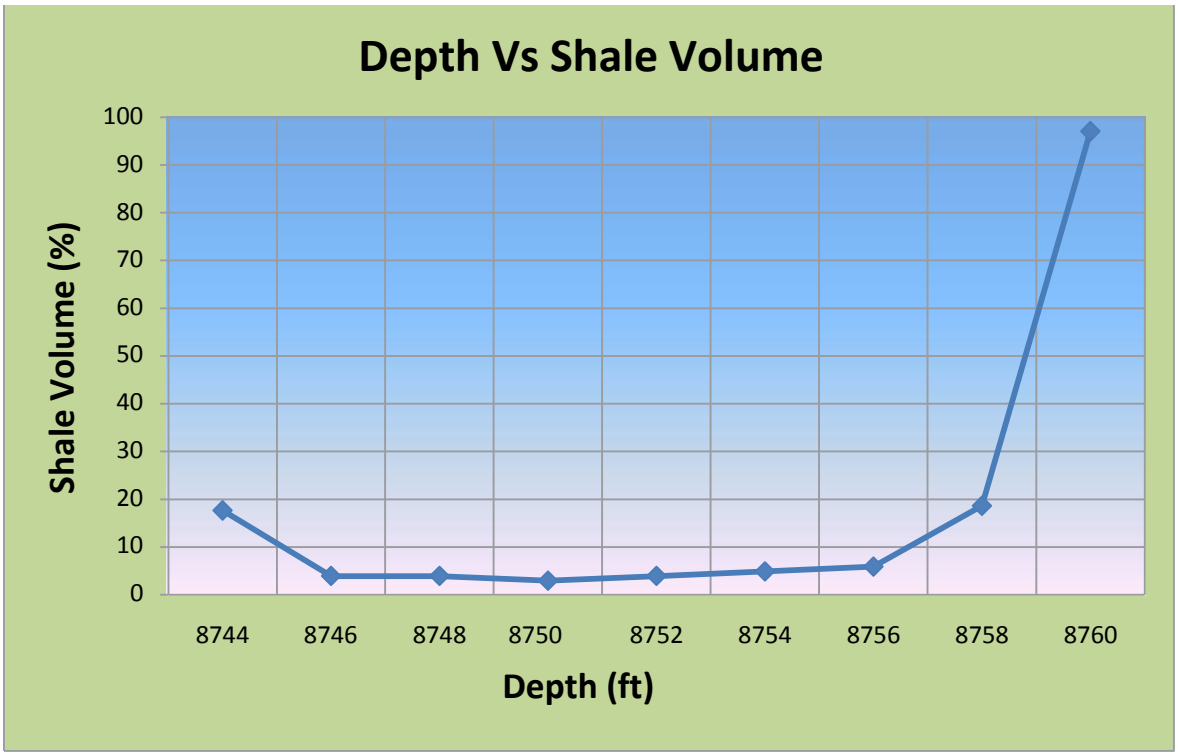

Graph 8.9: Graph showing relationship of shale volume with depth in zone 3, Mari deep 6, Central Indus Basin

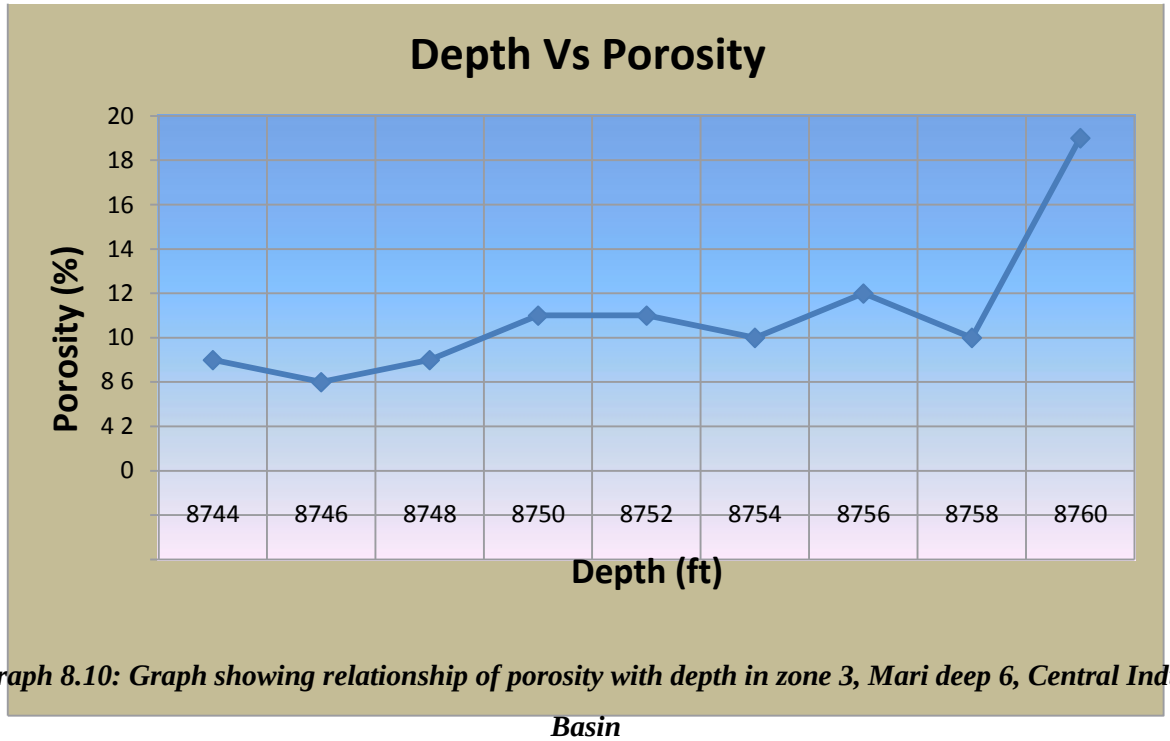

Graph 8.10: Graph showing relationship of porosity with depth in zone 3, Mari deep 6, Central Indus Basin

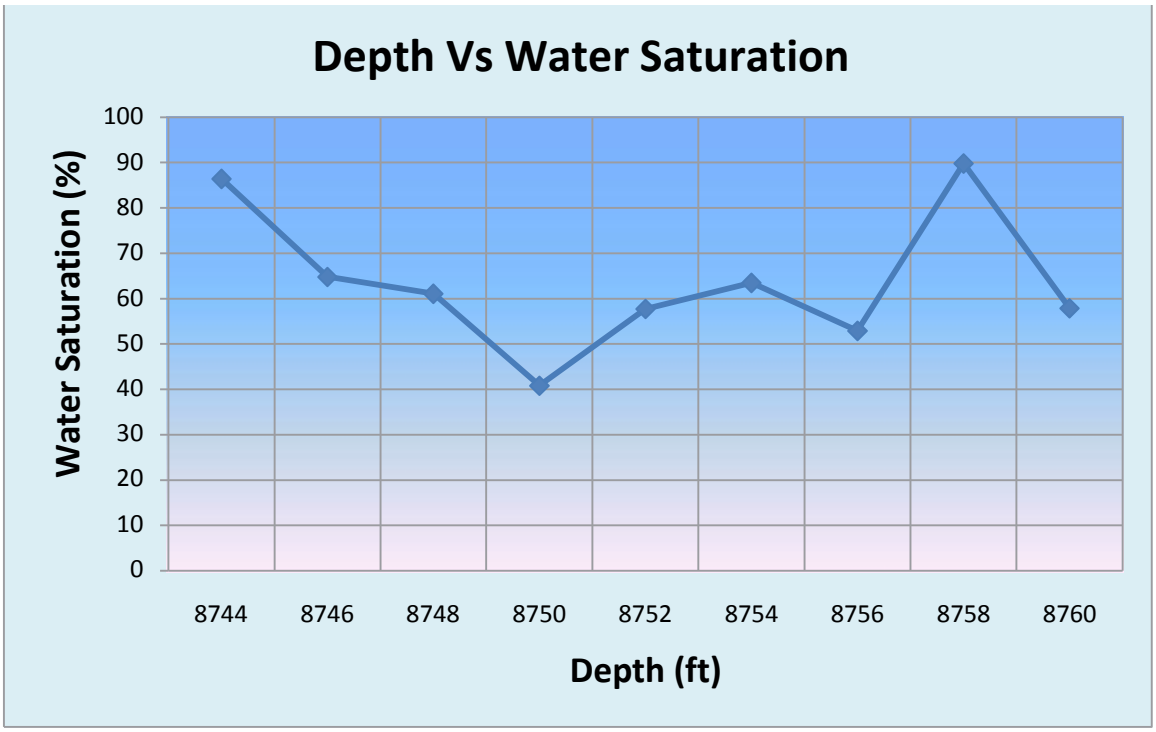

Graph 8.11: Graph showing relationship of water saturation with depth in zone 3, Mari deep 6, Central Indus Basin

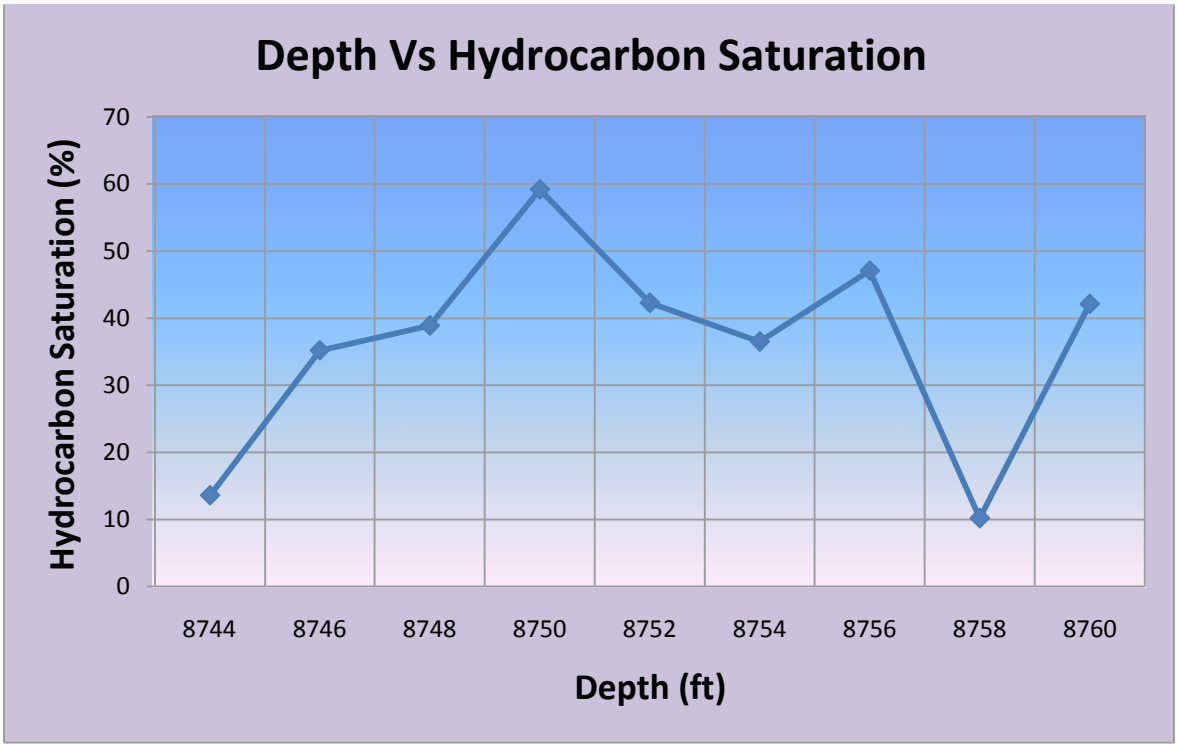

Graph 8.12: Graph showing relationship of hydrocarbon saturation with depth in zone 3, Mari deep 6, Central Indus Basin

Zone 4

Depth (ft)	Volume of Shale (V_{Sh}) (%)	Porosity (Φ) (%)	Water Resistivity (R_w) (Ωm)	Water Saturation (S_w) (%)	Saturation of Hydrocarbons (S_{hc}) (%)	Permeability	Lithology
8858	93.57798	13	0.121	63.06858	36.93142	N/A	Sandstone
8860	6.422018	11	0.121	22.36068	77.63932	10	Sandstone
8862	5.504587	9	0.121	31.55764	68.44236	2	Sandstone
8864	12.84404	8	0.121	35.50235	64.49765	1	Sandstone
8866	12.84404	9	0.121	38.65006	61.34994	1.5	Sandstone
8868	19.26606	10	0.121	33.16625	66.83375	3	Sandstone
8870	9.174312	9	0.121	30.55556	69.44444	2	Sandstone
8872	9.174312	8	0.121	38.13564	61.86436	1	Sandstone
8874	6.422018	8	0.121	43.48132	56.51868	0.7	Sandstone
8876	6.422018	9	0.121	53.59799	46.40201	0.8	Sandstone
8878	38.53211	11	0.121	53.45225	46.54775	2	Sandstone
8880	17.43119	9	0.121	52.11573	47.88427	0.8	Sandstone
8882	3.669725	10	0.121	24.59675	75.40325	5	Sandstone
8884	5.504587	10	0.121	28.40188	71.59812	4	Sandstone
8886	6.422018	9	0.121	40.74074	59.25926	1.3	Sandstone
8888	26.6055	9	0.121	28.0397	71.9603	3	Sandstone
8890	3.669725	13	0.121	13.37887	86.62113	65	Sandstone
8892	1.834862	12	0.121	16.73597	83.26403	30	Sandstone
8894	2.752294	11	0.121	20	80	14	Sandstone
8896	2.752294	11	0.121	15.81139	84.18861	20	Sandstone
8898	3.669725	14	0.121	11.11168	88.88832	130	Sandstone
8900	0	15	0.121	18.93459	81.06541	60	Sandstone
8902	6.422018	11	0.121	57.73503	42.26497	1.6	Sandstone
8904	58.7156	13	0.121	84.61538	15.38462	N/A	Sandstone

Table 8.4: Table showing interpretation of zone 4, Mari deep 6, Central Indus Basin

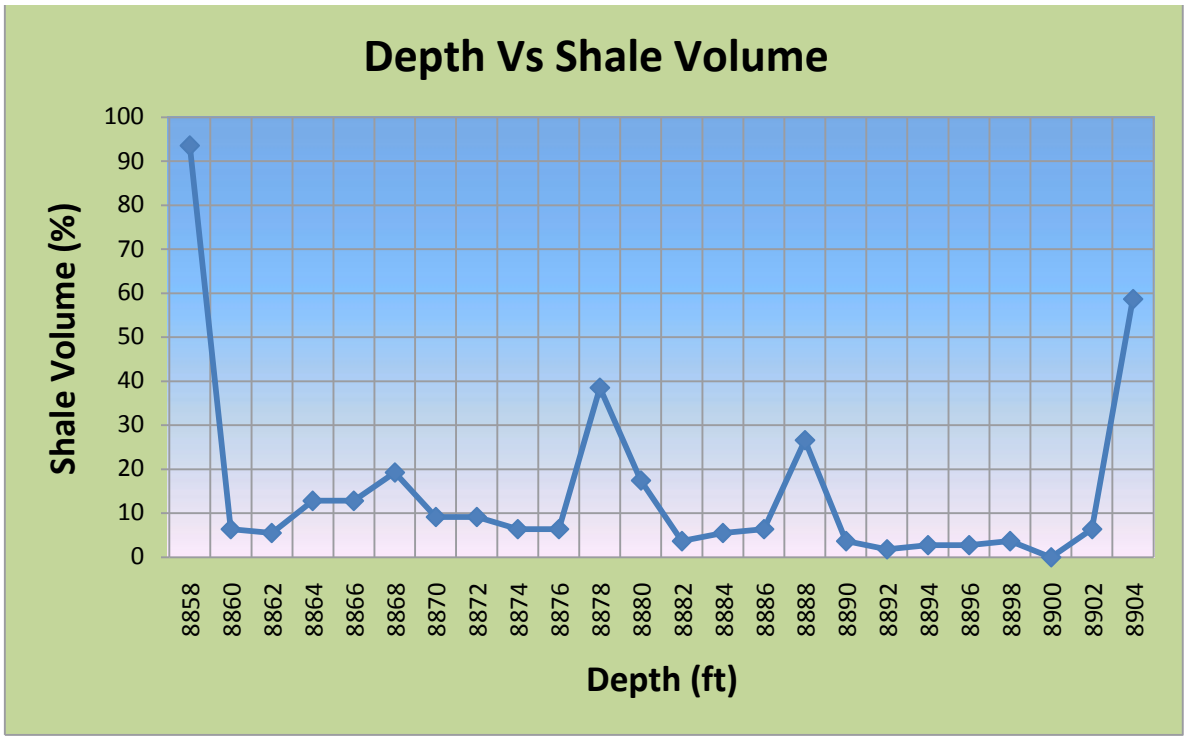

Graph 8.13: Graph showing relationship of Shale volume with depth in zone 4, Mari deep 6, Central Indus Basin

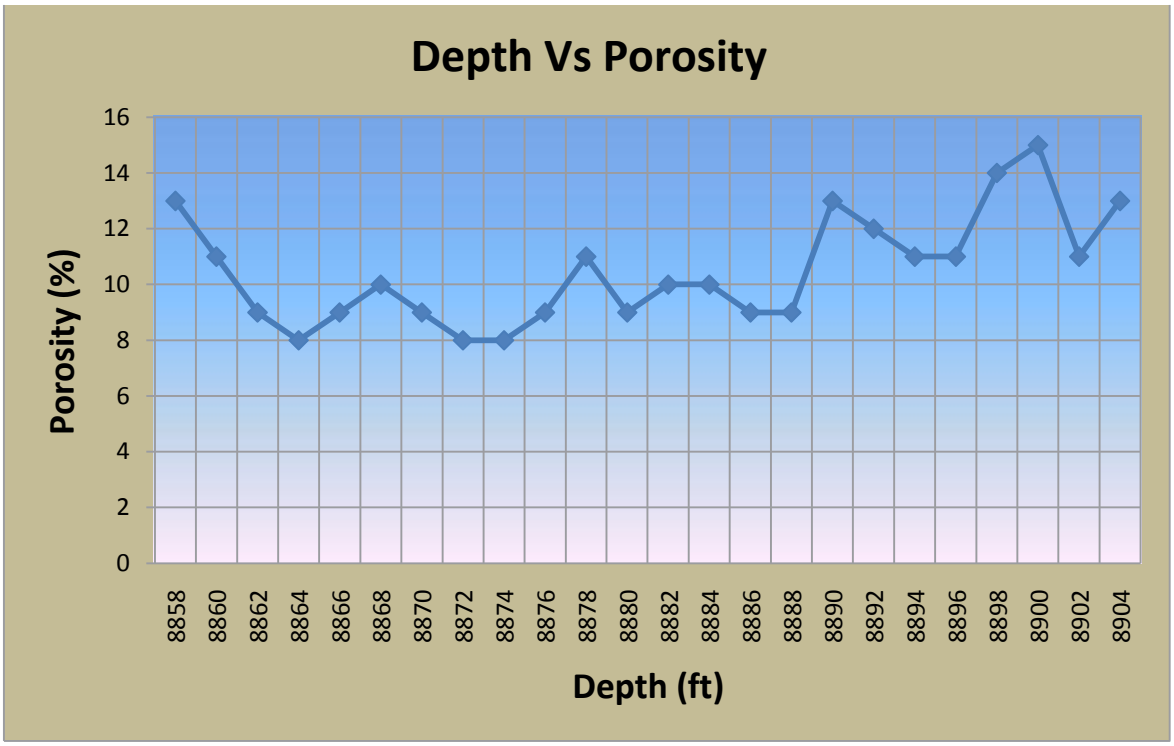

Graph 8.14: Graph showing relationship of porosity with depth in zone 4, Mari deep 6, Central Indus Basin

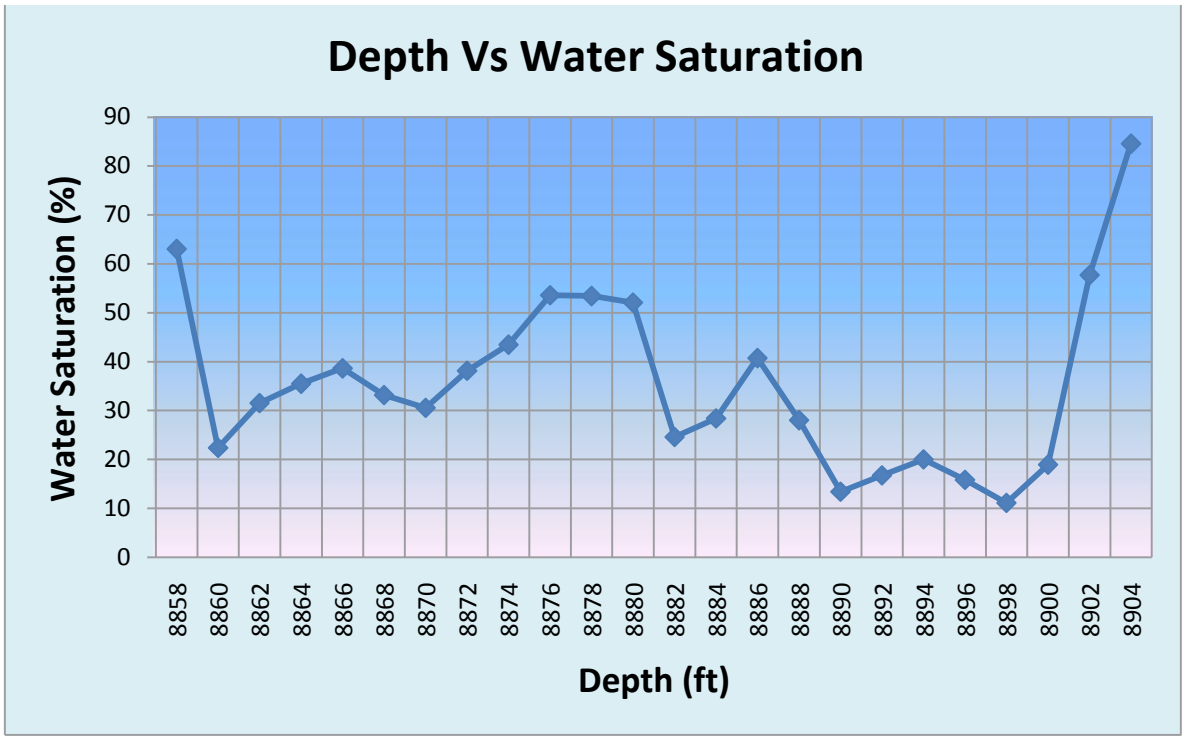

Graph 8.15: Graph showing relationship of water saturation with depth in zone 4, Mari deep 6, Central Indus Basin

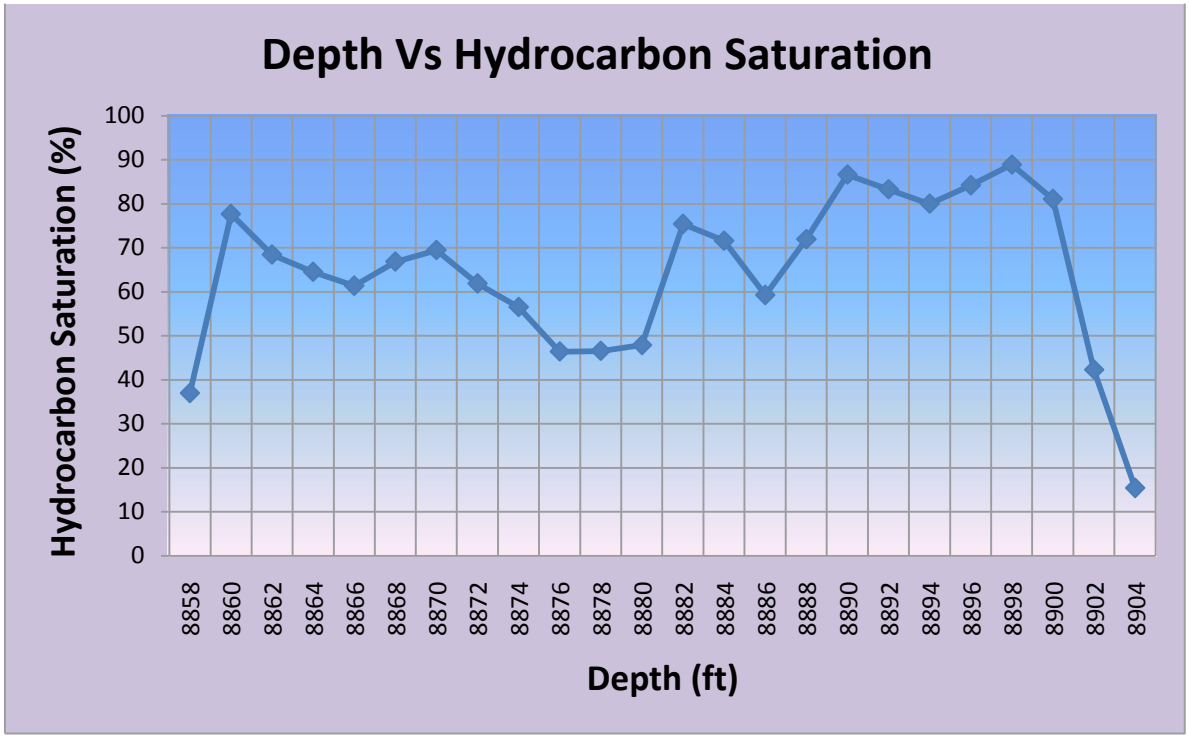

Graph 8.16: Graph showing relationship of hydrocarbon saturation with depth in zone 4, Mari deep 6, Central Indus Basin

Zone 5

Depth (ft)	Volume of Shale (V_{Sh}) (%)	Porosity (Φ) (%)	Water Resistivity (R_w) (Ωm)	Water Saturation (S_w) (%)	Saturation of Hydrocarbons (S_{hc}) (%)	Permeability	Lithology
8919	48	12	0.121	45.83333	54.16667	4	Sandstone
8920	33	13	0.121	37.84115	62.15885	8	Sandstone
8922	0	13	0.121	15.44858	84.55142	47	Sandstone
8924	0	12	0.121	23.66823	76.33177	15	Sandstone
8926	8	9	0.121	40.74074	59.25926	1.5	Sandstone
8928	6	10	0.121	33.16625	66.83375	3.5	Sandstone
8930	3	12	0.121	30.55556	69.44444	8	Sandstone
8932	9	11	0.121	31.62278	68.37722	5	Sandstone
8934	1	12	0.121	25.42376	74.57624	12	Sandstone
8936	2	13	0.121	21.8476	78.1524	25	Sandstone
8938	3	11	0.121	31.62278	68.37722	5	Sandstone
8940	8	9	0.121	36.85139	63.14861	1.8	Sandstone
8942	0	12	0.121	28.98755	71.01245	9	Sandstone
8944	8	11	0.121	31.62278	68.37722	5	Sandstone
8946	1	13	0.121	18.92058	81.07942	35	Sandstone
8948	3	13	0.121	21.8476	78.1524	20	Sandstone
8950	7	13	0.121	31.98161	68.01839	10	Sandstone
8952	1	12	0.121	23.66823	76.33177	15	Sandstone

8954	1	13	0.121	21.8476	78.1524	25	Sandstone
8956	0	14	0.121	15.71429	84.28571	70	Sandstone
8958	2	12	0.121	28.98755	71.01245	6	Sandstone
8960	0	13	0.121	33.18888	66.81112	10	Sandstone
8962	0	13	0.121	36.08012	63.91988	8	Sandstone
8964	6	11	0.121	70.71068	29.28932	N/A	Sandstone
8966	3	11	0.121	53.45225	46.54775	1.9	Sandstone
8968	3	11	0.121	47.14045	52.85955	2.5	Sandstone
8970	5	11	0.121	50	50	2	Sandstone
8972	3	11	0.121	53.45225	46.54775	1.8	Sandstone
8974	10	11	0.121	63.24555	36.75445	N/A	Sandstone
8976	11	10	0.121	77.78175	22.21825	N/A	Sandstone
8978	14	11	0.121	81.64966	18.35034	N/A	Sandstone
8980	13	10	0.121	89.81462	10.18538	N/A	Sandstone
8982	26	10	0.121	100	0	N/A	Sandstone
8984	23	9	0.121	100	0	N/A	Sandstone
8986	11	11	0.121	81.64966	18.35034	N/A	Sandstone
8988	20	9	0.121	100	0	N/A	Sandstone
8990	20	9	0.121	100	0	N/A	Sandstone
8991	63	10	0.121	100	0	N/A	Sandstone

Table 8.5: Table showing interpretation of zone 5, Mari deep 6, Central Indus Basin

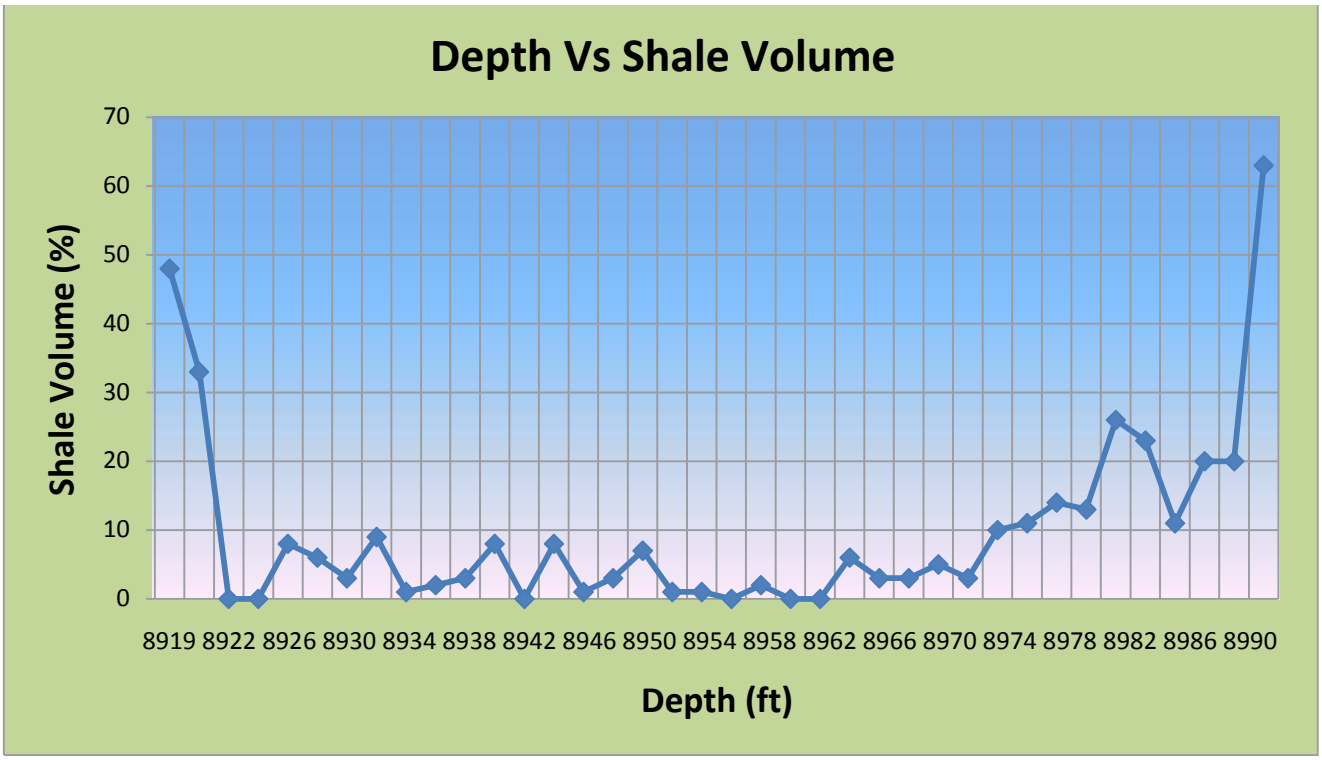

Graph 8.17: Graph showing relationship of shale volume with depth in zone 5, Mari deep 6, Central Indus Basin

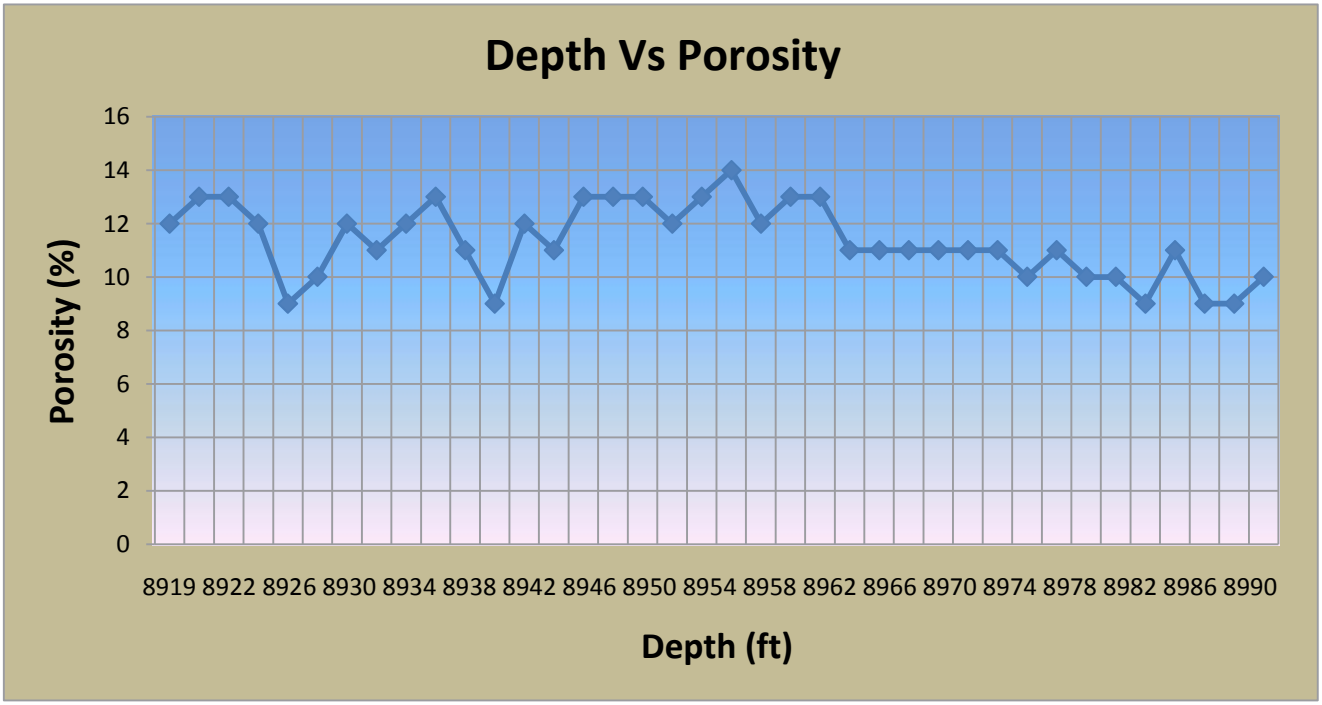

Graph 8.18: Graph showing relationship of porosity with depth in zone 5, Mari deep 6, Central Indus Basin

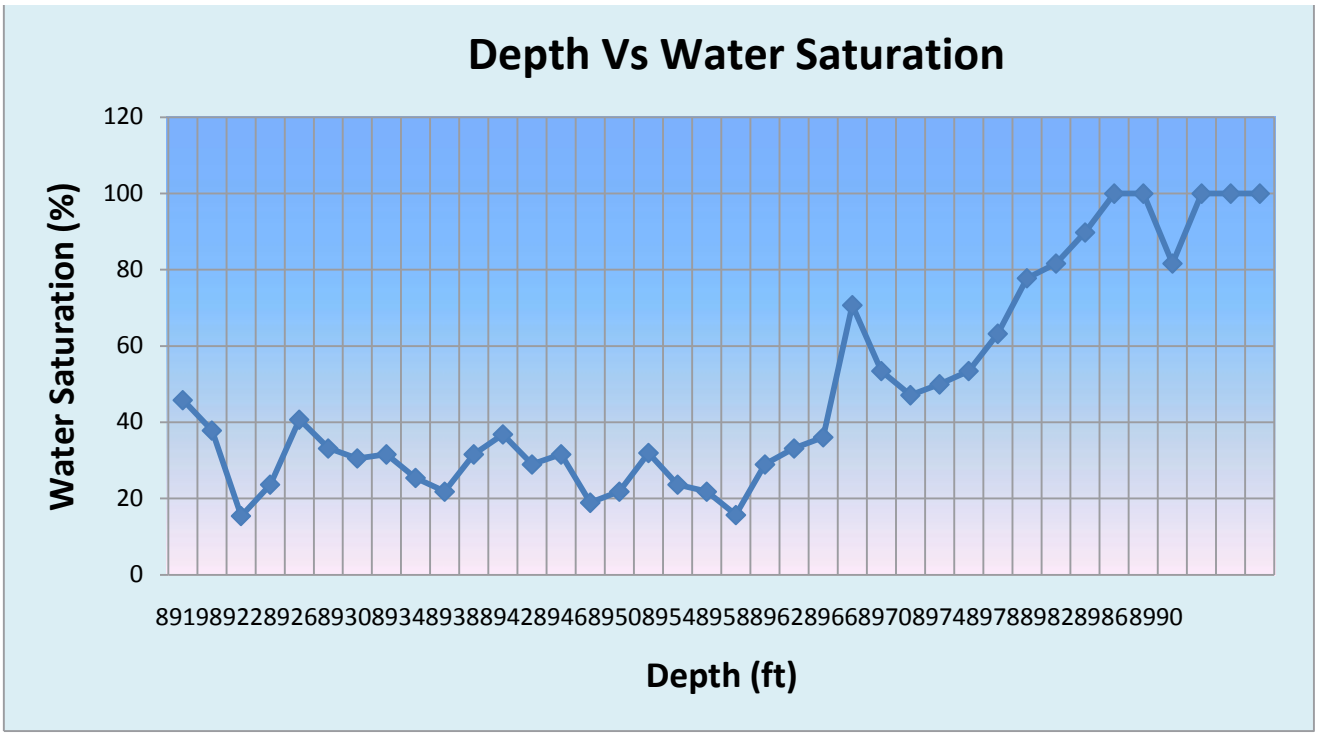

Graph 8.19: Graph showing relationship of water saturation with depth in zone 5, Mari deep 6, Central Indus Basin

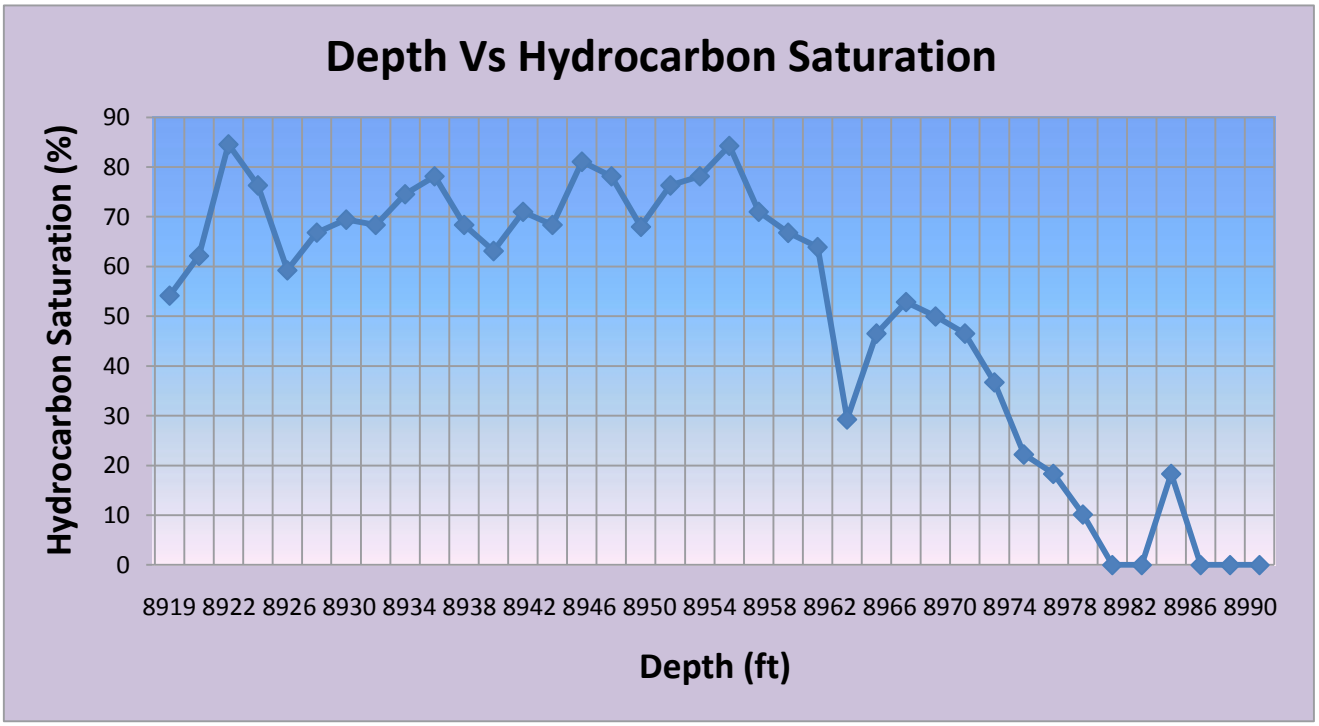

Graph 8.20: Graph showing relationship of hydrocarbon saturation with depth in zone 5, Mari deep 6, Central Indus Basin

Zone 6

Depth (ft)	Volume of Shale (V_{Sh}) (%)	Porosity (Φ) (%)	Water Resistivity (R_w) (Ωm)	Water Saturation (S_w) (%)	Saturation of Hydrocarbons (S_{hc}) (%)	Permeability	Lithology
9209	29.26829	14	0.121	100	0	N/A	Sandstone
9210	9.756098	14	0.121	100	0	N/A	Sandstone
9212	14.63415	13	0.121	100	0	N/A	Sandstone
9214	13.41463	13	0.121	100	0	N/A	Sandstone
9216	10.97561	12	0.121	100	0	N/A	Sandstone
9218	19.5122	11	0.121	100	0	N/A	Sandstone
9220	24.39024	14	0.121	100	0	N/A	Sandstone
9222	23.17073	14	0.121	100	0	N/A	Sandstone
9224	19.5122	16	0.121	100	0	N/A	Sandstone
9225	9.756098	12	0.121	100	0	N/A	Sandstone

Table 8.6: Table showing interpretation of zone 6, Mari deep 6, Central Indus Basin

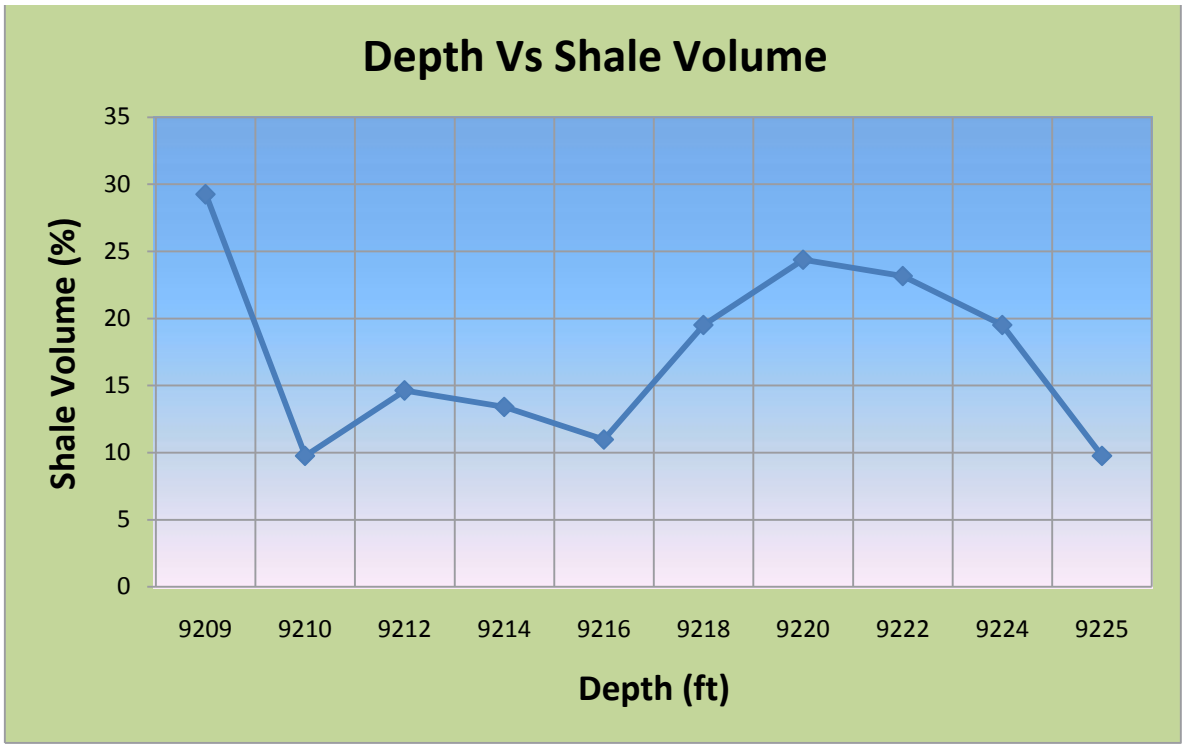

Graph 8.21: Graph showing relationship of shale volume with depth in zone 6, Mari deep 6, Central Indus Basin

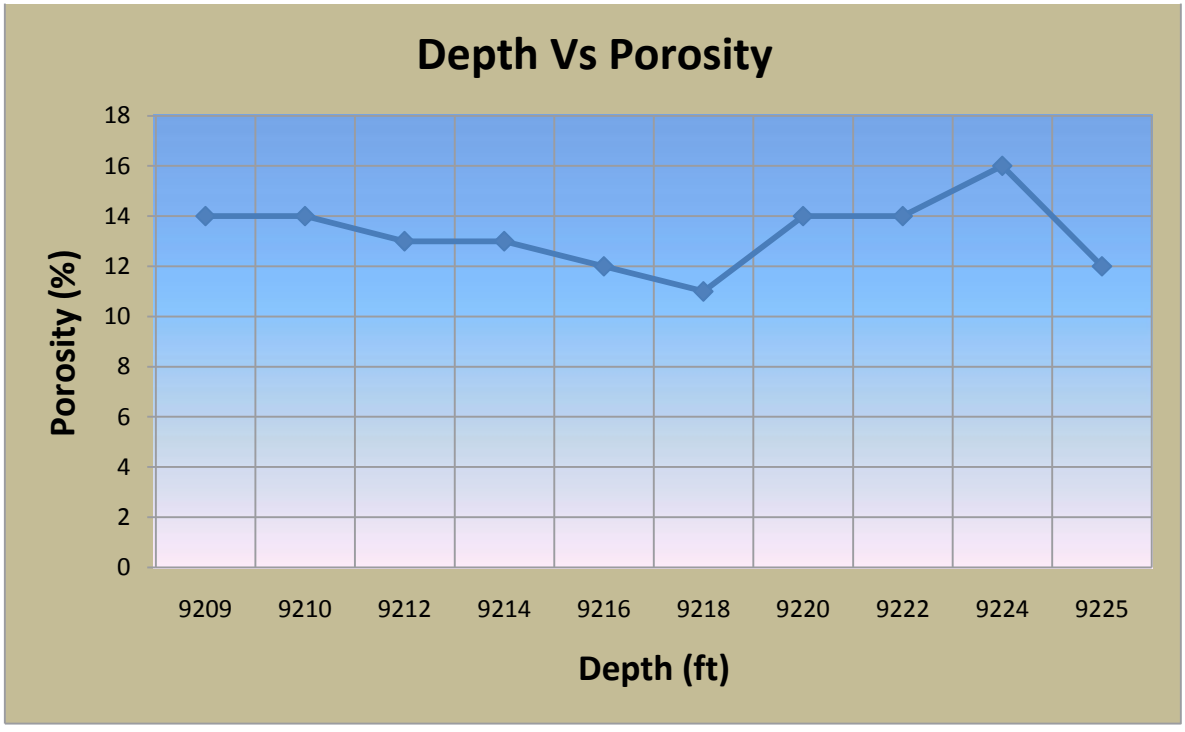

Graph 8.22: Graph showing relationship of porosity with depth in zone 6, Mari deep 6, Central Indus Basin

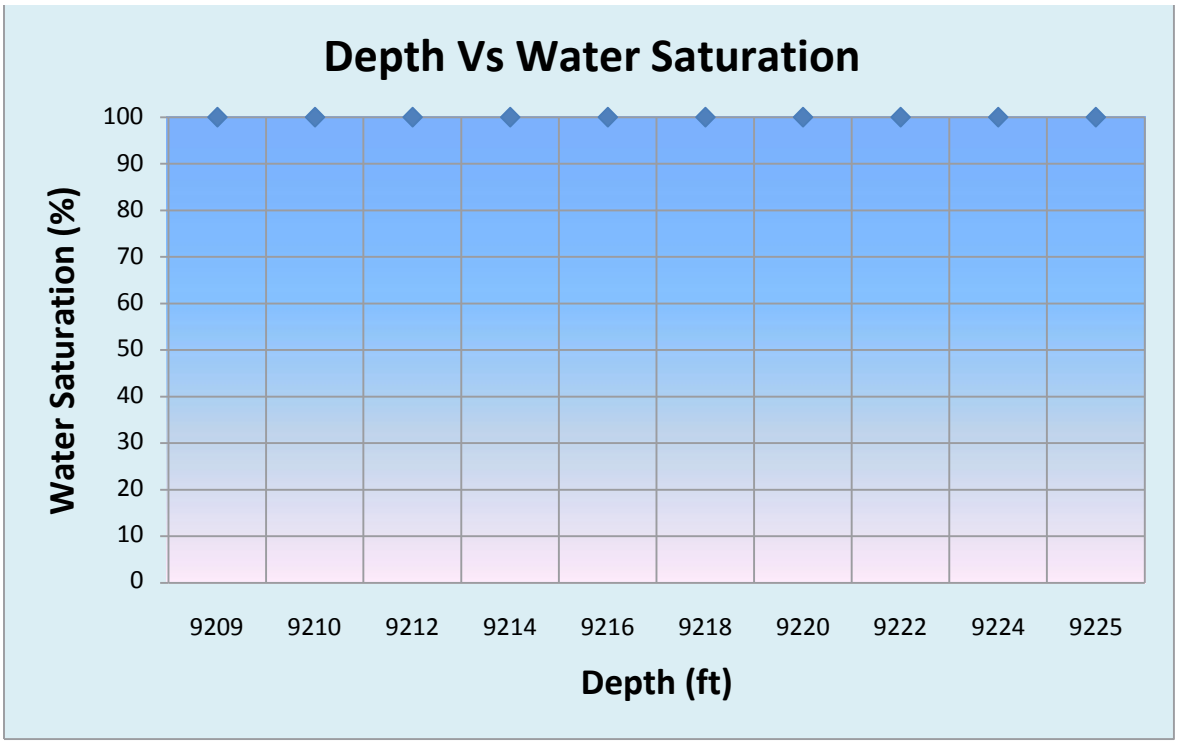

Graph 8.23: Graph showing relationship of water saturation with depth in zone 6, Mari deep 6, Central Indus Basin

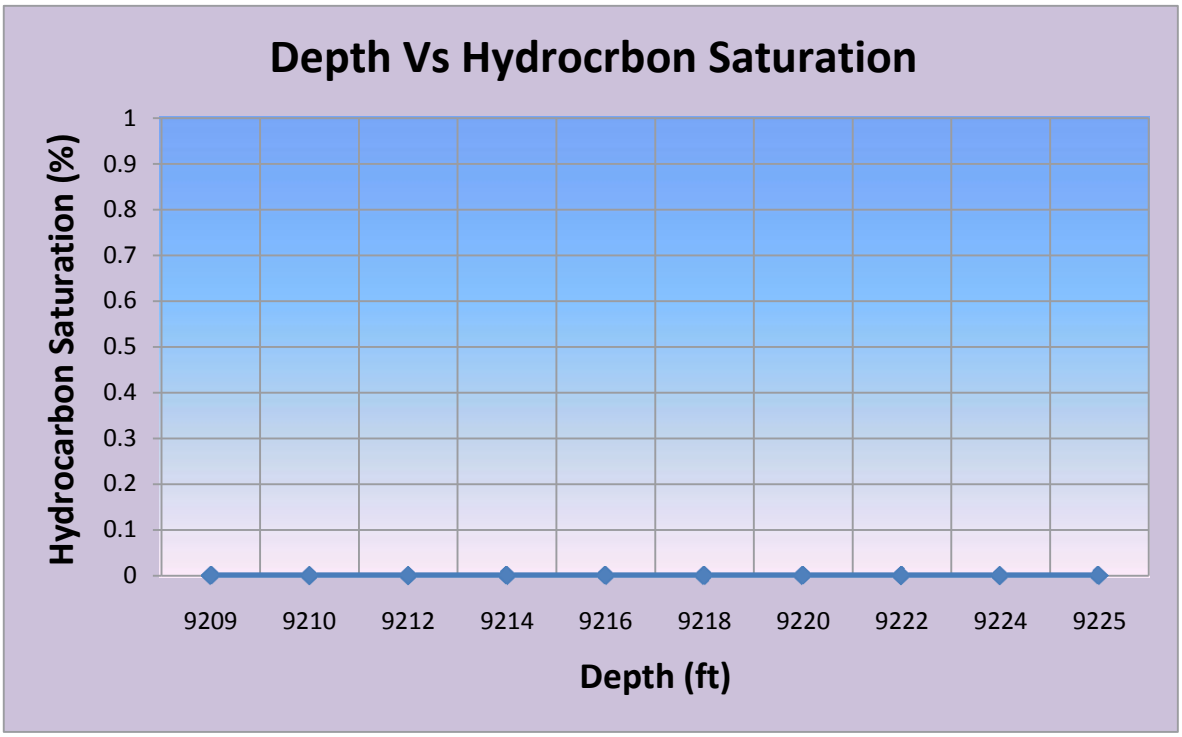

Graph 8.24: Graph showing relationship of hydrocarbon saturation with depth in zone 6, Mari deep 6, Central Indus Basin

8.2 Interpretation of Mari deep 9, Central Indus Basin

In Mari deep 9, we came across three zones which were interpreted in order to evaluate the hydrocarbon potential of this well. Different parameters calculated, which were discussed in previous chapter, are given below:

Zone 1

Depth (ft)	Volume of Shale (V_{sh}) (%)	Porosity (Φ) (%)	Water Resistivity (R_w) (Ωm)	Water Saturation (S_w) (%)	Saturation of Hydrocarbons (S_{hc}) (%)	Permeability	Lithology
8903	46.39175	30.5	0.121	19.27786	80.72214	1450	Sandstone
8904	15.46392	15.5	0.121	25.09089	74.90911	42	Sandstone
8905	1.030928	10	0.121	34.78505	65.21495	3	Sandstone
8906	1.030928	11	0.121	25.81989	74.18011	8	Sandstone
8907	2.061856	12	0.121	20.49729	79.50271	19	Sandstone
8908	0	11	0.121	25.81989	74.18011	8	Sandstone
8909	0	12	0.121	32.40906	67.59094	7	Sandstone
8910	1.030928	11	0.121	33.33333	66.66667	4	Sandstone
8911	0	10	0.121	36.66667	63.33333	3	Sandstone
8912	0	12	0.121	33.47193	66.52807	7	Sandstone
8913	1.030928	12	0.121	34.64674	65.35326	6	Sandstone
8914	2.061856	11.5	0.121	47.82609	52.17391	3	Sandstone
8915	3.092784	12	0.121	57.97509	42.02491	3	Sandstone
8916	15.46392	13	0.121	59.83211	40.16789	4	Sandstone
8917	22.68041	14	0.121	55.55839	44.44161	5	Sandstone
8918	17.52577	14	0.121	55.55839	44.44161	5	Sandstone
8919	15.46392	11	0.121	81.64966	18.35034	5	Sandstone
8920	16.49485	14	0.121	78.57143	21.42857	N/A	Sandstone
8921	46.39175	19	0.121	69.19745	30.80255	N/A	Sandstone
8922	69.07216	25.5	0.121	55.68996	44.31004	N/A	Sandstone
8923	53.60825	27	0.121	52.59607	47.40393	75	Sandstone
						100	Sandstone

Table 8.7: Table showing interpretation of zone 1, Mari deep 9, Central Indus Basin

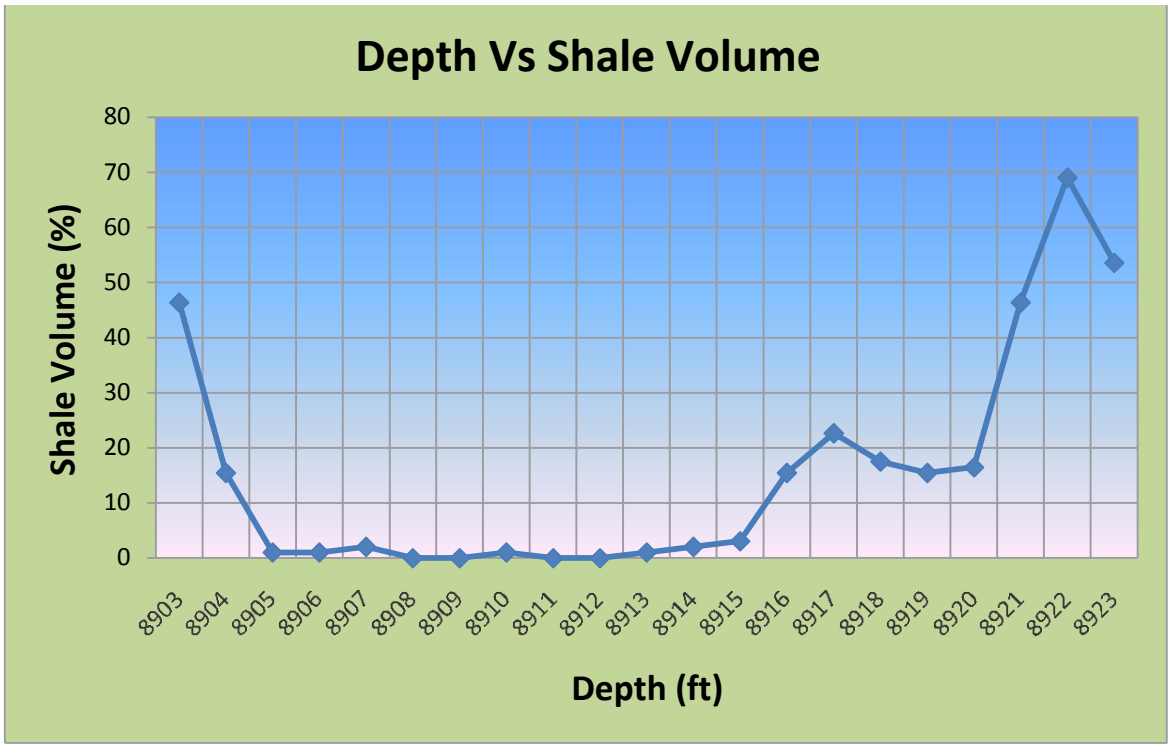

Graph 8.25: Graph showing relationship of shale volume with depth in zone 1, Mari deep 9, Central Indus Basin

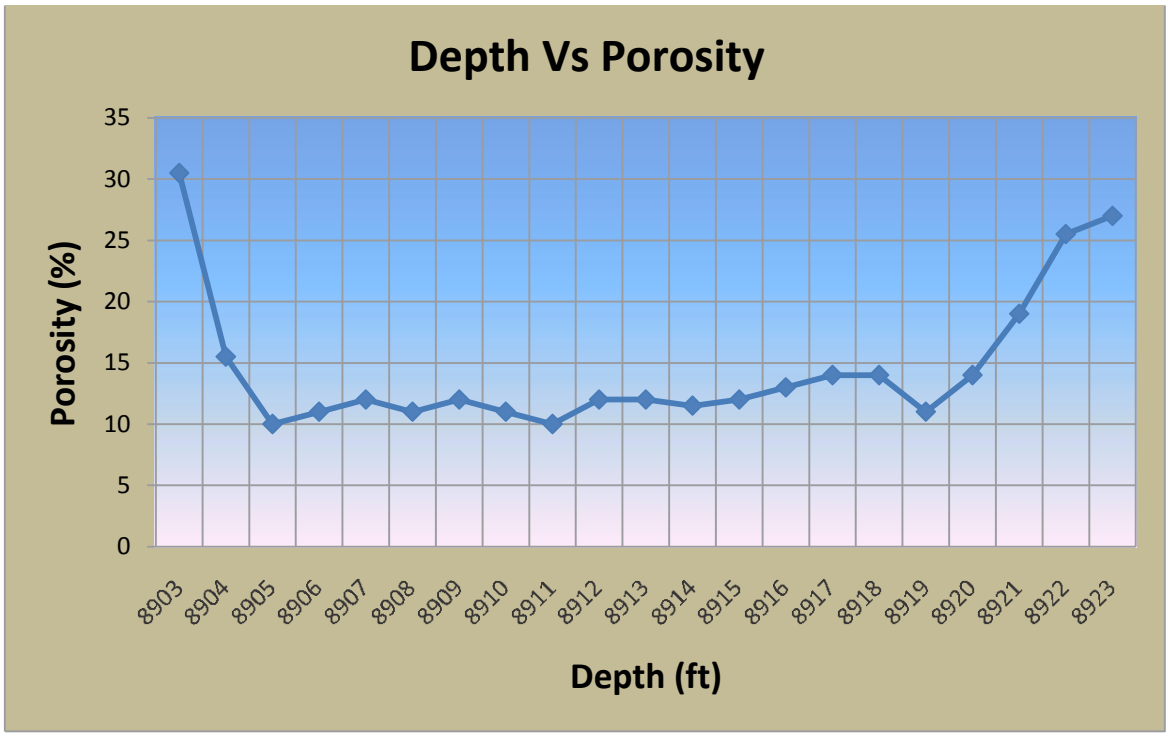

Graph 8.26: Graph showing relationship of porosity with depth in zone 1, Mari deep 9, Central Indus Basin

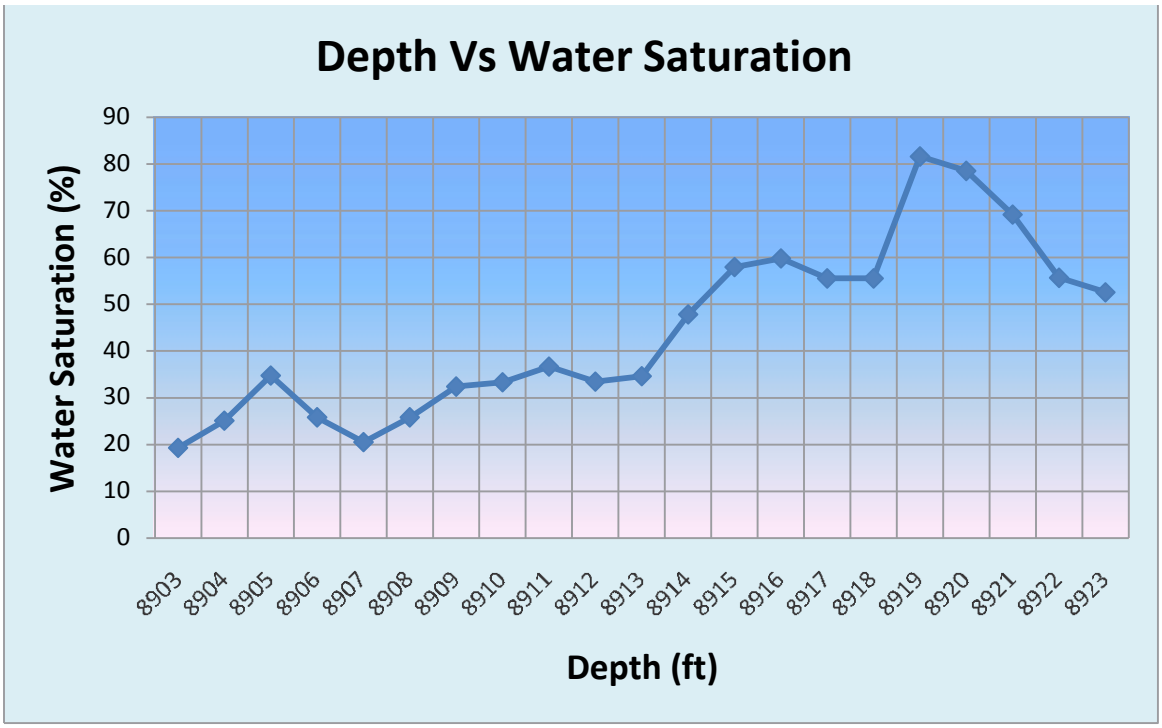

Graph 8.27: Graph showing relationship of water saturation with depth in zone 1, Mari deep 9, Central Indus Basin

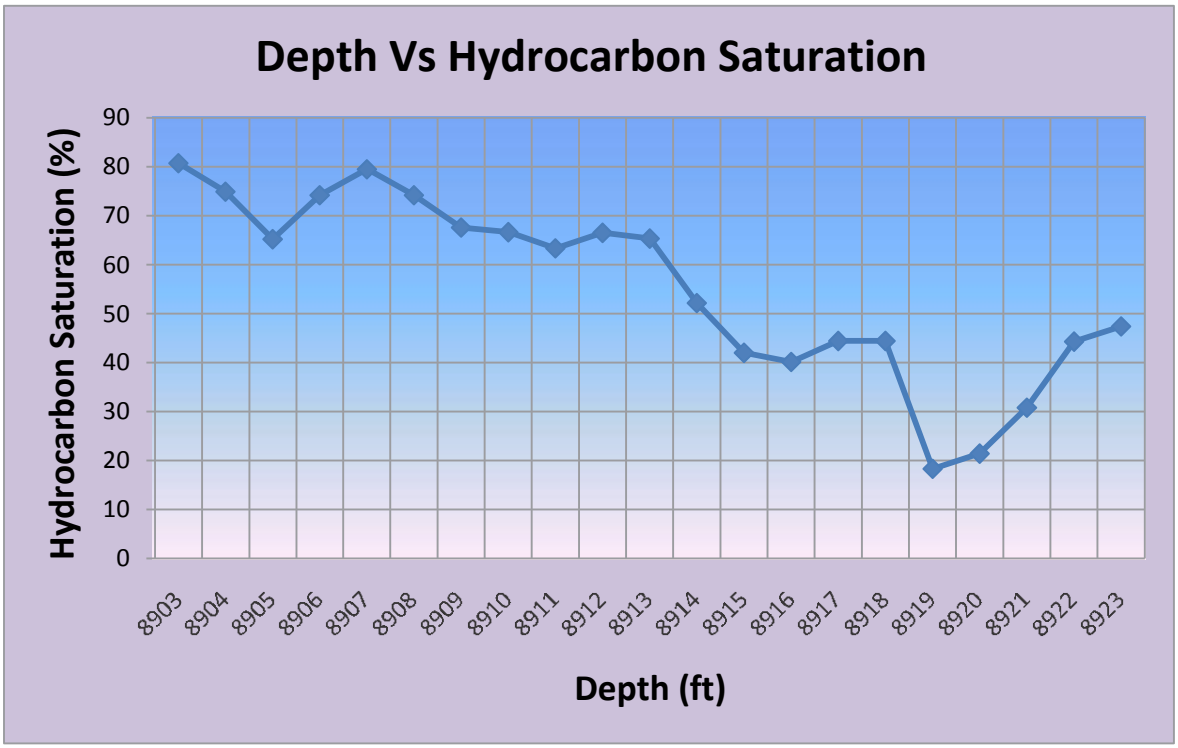

Graph 8.28: Graph showing relationship of hydrocarbon saturation with depth in zone 1, Mari deep 9, Central Indus Basin

Zone 2

Depth (ft)	Volume of Shale (V_{sh}) (%)	Porosity (Φ) (%)	Water Resistivity (R_w) (Ωm)	Water Saturation (S_w) (%)	Saturation of Hydrocarbons (S_{hc}) (%)	Permeability	Lithology
9010	3.370787	24	0.121	100	0	N/A	Sandstone
9011	0	18	0.121	100	0	N/A	Sandstone
9012	0	16	0.121	100	0	N/A	Sandstone
9013	0	17	0.121	100	0	N/A	Sandstone
9014	0	15	0.121	100	0	N/A	Sandstone
9015	2.247191	18	0.121	100	0	N/A	Sandstone
9016	2.247191	18	0.121	100	0	N/A	Sandstone
9017	2.247191	17	0.121	100	0	N/A	Sandstone
9018	2.247191	16	0.121	100	0	N/A	Sandstone
9019	7.865169	15	0.121	100	0	N/A	Sandstone
9020	6.741573	12	0.121	100	0	N/A	Sandstone
9021	2.247191	11	0.121	100	0	N/A	Sandstone
9022	0	12	0.121	100	0	N/A	Sandstone
9023	2.247191	12	0.121	100	0	N/A	Sandstone
9024	2.247191	12	0.121	100	0	N/A	Sandstone
9025	2.247191	12	0.121	100	0	N/A	Sandstone
9026	2.247191	14	0.121	100	0	N/A	Sandstone
9027	2.247191	14	0.121	100	0	N/A	Sandstone
9028	7.865169	14	0.121	100	0	N/A	Sandstone
9029	17.97753	12	0.121	100	0	N/A	Sandstone
9030	17.97753	11	0.121	100	0	N/A	Sandstone
9031	16.85393	12	0.121	100	0	N/A	Sandstone
9032	24.7191	20	0.121	77.78175	22.21825	N/A	Sandstone
9033	44.94382	23	0.121	57.16311	42.83689	N/A	Sandstone
9034	50.5618	25	0.121	44	56	45	Sandstone
9035	58.42697	30	0.121	36.66667	63.33333	100	Sandstone
9036	69.66292	27	0.121	38.84477	61.15523	375	Sandstone
						190	Sandstone

Table 8.8: Table showing interpretation of zone 2, Mari deep 9, Central Indus Basin

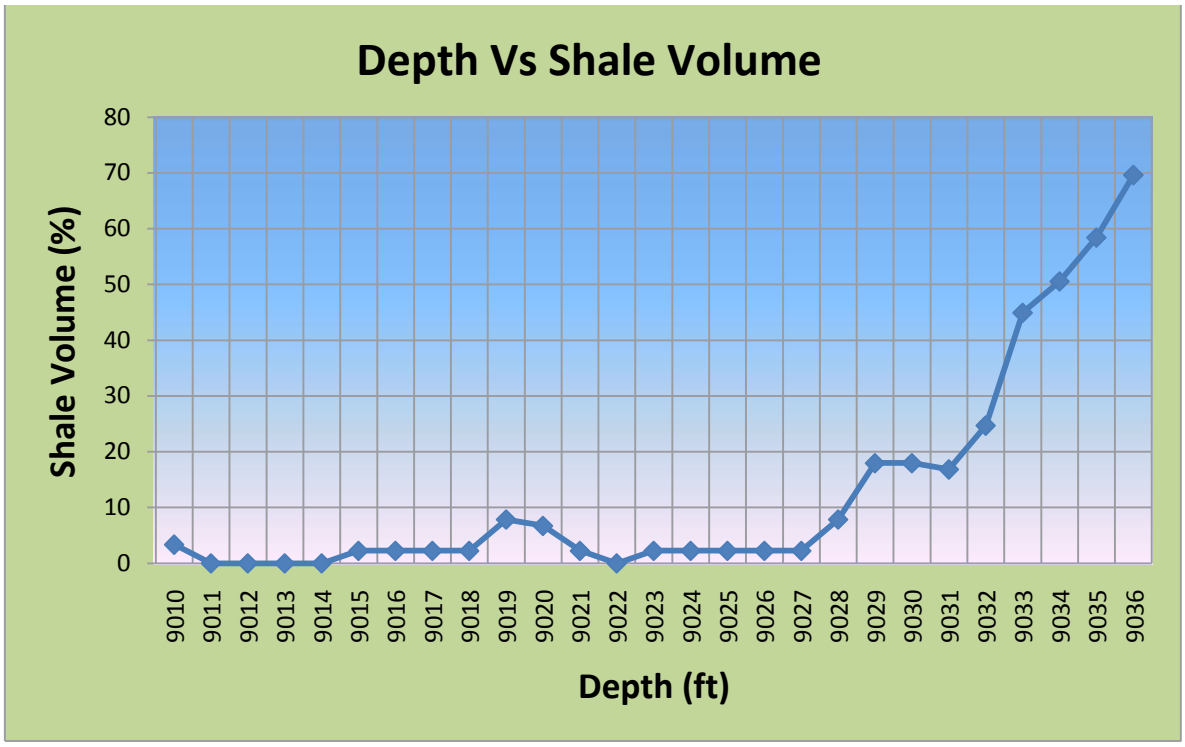

Graph 8.29: Graph showing relationship of shale volume with depth in zone 2, Mari deep 9, Central Indus Basin

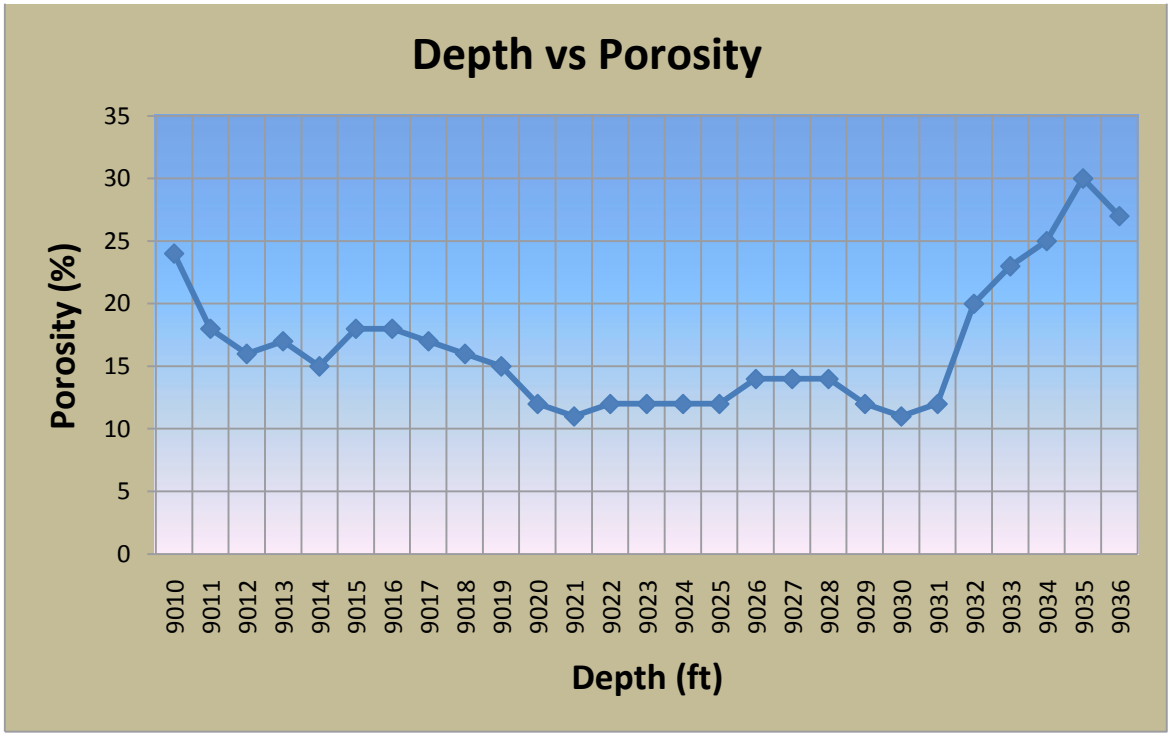

Graph 8.30: Graph showing relationship of porosity with depth in zone 2, Mari deep 9, Central Indus Basin

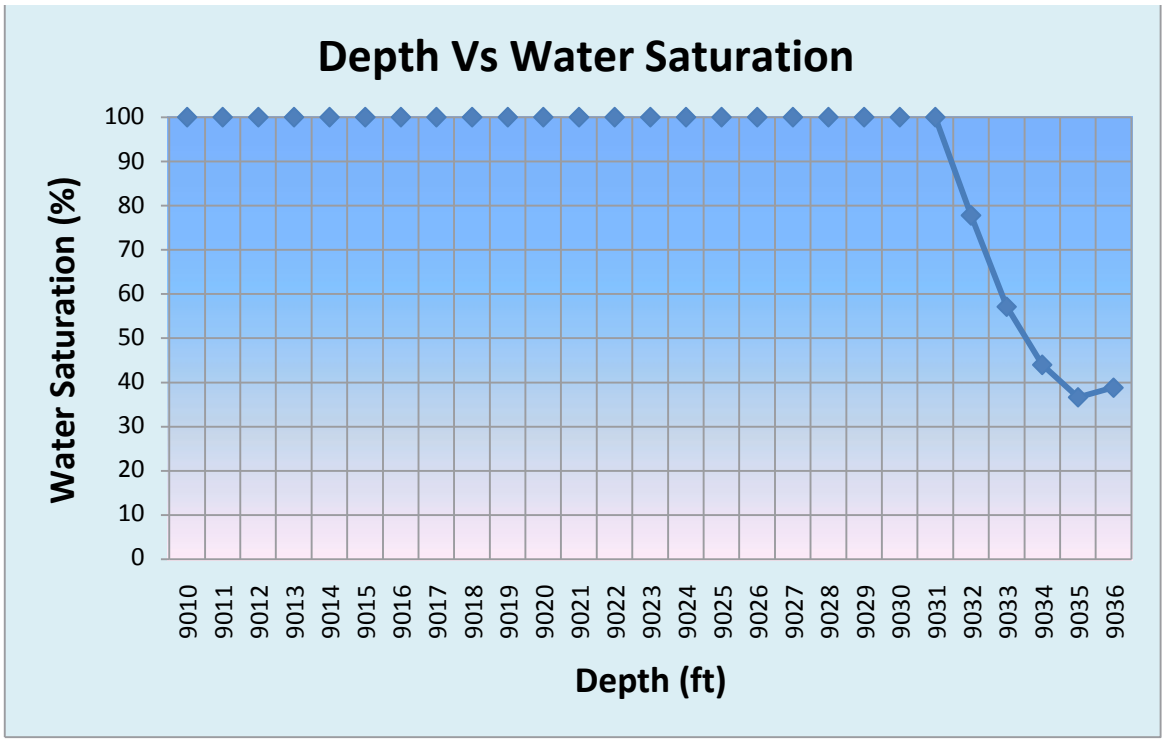

Graph 8.31: Graph showing relationship of water saturation with depth in zone 2, Mari deep 9, Central Indus Basin

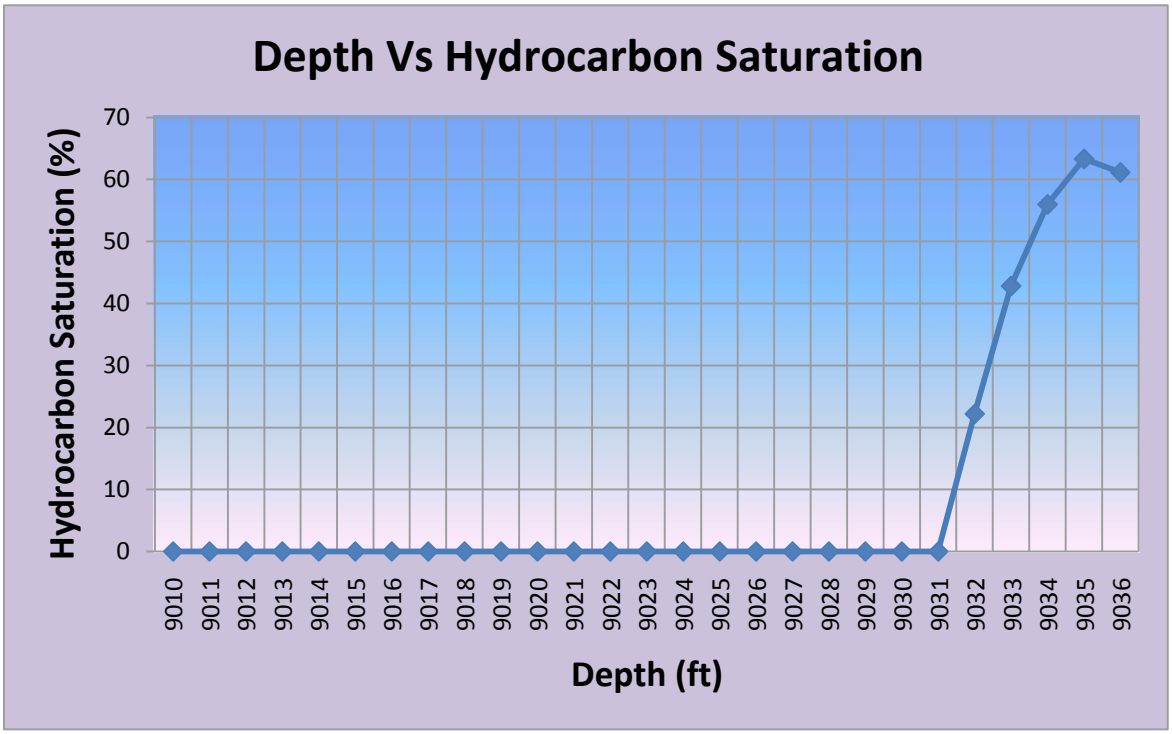

Graph 8.32: Graph showing relationship of hydrocarbon saturation with depth in zone 2, Mari deep 9, Central Indus Basin

Zone 3

Depth (ft)	Volume of Shale (V_{sh}) (%)	Porosity (Φ) (%)	Water Resistivity (R_w) (Ωm)	Water Saturation (S_w) (%)	Saturation of Hydrocarbons (S_{hc}) (%)	Permeability	Lithology
9212	27.88462	13	0.121	100	0	N/A	Sandstone
9213	13.46154	12	0.121	100	0	N/A	Sandstone
9214	10.57692	12	0.121	100	0	N/A	Sandstone
9215	3.846154	11	0.121	100	0	N/A	Sandstone
9216	0.961538	10	0.121	100	0	N/A	Sandstone
9217	5.769231	11	0.121	100	0	N/A	Sandstone
9218	13.46154	14	0.121	87.84553	12.15447	N/A	Sandstone
9219	18.26923	16	0.121	68.75	31.25	N/A	Sandstone
9220	10.57692	15	0.121	77.30012	22.69988	N/A	Sandstone
9221	1.923077	10	0.121	100	0	N/A	Sandstone
9222	2.884615	10	0.121	100	0	N/A	Sandstone
9223	3.846154	11	0.121	95.34626	4.653741	N/A	Sandstone
9224	2.884615	12	0.121	80.39699	19.60301	N/A	Sandstone
9225	8.653846	11	0.121	100	0	N/A	Sandstone
9226	15.38462	11	0.121	100	0	N/A	Sandstone
9227	25	16	0.121	82.17197	17.82803	N/A	Sandstone
9228	23.07692	18	0.121	68.3243	31.6757	N/A	Sandstone
9229	13.46154	16	0.121	82.17197	17.82803	N/A	Sandstone
9230	12.5	14	0.121	100	0	N/A	Sandstone
9231	10.57692	11	0.121	100	0	N/A	Sandstone
9232	12.5	9	0.121	100	0	N/A	Sandstone
9233	14.42308	10	0.121	100	0	N/A	Sandstone
9234	8.653846	8	0.121	100	0	N/A	Sandstone

Table 8.9: Table showing interpretation of zone 3, Mari deep 9, Central Indus Basin

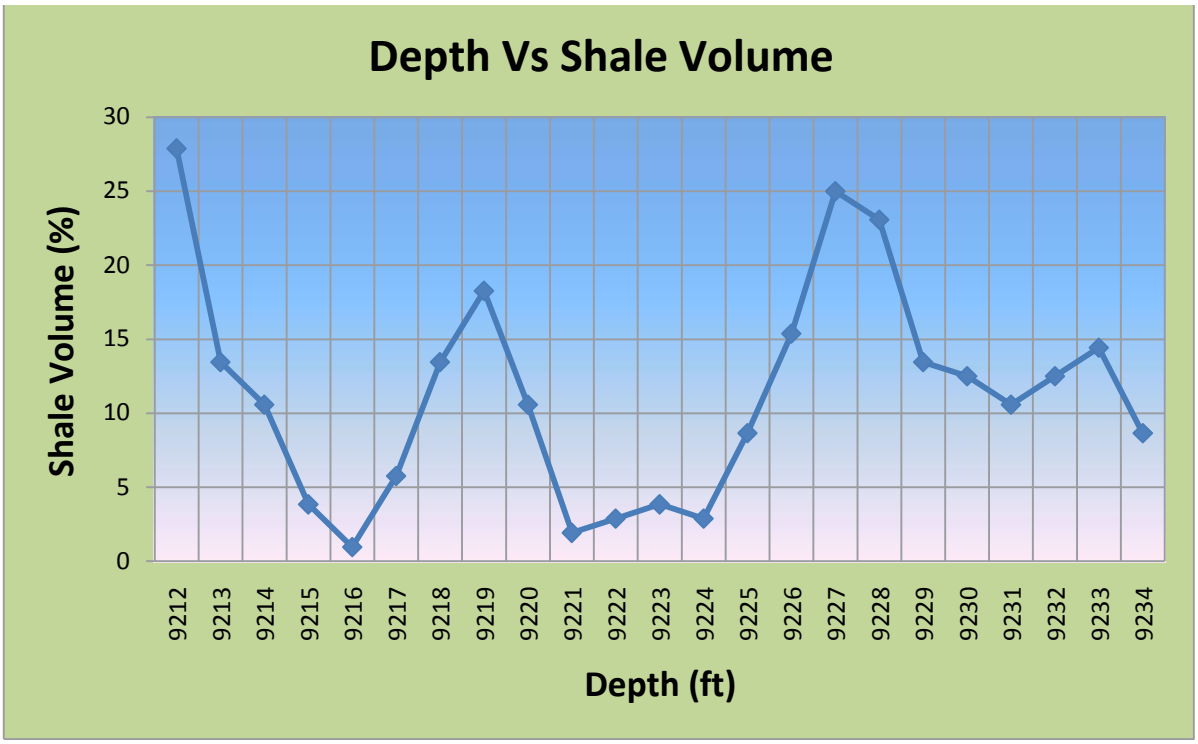

Graph 8.33: Graph showing relationship of shale volume with depth in zone 3, Mari deep 9, Central Indus Basin

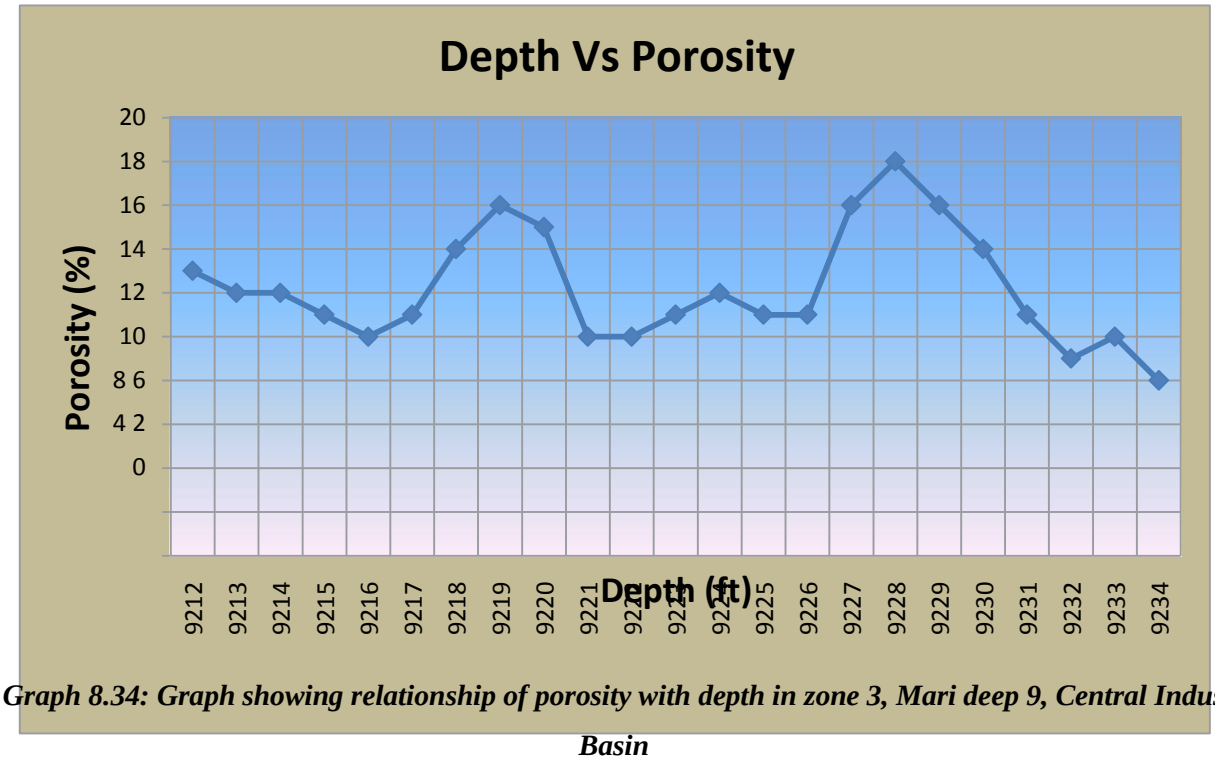

Graph 8.34: Graph showing relationship of porosity with depth in zone 3, Mari deep 9, Central Indus Basin

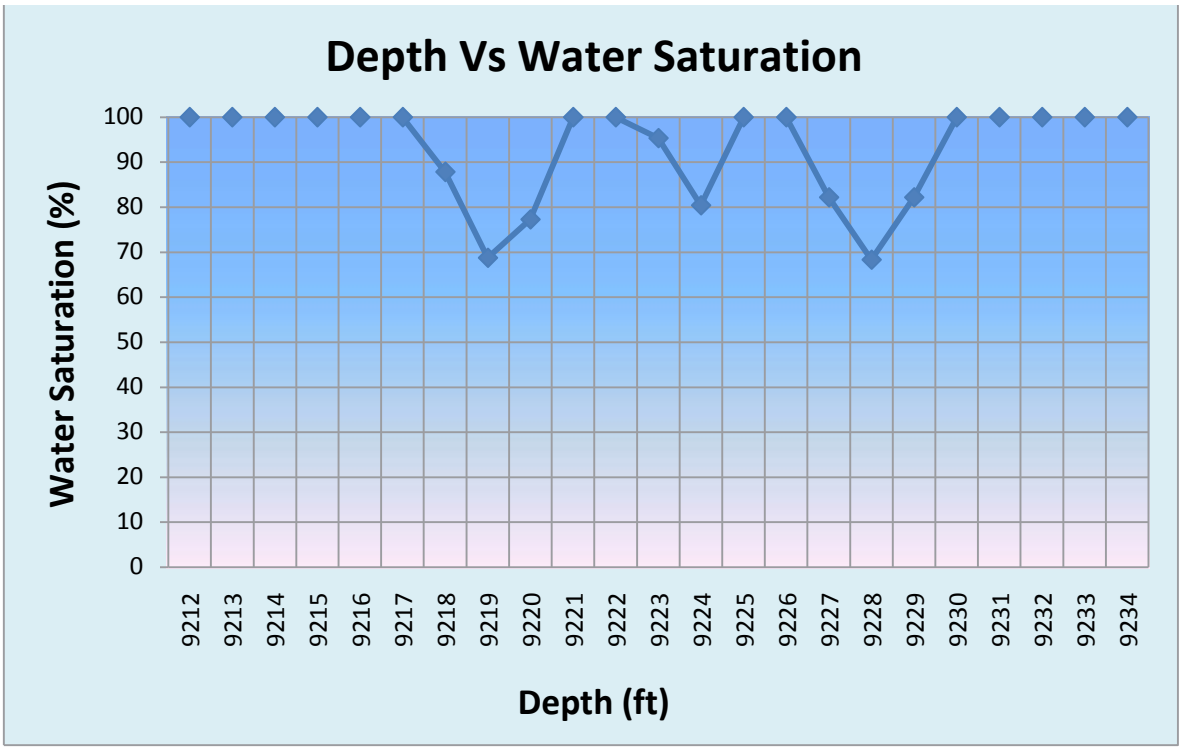

Graph 8.35: Graph showing relationship of water saturation with depth in zone 3, Mari deep 9, Central Indus Basin

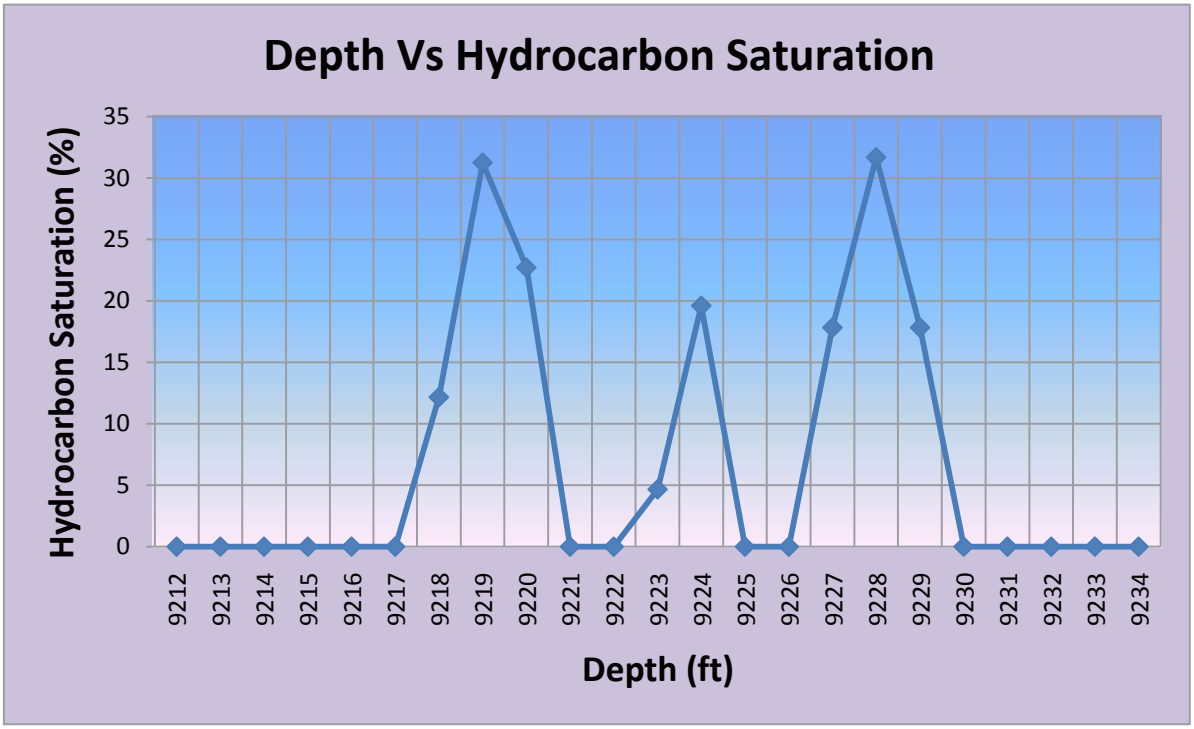

Graph 8.36: Graph showing relationship of hydrocarbon saturation with depth in zone 3, Mari deep 9, Central Indus Basin

CHAPTER # 9

Conclusion and Recommendations

9.1 Conclusion

Petrophysical interpretations were carried out successfully for Mari deep 6 and Mari deep 9, Central Indus Basin. Different petrophysical parameters were calculated i.e. shale volume, porosity, water saturation, hydrocarbon saturation, permeability and lithology using different logs. Three potential reservoirs were found, namely Pirkoh limestone, Habib Rahi limestone and Goru Sandstone.

During the interpretation of Mari Deep 6, first formation found, containing hydrocarbons was Pirkoh Formation. The average shale volume in this formation was calculated to be 44.6%, average porosity was calculated to be 22.7%, average water saturation was calculated to be 84.7% and average hydrocarbon saturation was calculated to be 15.3%. Second formation containing hydrocarbons was Habib Rahi limestone. The average shale volume in this formation was calculated to be 10.4%, average porosity was calculated to be 21.6%, average water saturation was calculated to be 29.1% and average hydrocarbon saturation was calculated to be 70.8%. Third formation containing hydrocarbons was Goru sandstone. In this formation, four zones were encountered. The average shale volume in this formation was calculated to be 14.9%, average porosity was calculated to be 11.5%, average water saturation was calculated to be 61.9% and average hydrocarbon saturation was calculated to be 38.1%.

During the interpretation of Mari Deep 9, the formation encountered was Goru sandstone. In this formation we marked three zones of interest. The average shale volume in this formation was calculated to be 13.3%, average porosity was calculated to be 14.6%, average water saturation was calculated to be 76.2% and average hydrocarbon saturation was calculated to be 23.8%.

Petrophysical analysis showed that Mari deep 6 has huge hydrocarbon reserves i.e. natural gas and is more economical, while in Mari deep 9, only first zone is hydrocarbon bearing zone and the rest of the zones encountered below were water zones.

9.2 Recommendations

1. Special core analysis should be done on reservoir rocks for better control on petrophysical interpretations.
2. MDT, FMI should be run in future wells.
3. TDT, RST should be run in production wells to measure the water level in reservoir.
4. Best drilling and mud parameters should be used in future wells to minimize the well damage.

REFERENCES

- Ahmed, N., Fink,P., Sturrock, S., Mahmood, T. and Ibrahim, M., 2004, Sequence Stratigraphy as Predictive Tool In Lower Goru Fairway, Lower and Middle Indus Platform, Pakistan. Proceedings of the ATC Conference, Islamabad, Pakistan, 2004, p.85-87.
- Abbasi, M.A. and Siddique, M.S., 1998, Mari Gas Field: The Habib Rahi Limestone Reservoir. Proceedings of the SPE-PAPG Conference, Islamabad, Pakistan, 1998, p.90-99.
- Basan, P.B.; Lowden, B.D. ;Attard, J.J. "Visualisation with quantification: New approaches to reservoir petrophysics, 1996.
- Brown, A Mathematical Comparison of Common Saturation Equations, SPWLA twenty-seventh annual logging symposium, June, 1986, paper T, appendix 1.
- Hemphill, Kazmi, A.H. and Meissner 1977. Middle Eocene. In: Ibrahim Shah, dS.M.(ed): Stratigraphy of Pakistan. Geological Survey Pakistan, Mem,V.12, p. 70-72.
- Kadri, I.B., 1995, Petroleum Geology of Pakistan, Pakistan Petroleum Limited. Karachi, p.275.
- Kazmi A.H. & Jan, M.Q, 1997, "Geology & Tectonic of Pakistan", Graphic Publishers, Karachi, Pakistan. p. 232-249.
- Khan, J. M., Moghal, M.A. and Jami,M.A.,1999, Evolution of Shelf Margin and Distribution of Reservoir Facies In Early Cretaceous of Central Indus Basin, Pakistan. Proceedings of the SPE-PAPG Conference, Islamabad, Pakistan, 1999, p.1-13.
- Khan, M.N., 1998, Introduction to wire line log interpretation.
- Naseer, A.M, khoso, T., Alam, M.S., Amir, S., Saqib, M., 2007, Formation Pressure Prediction Using Seismic Inversion Technique in Mari Gas Field, Central Indus Basin, Pakistan. Proceedings of the ATC Conference, Islamabad, Pakistan, 2007, p. 85-88.
- Poupon, Clavier, Dumanoir, Gaymard, and Misk, Journal of Petroleum Technology, July, 1970, p. 868.
- Raza, H.A., Ahmed, R., Ali, S.M., Ahmed, J., 1989, ”Petroleum prospects: Sulaiman sub-Basin, Pakistan”, Pakistan Journal of Hydrocarbon Research, v.1, No.2, p. 21 - 56.
- Serra.O., 1984, Fundamentals of Well Log Interpretation.

- Sheikh, R.A., Jamil, M.A., Abbas, G., and Saqi, M.I., 2004. The Reservoir Potential of Carbonate Horizons of Kirthar Formation, Eastern Sulaiman Range, Central Indus Basin Pakistan. Proceedings of the ATC Conference, Islamabad, Pakistan, 2004, p. 61-70.
- Williams, 1977 Oligocene. In: Ibrahim Shah, S.M.(ed): Stratigraphy of Pakistan. Geological Survey Pakistan, Mem, v.12, p.47-83.
- http://www.marigas.com.pk/Production%20Graphs.htm